Dynamique et contrôle actif avec délai de la dynamique des structures mécaniques à potentiel $\phi6$ monostable non bornés

Blaise Romeo Nana Nbendjo

HAL Id: tel-00009933

https://theses.hal.science/tel-00009933

Submitted on 12 Aug 2005

DYNAMICS AND ACTIVE CONTROL WITH DELAY OF THE DYNAMICS OF UNBOUNDED MONOSTABLE MECHANICAL STRUCTURES WITH ϕ^6 POTENTIAL

NANA NBENDJO Blaise Roméo

Laboratoire de Mécanique, Faculté des Sciences, Université de Yaoundé I, B. P. 812 Yaoundé, Cameroun

Email : brnana@uycdc.uninet.cm & nananbendjo@yahoo.com

Directed by :

WOAFO Paul
Associate Professor
University of Yaoundé I

Email : pwoafo1@yahoo.fr & pwoafo@uycdc.uninet.cm

Academic year 2004

TABLE OF CONTENTS

TABLE OF CONTENTS

CHAPTER II : CONTROL BY SANDWICH AND WITH PIEZOELECTRIC ABSORBER OF THE DYNAMICS OF UNBOUNDED MONOSTABLE MECHANICAL STRUCTURES WITH ϕ^6 POTENTIAL

CHAPTER III : ACTIVE CONTROL WITH DELAY OF THE DYNAMICS OF UNBOUNDED MECHANICAL STRUTURES WITH ϕ^6 POTENTIAL

6

ABSTRACT

ABSTRACT

Dynamics and active control with delay of the dynamics of unbounded monostable mechanical structures with ϕ^6 potentials, that is the main purpose of this work. It may be viewed as a contribution to the study of the control of the dynamics of physical systems in which the potential have a catastrophic single well ϕ^6 configuration. Active structural enhancement consists of the use of active control to modify the structural behaviour.

We present in chapter I, some important physical systems related to the non-linear mechanical structures with catastrophic single well ϕ^6 potential. It is shown that, the mathematical model of various non-linear structures (inverted pendulum, articulated beam, elastic beam fixed at its base and free at the top) is that of a particle moving in a catastrophic single well ϕ^6 potential. The condition for escape from a potential well are obtained and the criteria for the appearance of horseshoes chaos are derived using the Melnikov theory. Numerical simulation of the original equation is carried out to complement our analysis and metamorphism of the basin of attraction is observed.

Chapter II is devoted to the control by sandwich and with piezoelectric absorber of the dynamics of mechanical structures as presented in chapter I. The first control strategy consists of coupling the non-linear beam by a linear one. The linear one serves as control element used to reduce the amplitude of vibration of the non-linear beam. The effects of the control parameters on the dynamical behaviour of the system is analysed and the conditions for the effectiveness of the control as well are obtained. Approximate criterion for the appearance of Melnikov in the control model is derived and the effects of control gain parameters are analysed.

In chapter III, we consider the effect of time-delay between the detection of the structure's motion and the restoring action of the control system. The stability of the control system under control is studied using the Lyapunov

concept and the domain subdivision method. The effect of time delays in the critical force leading to the reduction of amplitude and escape from a potential well is obtained analytically and verified numerically. The effects of the control strategy and time-delays in the onset of Melnikov chaos is presented.

Our study ends with a general conclusion summarising the most important results obtained and listing some other problems encountered. We also present the other perspectives open by this work.

RESUME

Dynamique et contrôle actif avec délai de la dynamique des structures mécaniques à potentiel ϕ^6 monostable non borné, tel est le thème de ce travail qui se veut être une contribution à l'étude du contrôle de la dynamique des structures mécaniques régis par le potentiel ϕ^6 monostable catastrophique. Le renchérissement actif de la structure consiste à utiliser le control actif pour modifier le mouvement de la structure.

Nous présentons au chapitre I des systèmes physiques pouvant être modélisés par le modèle potentiel ϕ^6 monostable catastrophique. Nous établissons que, les systèmes suivants : pendule inversé, poutres articulées aux deux extrémités, poutre élastique libre à une extrémité et fixée à l'autre, sont décrits par une équation identique à celle d'une particule se mouvant dans un potentiel ϕ^6 monostable catastrophique. La condition du saut de puits de potentiel est obtenue de même que le critère d'apparition du chaos du fer à cheval, en utilisant la théorie de Melnikov. La simulation numérique de l'équation originale est faite pour compléter les analyses et les métamorphoses du bassin d'attraction sont observées.

Le chapitre II est consacré au contrôle par sandwich et avec absorbeur piézoélectrique de la dynamique des structures mécaniques tel que présentés au chapitre I. Nous considérons dans le cas du contrôle par sandwich une stratégie consistant à coupler la structure non-linéare à une autre linéaire, la structure linéaire ici servant d'élément de contrôle utilisé pour réduire l'amplitude des vibrations de la structure non-linéaire. L'effet des paramètres de contrôle sur la dynamique du système sont analysés et la condition d'efficience du contrôle est obtenue. Nous obtenons approximativement le critère d'apparition du chaos dans le modèle contrôlé et l'effet des paramètres de gain de contrôle est analysé.

Au chapitre III, nous considérons l'effet du retard entre la détection du mouvement de la structure et l'action restitué du système de contrôle. La

stabilité du système sous contrôle est étudiée en utilisant le concept de Lyapunov et la méthode de subdivision du domaine. L'effet du délai sur la force critique conduisant à la réduction d'amplitude ou au saut du puits de potentiel est obtenu analytiquement et vérifié numériquement. L'effet de la stratégie de contrôle et du retard sur l'apparition du chaos de Melnikov est présenté.

Notre étude s'achève par une conclusion générale résumant les résultats importants obtenus et faisant état de quelques problèmes rencontrés au cours de l'étude, puis de quelques perspectives en rapport avec le travail effectué.

PhD Thesis in Non-linear Mechanics

GENERAL INTRODUCTION

GENERAL INTRODUCTION
1°) Generalities on mechanical structures with ϕ^6 potential

The non linear dynamics in mechanical structures has been investigated by an increasing number of researchers in recent years. The reason for this high interest is due to the fact that non linear modelling permits to explain various phenomena in chemistry, economy, biology, etc and especially in all the branches of physics. Basically, all the problems in mechanics are non linear from the out set. The linearisations commonly practised are approximating devices that are good enough or quite satisfactory for must purposes. There are however, also certain cases in which linear treatments may not be applicable at all [1]. In this line, particular attention had been paid to the modelling of mechanical structures by the Duffing oscillator (oscillator with ϕ^4 potential) [2-5]. For instance taking the case of softening Duffing oscillator [6], a large number of studies permit to explain that it modelises a variety of physical phenomena such as the rolling motion of a ship, Josehpson oscillators, Foucoult's pendulum, etc [7]. These studies have revealed various types of interesting behaviours: hysteresis, multistability, period-doubling bifurcation, intermittent transition to chaos, fractal basin boundarie etc [8-12]. Another model which deserves particular attention is the extended Duffing oscillator (oscillator with ϕ^6 potential). This potential can present many configurations which may be classified in two groups: bounded configurations (with one well, two or three wells) and unbounded or catastrophic configuration (with one well or two wells). The first group always leads to bounded dynamics while the second group can give rise to unbounded motion resulting to catastrophic consequences. The interest devoted to the model, is due to the fact that in addition to results obtained from the classical Duffing oscillator, it can permit us to have more information about the dynamics of the system and in certain cases to foresee the failure of the structure. The first analysis of that model has been done in 1991 by Debnath and Chawdhury [13] who studied the stability, the response of the models and the onset of period-doubling through the harmonic balance method. In the same way, Li and Moon [14] studied the dynamics of a cantilever steel beam

with free ends and subjected to the action of three magnets placed in a regular manner to give the bounded tristable configuration. In 1999, Lenci *et al* [15] considered the dynamics of slender column fixed at its base and resting on a Winkler foundation. By extending the reactive force exerted by the foundation on the column to include a fifth order term, they found that depending on the value of the vertical load applied to the free end, the single mode dynamics can be described by bounded potential with two or three wells. They then derived the criteria for the occurrence of Melnikov chaos. Recently, Tchoukuegno [16] shed some light on other aspects of this ϕ^6 model, but his attention was focused only in the case of ϕ^6 potential with three wells and catastrophic two wells configurations.

In this thesis, we will continue to throw more light on the other aspects of this ϕ^6 model. Our attention will be paid on the unbounded single well ϕ^6 potential Some of the questions like which types of mechanical structures can be modelised by this model and what is the advantage of using this model will be answered.

2°) Control of the dynamics of mechanical structures

All mechanical systems exhibit vibrating responses when subjected to time varying disturbances. The predictions and control of these disturbances is fundamental to the design and operation of mechanical equipment. For instance, in automobile and aeronautic industries, one of the most dangerous effects is the influence of parasite perturbation, notably in the propulsion jet, propeller shaft and crankshaft. Around us, one can remind himself about the state of roads, bridges, agriculture and the shakes in industries. Further, one can see the turbulent zone in aircraft. Very often these perturbations forestall the growing of agriculture structures and can lead them to catastrophic failure.

Considerable efforts have been devoted to the control of linear and non linear vibrating structures. Among the control strategies, the active control plays a particular role [17-20]. Another reason that active control has been receiving an increasing amount of attention has to do with the rapid advances that have been taking place in allied technologies. The development of the active control must go hand-in hand with advanced areas such as computers, electronics, measurement

techniques, instrumentations, controllers, actuators, materials etc [21]. Consequently, the study of active control in dynamical structures has given rise to considerable development in many domains such as industries. One of the first application was in the increment of critical speed of aircraft modulation [22]. Recently, due to new technologies, the use of control theory in mechanical system has increased a lot. For instance in reference [23], the author gives a thorough review of the description and the main results are that, control scheme mitigates the effects of the dynamic loading on the vibration amplitude and prevent dangerous instability phenomena, with a load carrying capacity of buckled beams increasing with the degree of non linearity of the control strategy. In 1985, Bailey *et al.* [25] introduced piezoelectric actuators to active vibration control. They used the actuators bonded to the surface of a cantilever beam in their feedback vibration damping design. Demitriadis *et al* [26] in 1991 performed a two-dimensional extension of Crawley and Deluis work [27], applying pair of laminated piezoelectric actuators to a plate. They demonstrated that the location and shape of the actuator dramatically affected the vibration response of the plate. Recently in 2002, Morgan *et al.* [24] proposed a semi active piezoelectric absorber for suppressing harmonic excitation with varying frequency.

Another effect which arises in control strategies is the inevitable time-delay between the detection of the structure motion and the restoring action of the control. In reference [28], the authors considered such a problem in linear structures and showed that time-delay can even lead to the instability of the whole structure. Thus it is of interest to pursue this study in non-linear structures. In this dissertation we consider many control strategies with the effect of time delay on the control strategy.

3°) Problematic and organisation of the thesis

The aim of this thesis is to study the dynamics and control of mechanical structures with unbounded single well ϕ^6 potential.

In chapter I, we present the modelling of mechanical structures with unbounded single well ϕ^6 potential. Later, we derive the condition for escape from

the potential well [29]. At the end of this chapter, we will follow the Melnikov method [30] to derive the criteria for the occurrence of fractal basin boundaries for the heteroclinic orbit.

In chapter II, we describe two types of control strategy (sandwich control and piezoelectric control). After the establishment of the resultant equations of motion of the models, we derive the range of control gain parameters that can produce an effective control (stability of the model and reduction of amplitude) along with the condition for the escape from a potential well. The other part of this chapter deals with the derivation of Melnikov criterion for suppressing chaos and the effect of the control gain parameters on the basin of attractions.

Chapter III deals with the study of the effects of time delays in the control strategy. We find the stability of the system under control using the Lyapunov concept and D-subdivision method. The effect of time delays in the amplitude and critical forcing for catastrophic and Melnikov chaos are analysed.

We end the thesis with a general conclusion and the perspectives offered by our investigations.

REFERENCES

[1]- T. T. Soong, "Active Structural Control: Theory and Practice", John Wiley & Sons, Inc, New York,1950.

[2]-J. J. Stokker, "Non-linear Vibrations" , Interscience, New-York, 1950.

[3]- C. Hayashi, "Non-linear Oscillations in Physical Systems" McGraw-Hill, New-York, 1964

[4]-A H. Nayfey, D. T. Mook, "Non-linear Oscillations" Wiley, New York, 1996.

[5]- J. M. T. Thompson, H. B. Stewart, "Non-linear Dynamics and Chaos" Wiley New york, 1986.

[6]-A H. Nayfey, N. E. Sanchez, Int. J. Nonlinear Mech. 24 (1989) 483.

[7]-P. Holmes, Philos-trans. R. Soc. London ser 282 (1979) 419

[9]-J. Guckenheimer, P. J. Holmes, "Non-linear Oscillations, Dynamical Systems and Bifurcation of Vector Fields", Springer, New york, 1983

[10]- M. S. Sato, Y Sawada, Phys. Rev A 28 (1983)1654

[11]-B. H. Hurberman, J. P. Crutchfied, Phys. Rev. Lett 43 (1979) 1743

[12]-H. Fotsin, C. Chedjou and P. Woafo, Phys. Scripta 54 (1996) 545

[13]-M. Debnath, A. R. Chawdhury, Phys. Rev. A 44 (1991) 1049

[14]-G. X. Li and F. C. Moon, J. Sound and Vibration 136 (1990) 17

[15]-S. Lenci, G. Menditto, A.M. Tarantino, Int. J. Non-linear Mech.34 (1999) 615

[16]- R. Tchoukuegno, "Dynamique et Contrôle des Vibrations des Poutres modélisées par le potentiel phi-6 tristable et bistable catastrophique", Ph.D Thesis, Université de Yaoundé I, 2003

[17]-C. R. Fuller, S. J. Eliot, P. A. Nelson " Active Control of Vibration", London Academic 1997

[18]-K. Hackl, C.Y. Yang, AHD Cheng, Int. J. Nonlinear Mech.28 (1993) 441

[19]-AHD Cheng, Y Yang, K. Hackl, M. J. Chaves, Int. J. Nonlinear Mech. 28 (1999) 549

[20]- R. Tchoukuegno, P. Woafo, Physica D 167 (2002) 86

[21]- T.Aida, K.Kawazoe, S. Toda, J. Vibration and Acoustics117 (1995) 332

[22]- Jezequel, "Active Control in Mechanical Engineering ", Editions Hermes, 1995

[23]- O. C. Pinto, P. B. Goncalves, Chaos, Solitons and Fractals 14 (2002) 227

[24]- R. A. Morgan, k. W. Wang, J. Vib. Acoustics 124 (2002) 77

[25]-T. Bailey, J. E. Hubbard, Journal of Guidance, Control, and Dynamics 8 (1985) 605

[26]-E. K. Dimitriadis, C. R. Fuller, C. A. Rogers, Journal of vibration and acoustics 113 (1991) 100

[27]-E. F. Crawley, J. Luis, AIAA Journal 25 (1987) 1373

[28]-L. Zhang, C. Y. Yang, M. J. Chaves, AHD Cheng, J. Engng. Mech. Div. ASCE 119 (1993) 1017

[29]- N. Virgin, R. H Plaut, C. C. Cheng, Int. J. of Non-linear Mech. 27 (1992) 357

[30]- V. K. Melnikov, Trans. Moscow. Math. Soc 12 (1963)1.

CHAPTER I
MODELLING AND DYNAMICS OF UNBOUNDED
MONOSTABLE MECHANICAL STRUCTURES WITH
ϕ^6 POTENTIAL

CHAPTER I: MODELLING AND DYNAMICS OF
UNBOUNDED MONOSTABLE MECHANICAL
STRUCTURES WITH ϕ^6 POTENTIAL

I-INTRODUCTION

In recent years, considerable efforts have been devoted to the study of non-linear vibrating structures. This is due to the fact that they appear in various fields of fundamental and applied sciences [1-5]. Among these studies, particular attention has been paid on the dynamics of Duffing structures. The Duffing oscillator is beside the Van der Pol oscillator [6,7] one of the non-linear oscillator that has received a lot of attention in recent years, since it modelises a large variety of systems in physical sciences. Another model of interest is the extended Duffing oscillator with non-linear terms of order greater than four. When one restricts the development to the sixth order term, the potential is called the ϕ^6 potential and is given by

$$V(x) = \frac{1}{2}bx^2 + \frac{1}{4}cx^4 + \frac{1}{6}dx^6 \qquad (I-1)$$

where b, c, d are constants.

This potential permits to foresee the behaviour of structures when the amplitude of the oscillation is large. It gives rise to many configurations depending on the nature and the environment of the structure in movement. The configurations can be classified into two groups as follow.

- The hard spring systems (see figure I-1a): for these systems, as the amplitude of the external excitation increases, the system becomes tense and the natural frequency of the free vibrations increases. The curve of the energy versus the deformation is concave towards the up. These systems can possess one, two or three potential wells according to the values of c and d.
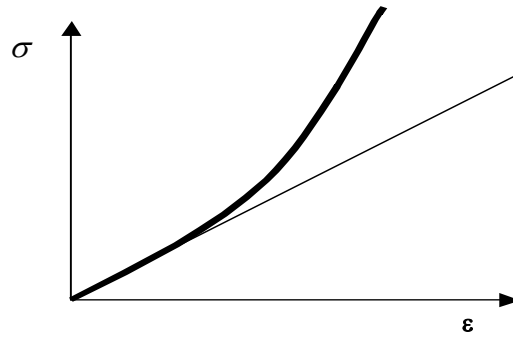
Figure. I-1a: Evolution of the energy versus the
deformation in the case of hard spring systems

•The soft spring system (see figure I-1b): in these systems, the energy versus the
deformation is concave downward as presented below.
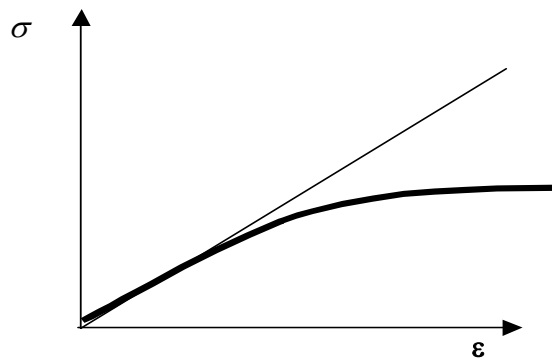
Figure I-1b: Evolution of the energy versus the
deformation in the case of soft spring systems

The soft spring systems can be described by the ϕ^6 potential with one or two
potential wells according to the consistence of the environment in which it is
found.

In this chapter, we will focus our attention on a soft spring system
corresponding to a catastrophic or unbounded potential well. Section II deals with
the modelling of physical systems described by the unbounded monostable ϕ^6
potential. In each system, the interest of using a ϕ^6 potential is clarified. Section III
deals with the general dynamics of the system and section IV summarises the
chapter.

II-MODELLING OF THE DYNAMICS OF MECHANICAL STRUCTURES BY AN UNBOUNDED SINGLE WELL ϕ^6 POTENTIAL

II-1- An inverted pendulum

The inverted pendulum is considered as a rigid rod attached to the soil by a rotary spring and dashpot (viscous damper) as shown in figure I-2. The forces acting on this system are: the weight and the reaction of the soil.
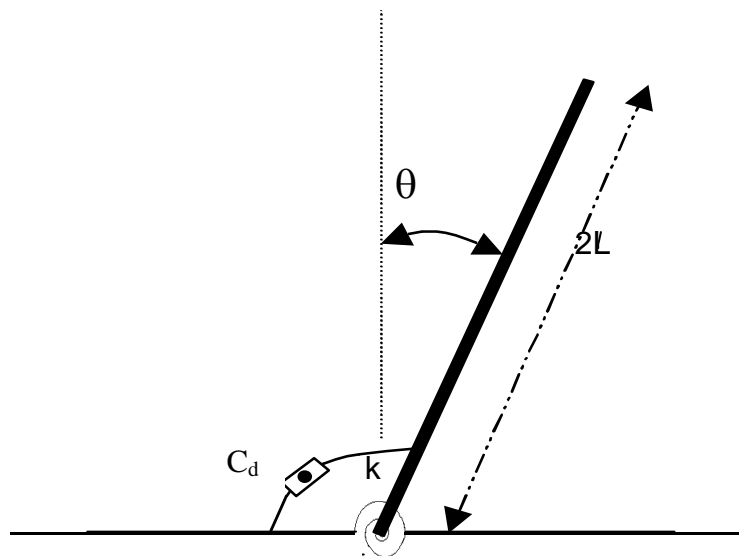
Figure I-2 : An inverted pendulum

This reaction is related to the mechanical properties of the soil. The coefficients of the reaction (damping and elastic coefficients) of each structure can be deduced from a free vibration test. The inclination of the rod must be less than the critical amplitude, if not the structure will break. We encounter this type of structure in various domains.

♦In agriculture, it represents rigid plants such as corn plant and tree [8-10]. In this case, the reaction is also related to the depth and the configuration of the roots.

♦In civil engineering, we have electrical poles either in wood or in iron. We also have the one-dimensional version of a rocket on take-off, the vehicle being balanced by an engine thrust [11].

♦In biomechanics the prosthetic limb for physically disabled persons [11] can also be described by such a model.

Under the action of the external excitation, the motion of the inverted pendulum is obtained using the fundamental equation governing the dynamics of the system in rotation and it is given by

$$J \frac{d^2\theta}{dt^2} + C_d \frac{d\theta}{dt} + k\theta - mgl \sin\theta = M'(t) \qquad \text{(I-2)}$$

where J is the moment of inertia , m the rod mass and l the height at mid length of the rod. g, C_d and k are respectively the gravitational acceleration, the damping coefficient and the spring constant. θ is the angle the rod makes with the equilibrium position and $M'(t)$ stands for the external forces. $M'(t)$ can be the effects of wind or the action of machine used to uproot the mechanical structure. Very often, these forces are stochastic and when the amplitude is small, one can assimilate it to a gaussian white noise [12]. They can also be approximated by periodic functions whose amplitude and frequency are deduced by using averaging procedures (statistics analysis, Fourier analysis, noise analysis, etc..).

An interesting case of this study is to foresee the critical amplitude of the external excitation for which the failure appears. Using equation (I-2), the potential energy is given by

$$V(\theta) = \frac{1}{2}k\theta^2 + D\cos\theta \qquad\qquad \text{Where D}=mgl \qquad \text{(I-3)}$$

The critical amplitude θ_u is obtained when the following conditions are satisfied

$$V'(\theta) = 0 \qquad \text{and} \qquad V''(\theta) \succ 0 \qquad \text{(I-4)}$$

But obtaining the analytical expression using equation (I-3) is not possible. That is why, we carry out the expansion of $\cos\theta$ up to the sixth order around the equilibrium position *θ=0*, to obtain

$$V(\theta) \simeq D + \frac{1}{2}(k-D)\theta^2 + \frac{1}{24}D\theta^4 - \frac{1}{120}D\theta^6 \qquad \text{(I-5)}$$

Since $\left(-\frac{1}{720}D\theta^6\right)$ is negative, we have a ϕ^6 potential [13], showing one stable

equilibrium point *(θ=0)* and two unstable equilibrium points at

$\theta_u = \pm\left(10 + \sqrt{20\left(\frac{6k}{D}-1\right)}\right)^{1/2}$ as it appears in figure I-3. Thus, unbounded motion can

appear for $|\theta| \geq |\theta_u|$.

Following equation (I-5), equation (I-2) becomes

$$J\frac{d^2\theta}{dt^2} + C_d\frac{d\theta}{dt} + (k-D)\theta + \frac{1}{6}D\theta^3 - \frac{1}{120}D\theta^5 = M'(t) \qquad \text{(I-6)}$$

Using the following dimensionless quantities

$$\lambda = \frac{C_d}{J\omega_0}, \ b = 1 - \frac{D}{k}, \ c = \frac{D\theta_0^2}{6k}, \ d = -\frac{D\theta_0^4}{720k}, \ \tau = \omega_0 t, \ M(\tau) = \frac{M'(t)}{J\omega_0^2\theta_0}, \ q = \frac{\theta}{\theta_0} \ \text{and} \ \omega_0^2 = \frac{k}{J}, \qquad \text{(I-7)}$$

Where θ_0 is a reference amplitude

We obtain

$$\frac{d^2q}{d\tau^2} + \lambda\frac{dq}{d\tau} + bq + cq^3 + dq^5 = M(\tau) \qquad \text{(I-8)}$$

As an example, we consider a structure having the following parameters: mass *m=2 kg*, length of the stalk *2l=2.5 meter*, damping coefficient *C$_d$=0.15 Ns/meter*, natural frequency *ω_0=8.8 rad/s* and gravity acceleration given by *g=9.8 meter/s^2*. Such a structure is compatible with a corn plant as reported in reference [9]. We thus obtain the following values for the dimensionless parameters:

λ=0.009, b=0.92, c=0.013 and *d=-0.0008*

Throughout the thesis we will use this set of dimensionless parameters.
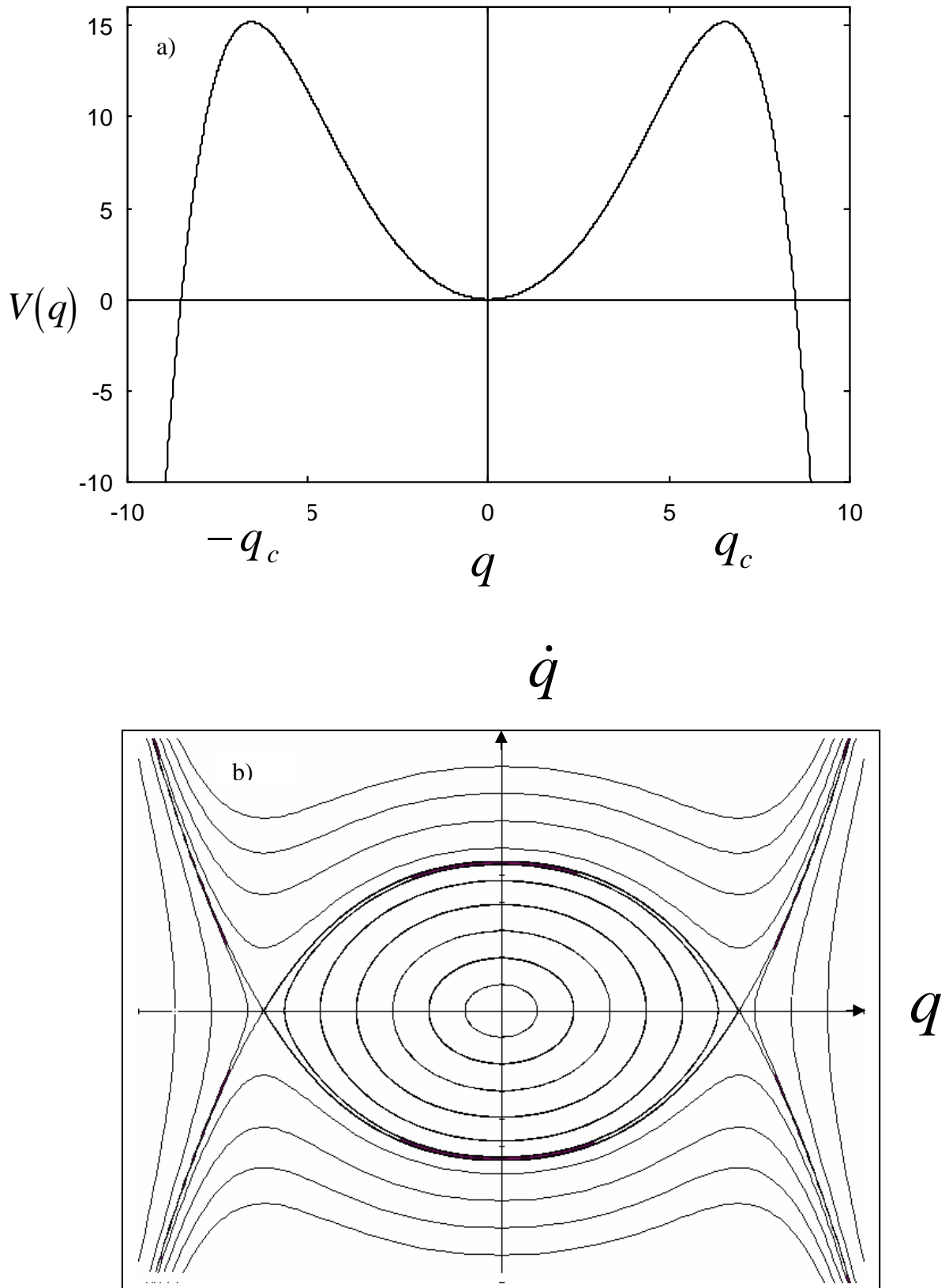
Figure I-3 : a) Catastrophic single-well ϕ^6 potential with the following parameters $\omega_0^2 = b = 0.92$, $c = 0.013$ and $d = -0.0008$.
b) Corresponding phase diagram of the oscillator

II-2 Beam with articulated ends under transversal excitation

The model is a strongly non-linear beam of length l with articulated ends subjected to the action of a transversal excitation P (figure I-4).
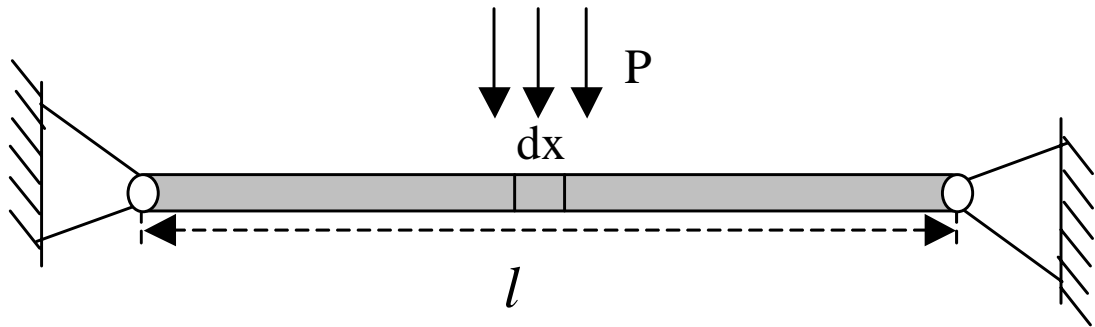
Figure I-4: Articulated beam under transversal excitation

This model is generally found in civil and mechanical engineering.

In civil engineering, it is used in building construction where it serves as an element of skeleton, floor-plates and in cross over like bridges and viaducts. The transversal excitation can be the movement of vehicles or people on the bridge, the movement of robots or vibrating machines on the floor-plates (for example in industries). It can also result from the action of seismic waves on engineering structures.
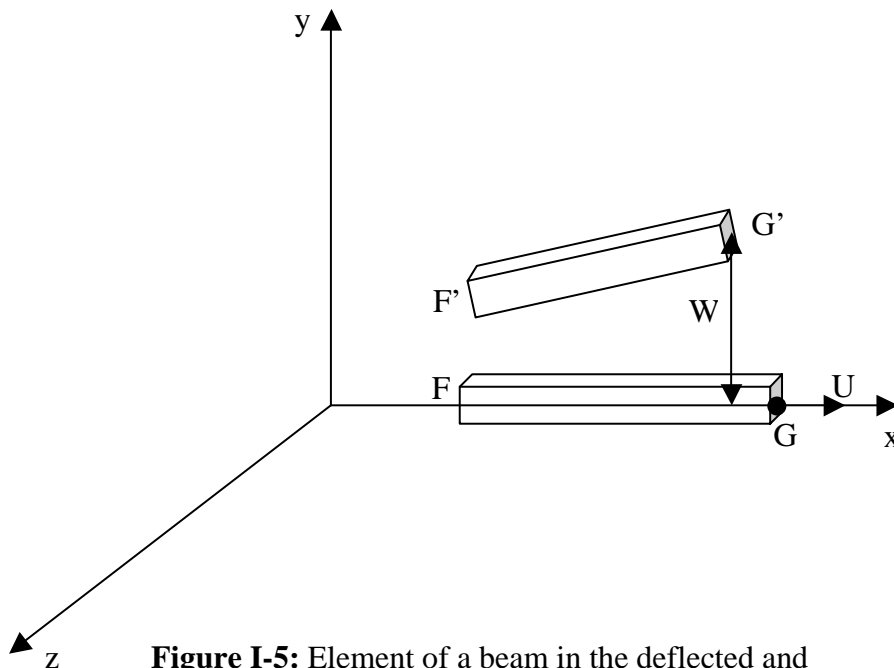
Figure I-5: Element of a beam in the deflected and undeflected positions

To deal with the modelling, let w and u be the transversal and longitudinal displacements respectively. We consider an element of the beam of length dx at rest (figure I-5). We label the end of an infinitesimal length of string by F and G in the undeformed position and F' and G' in the deformed position. The displacement of F is given by

$$\overrightarrow{\Delta F} = u(x,t)\vec{i} + w(x,t)\vec{j} \tag{I-9}$$

and the displacement of G is given by

$$\overrightarrow{\Delta G} = \left(u + \frac{\partial u}{\partial x}dx\right)\vec{i} + \left(w + \frac{\partial w}{\partial x}dx\right)\vec{j} \tag{I-10}$$

It follows from figure I-5 that

$$\overrightarrow{\Delta F} + \overrightarrow{\Delta F'G'} = \overrightarrow{\Delta F} + dx\vec{i} \tag{I-11}$$

where $\overrightarrow{\Delta F'G'}$ is the vector giving the position G' relative to F'

Let ds be the corresponding length when the beam is deflected. It is given by

$$ds = \left|\overrightarrow{\Delta F'G'}\right| = \left[\left(1 + \frac{\partial u}{\partial x}\right)^2 + \left(\frac{\partial w}{\partial x}\right)^2\right]^{\frac{1}{2}} dx \tag{I-12}$$

The unit vector parallel to this deflected element can be expressed as

$$\frac{\overrightarrow{\Delta F'G'}}{\left|\overrightarrow{\Delta F'G'}\right|} = \vec{n} = \left(\left(1 + \frac{\partial u}{\partial x}\right)\vec{i} + \frac{\partial w}{\partial x}\vec{j}\right)\frac{ds}{dx} \tag{I-13}$$

where

$\frac{\partial u}{\partial x}, \frac{\partial w}{\partial x}$ are partial derivatives with respect to x. $\vec{i}$ and $\vec{j}$ are the unit vectors in the u and w directions respectively.

During the motion the length of the string changes and hence the tension in the string changes. The instantaneous value of the tension is given by

$$N = \sigma S \text{ with } \sigma = E\frac{\Delta(dx)}{dx} = E\left(\frac{ds - dx}{dx}\right)$$
$$\text{thus, } N = ES\left(\frac{ds - dx}{dx}\right) \tag{I-14}$$

where E and S are respectively the Young's modulus and cross sectional area of the beam. We consider the presence of a viscous damping of coefficient δ in the w

direction. The dynamical behaviour of the beam is therefore described by the following equations:

$$\begin{cases} m\dfrac{\partial^2 u}{\partial t^2} = \dfrac{\partial}{\partial x}\left(N\vec{n}\right)\vec{i} \\[2mm] m\dfrac{\partial^2 w}{\partial t^2} + EI\dfrac{\partial V}{\partial x} + \delta\dfrac{\partial w}{\partial t} = \dfrac{\partial}{\partial x}\left(N\vec{n}\right)\vec{j} + P(t) \end{cases} \tag{I-15}$$

where $P(t)$ is the transversal load per unit length and m the mass per unit length and V the shear force. Knowing that the relation between the bending moment (M) and the shear force is $V - \dfrac{\partial M}{\partial x} = 0$ and M=EI$\dfrac{\partial^2 w}{\partial x^2}$ where I is the moment of inertia, equation (I-15) becomes

$$\begin{cases} m\dfrac{\partial^2 u}{\partial t^2} = \dfrac{\partial}{\partial x}\left(N\vec{n}\right)\vec{i} \\[2mm] m\dfrac{\partial^2 w}{\partial t^2} + EI\dfrac{\partial^4 w}{\partial x^4} + \delta\dfrac{\partial w}{\partial t} = \dfrac{\partial}{\partial x}\left(N\vec{n}\right)\vec{j} + P(t) \end{cases} \tag{I-16}$$

Carrying out the development of $\dfrac{dx}{ds}$ up to the second order, we obtain

$$\frac{dx}{ds} = 1 - \frac{1}{2}\left(2\frac{\partial u}{\partial x} + \left(\frac{\partial u}{\partial x}\right)^2 + \left(\frac{\partial w}{\partial x}\right)^2\right) + \frac{3}{8}\left(2\frac{\partial u}{\partial x} + \left(\frac{\partial u}{\partial x}\right)^2 + \left(\frac{\partial w}{\partial x}\right)^2\right)^2 \tag{I-17}$$

Inserting equations (I-13) and (I-17) in equation (I-16), the evolution of the system is governed by the following set of equations

$$\begin{cases} m\dfrac{\partial^2 u}{\partial t^2} - ES\dfrac{\partial^2 u}{\partial x^2} = \dfrac{1}{2}ES\dfrac{\partial}{\partial x}\left[\left(\dfrac{\partial w}{\partial x}\right)^2 - 5\left(\dfrac{\partial u}{\partial x}\right)^3 - 2\left(\dfrac{\partial u}{\partial x}\right)\left(\dfrac{\partial w}{\partial x}\right)^3 - \dfrac{3}{4}\left(\left(\dfrac{\partial u}{\partial x}\right)^2 + \left(\dfrac{\partial w}{\partial x}\right)^2\right)^2 \right. \\[4mm] \qquad\qquad \left. -3\left(\dfrac{\partial \mathrm{w}}{\partial x}\right)^2\left(\left(\dfrac{\partial u}{\partial x}\right)^2 + \left(\dfrac{\partial w}{\partial x}\right)^2\right) - \dfrac{3}{4}\left(\dfrac{\partial u}{\partial x}\right)\left(\left(\dfrac{\partial u}{\partial x}\right)^2 + \left(\dfrac{\partial w}{\partial x}\right)^2\right)^2 \right] \\[4mm] m\dfrac{\partial^2 w}{\partial t^2} + EI\dfrac{\partial^4 w}{\partial x^4} + \delta\dfrac{\partial w}{\partial t} = ES\dfrac{\partial}{\partial x}\left(e\dfrac{\partial w}{\partial x}\right) + P(x,t) \end{cases} \tag{I-18}$$

where

$$e = \frac{\partial u}{\partial x} - \left(\frac{\partial u}{\partial x}\right)^2 + \frac{1}{2}\left(\frac{\partial w}{\partial x}\right)^2 - \frac{3}{2}\frac{\partial u}{\partial x}\left(\left(\frac{\partial u}{\partial x}\right)^2 + \left(\frac{\partial w}{\partial x}\right)^2\right) - \frac{3}{8}\left(\left(\frac{\partial u}{\partial x}\right)^2 + \left(\frac{\partial w}{\partial x}\right)^2\right)^2 \tag{I-19}$$

The system of equation (I-18) contains the first, second third and fourth order power of u arising from the deflection induced by the motion. Only the first order approximation of u will be considered here. This means that the transversal displacement is more important than the longitudinal one. It follows that the following assumption can be made $u=O(w^4)$. We therefore neglect the following terms u_x^2, $u_x w_x^2$, u_x^3, $u_x^2\left(u_x^2 + w_x^2\right)$ and equation (I-17) becomes

$$e = \frac{\partial u}{\partial x} + \frac{1}{2}\left(\frac{\partial w}{\partial x}\right)^2 - \frac{3}{8}\left(\frac{\partial w}{\partial x}\right)^4 \tag{I-20}$$

Then the system of equation (I-18) becomes

$$\begin{cases} m\dfrac{\partial^2 u}{\partial t^2} - ES\dfrac{\partial^2 u}{\partial x^2} = \dfrac{1}{2}ES\left(\dfrac{\partial w}{\partial x} - \dfrac{3}{2}\left(\dfrac{\partial w}{\partial x}\right)^3\right)\dfrac{\partial^2 w}{\partial x^2} \\[4mm] m\dfrac{\partial^2 w}{\partial t^2} + EI\dfrac{\partial^4 w}{\partial x^4} + \delta\dfrac{\partial w}{\partial t} = ES\dfrac{\partial}{\partial x}\left(e\dfrac{\partial w}{\partial x}\right) + P(t) \end{cases} \tag{I-21}$$

We use the following boundaries conditions:

$$u(0,t) = u(l,t) = 0 \tag{I-22}$$

This means that the boundaries do not move longitudinally. Due to the complexity of equation (I-21), approximated methods are usually employed to seek for the solutions. The appropriate approximation parameter is the radius of gyration r. Assuming that r is small enough, the longitudinal inertia $\dfrac{\partial^2 u}{\partial t^2}$ is small compared to the restoring force. Using the boundaries conditions (I-22) and after some simplification its comes the following equation

$$e = \frac{1}{2l}\int_0^l\left(\frac{\partial w}{\partial x}\right)^2 dx - \frac{3}{8l}\int_0^l\left(\frac{\partial w}{\partial x}\right)^4 dx \tag{I-23}$$

Thus the general equation governing the behaviour of the beam with articulated ends is given by

$$m\frac{\partial^2 w}{\partial t^2} + EI\frac{\partial^4 w}{\partial x^4} + \delta\frac{\partial w}{\partial t} - ES\left[\frac{1}{2l}\int_0^l\left(\frac{\partial w}{\partial x}\right)^2 dx - \frac{3}{8l}\int_0^l\left(\frac{\partial w}{\partial x}\right)^4 dx\right]\frac{\partial^2 w}{\partial x^2} = P(t) \tag{I-24}$$

We stress here the presence of the fourth order term $\dfrac{3}{8l}\int_0^l\left(\dfrac{\partial w}{\partial x}\right)^4 dx$ in the equation. Since the pioneering work of Holmes [14], investigations had always

neglected this term. Its consideration brings the sixth order non-linearity and new dynamics for the beam. Consider the following dimensionless quantities:

$$W = \frac{w}{r}, \; z = \frac{x}{L}, \; l^* = \frac{l}{L}, \; \tau = \frac{t}{L^2}\sqrt{\frac{EI}{m}}, \; F(z,\tau) = \frac{P(t)L^4}{EIr}$$

$$k = \frac{Ar^2}{I}, \; \lambda = \frac{\delta L^2}{\sqrt{mEI}}, \; k_1 = \left(\frac{r}{L}\right)^2 \; \text{and} \; r = \left(\frac{I}{A}\right)^{\frac{1}{2}}$$

where L is a reference length. The non-dimensional equation of motion is given by

$$\frac{\partial^2 W}{\partial \tau^2} + \frac{\partial^4 W}{\partial z^4} + \lambda \frac{\partial W}{\partial \tau} - k\left[\frac{1}{2l^*}\int_0^{l^*}\left(\frac{\partial W}{\partial z}\right)^2 dz - \frac{3k_1}{8l^*}\int_0^{l^*}\left(\frac{\partial W}{\partial z}\right)^4 dz\right]\frac{\partial^2 W}{\partial z^2} = F(\tau) \qquad (I\text{-}25)$$

We assume for beam simply supported boundaries conditions:

$$\begin{aligned} W(0,\tau) &= W(l^*,\tau) = 0 \\ W''(0,\tau) &= W''(l^*,\tau) = 0 \end{aligned} \qquad (I\text{-}26)$$

We assume that the external excitation $F(\tau)$ is a periodic force coinciding with the first mode of the beam. That is

$$F(\tau) = F_o \cos(\Omega\tau) \qquad (I\text{-}27a)$$

Taking into account the boundaries conditions, we set

$$W(z,\tau) = \sum_{j=1}^{n} q_j(\tau)\sin(\pi j z) \qquad (I\text{-}27b)$$

Inserting equation (I-27) in equation (I-25), multiplying the result by $\sin(\pi z)$ and performing the integration from 0 to l^*, we obtain the normalised equation given by

$$\frac{d^2 q_j}{d\tau^2} + \lambda\frac{dq_j}{d\tau} + j^2\pi^4 q_j + \frac{j^2 k\pi^4}{4}\left[\sum_{r=1}^{n} r^2 q_r - \frac{9k_1\pi^2}{16}\sum_{r=1}^{n} r^4 q_r^4\right]q_j = F_o\cos(\Omega\tau)\delta_{1j} \qquad (I\text{-}28a)$$

For the first mode of vibration, we obtain

$$\frac{d^2 q}{d\tau^2} + \lambda\frac{dq}{d\tau} + \pi^4 q + cq^3 + dq^5 = F_o\cos(\Omega\tau) \qquad (I\text{-}28b)$$

Where $\quad c = \frac{1}{4}k\pi^4 \quad$ and $\quad$ d$= -\frac{9}{64}k\pi^6 k_1$

Taking for example a single rectangular steel beam (flexural rigidity $E = 200.10^9$ N/m^2 and density $\rho = 7850$ kg/m^3) of length $l = 2m$ and section $S = 0.05x0.03m^2$, we obtain after some calculations $c = 24.3$ and $d = -0.01$. Therefore, the model

describing the single mode dynamics behaviour of the non-linear beam with articulated ends is that of a particle moving in a catastrophic single well ϕ^6 potential. The same equation has been obtained by Tchoukuegno [15].

II-3 Elastic beam fixed at its base and free at the top

Figure I-6, shows an elastic beam fixed at its base, subjected to a transversal load. The beam is presumed to be a slender, isotropic, uniform rod whose bending moment depends linearly on the curvature. We encounter these types of structures in many areas such as flexible plants (wheat, tree [8,10]), telecommunication antennas and musical instruments like diapason. In engineering, it also describes a model for tall buildings [16,17], thin poles (used as pole vaulting for example) and many other structures in building construction and mechanical engineering.

When forces are applied transversally to the beam, it bends. Consider y as the lateral displacement of the center line and x its vertical location, the bending moment due to the couple is given by [18]

$$M = \frac{EI}{R} \text{ where } \frac{1}{R} = \frac{\dfrac{d^2 y}{dx^2}}{\left(1 + \left(\dfrac{dy}{dx}\right)^2\right)^{3/2}} \tag{I-29}$$

R being the radius of curvature and *EI* the flexural rigidity. Since that the moment varies from one point to another, there also exists a shear force which is added to the parallel forces to the *x* axis. Let V be that shear force in a section of the beam, knowing that the different forces acting in this section lead to a dynamical equilibrium, we obtain the following relation:

$$T + \frac{\partial M}{\partial x} = 0 \tag{I-30}$$

Let us assume now that the forces of volume exist (for example inertia forces). If G is the resultant volume forces per unit length of the beam, then at the equilibrium, we have

$$G + \frac{\partial T}{\partial x} = 0 \tag{I-31}$$
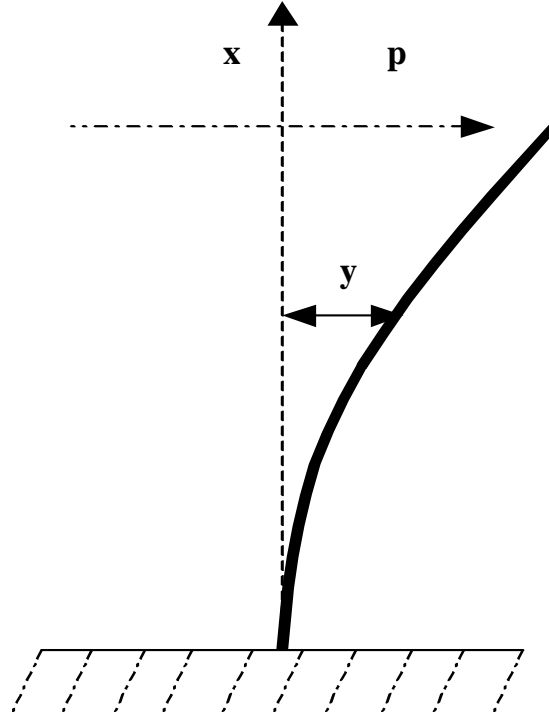
Figure I-6: Elastic beam

If that volume forces are only due to the inertia, G will be defined by

$$G = -\rho S \frac{\partial^2 y}{\partial t^2}$$

(I-32)

Where ρ is the density and S the section area of the beam. Consequently the equilibrium equation is given by:

$$\rho S \frac{\partial^2 y}{\partial t^2} = \frac{\partial T}{\partial x}$$

(I-33)

Inserting equation (I-30) into equation (I-33) it leads to

$$\rho S \frac{\partial^2 y}{\partial t^2} + \frac{\partial^2 M}{\partial x^2} = 0$$

(I-34)

Considering the expression of M given by equation (I-29), we arrive at the following equation:

$$\rho S \frac{\partial^2 y}{\partial t^2} + EI \frac{\partial^2}{\partial x^2}\left(\frac{1}{R}\right) = 0$$

(I-35)

We obtain here a general equation governing the transversal vibration of a prismatic bar. In an attempt to go closer to reality and knowing that at the

elasticity limit the gradient $\dfrac{\partial y}{\partial x} \lll 1$, we carry out the expansion of $\dfrac{1}{R}$ up to the fourth order. This leads us to

$$\rho S \frac{\partial^2 y}{\partial t^2} + EI \frac{\partial^2}{\partial x^2}\left[\frac{\partial^2 y}{\partial x^2}\left(1 - \frac{3}{2}\left(\frac{\partial y}{\partial x}\right)^2 + \frac{5}{8}\left(\frac{\partial y}{\partial x}\right)^4\right)\right] = 0 \qquad (I\text{-}36)$$

When we neglect the non-linear terms, we obtain the well-known linear equation given by [16,19]

$$\rho S \frac{\partial^2 y}{\partial t^2} + EI \frac{\partial^4 y}{\partial x^4} = 0 \qquad (I\text{-}37)$$

When the external excitation is large, the equation with non-linear terms can permit us to foresee the behaviour of the structure. Taking into account the dissipation and the external excitation, we obtain

$$\rho S \frac{\partial^2 y}{\partial t^2} + \delta \frac{\partial y}{\partial t} + EI \frac{\partial^2}{\partial x}\left[\frac{\partial^2 y}{\partial x^2}\left(1 - \frac{3}{2}\left(\frac{\partial y}{\partial x}\right)^2 + \frac{5}{8}\left(\frac{\partial y}{\partial x}\right)^4\right)\right] = P(t) \qquad (I\text{-}38)$$

where δ is the damping coefficient and $P(t)$ the external excitation per unit length. Looking now the equation of a single mode dynamics, we can express y in the form

$$y = X_n(x)Q_n(t) \qquad (I\text{-}39)$$

where X_n is the solution of the eigen value problem obtained by solving equation (I-37) the linear equation without damping excitation. $q_n(t)$ is the amplitude of the nth mode and its dynamical equation is obtained by inserting equation (I-39) into equation (I-38). Considering the case of our model as presented above, the boundary conditions are given as follows:

$$\left. \begin{array}{l} y(x=0,t)=0 \;\; ; \;\; \left(\dfrac{\partial y}{\partial x}\right)_{x=0} = 0 \\[2mm] M(x=l,t)=0 \;\; ; \;\; \left(\dfrac{\partial^3 y}{\partial x^3}\right)_{x=l} = 0 \end{array} \right\} \; 0 \le t \le \infty \qquad (I\text{-}40)$$

and $X_n(x)$ is given by

$$X_n(x) = -\frac{\sin(k_n l) + \sinh(k_n l)}{\cos(k_n l) + \cosh(k_n l)}\left[\cos(k_n x) - \cosh(k_n x)\right] + \left[\sin(k_n x) - \sinh(k_n x)\right] \quad (I\text{-}41)$$

where k_n is the solution of the transcendental equation $\cos(k_n l)\cosh(k_n l) = -1$ [16,19]. Here we will consider only the first mode of vibrations on which the major part of the energy is concentrated. Assuming that the frequency of the external excitation is close to that of natural vibration of the first mode, we thus insert equation (I-41) and equation (I-39) for *n=1* (according to [19], $k_1 = \dfrac{1.875}{l}$) into equation (I-38). Multiplying the result and performing the integral from 0 to l (l is the length of the beam), we obtain

$$\frac{d^2 q}{d\tau^2} + \lambda \frac{dq}{d\tau} + q + cq^3 + dq^5 = f(\tau) \tag{I-42}$$

where $q = \dfrac{Q}{L}$; $\tau = \omega_0 t$; $\delta = \dfrac{\delta}{\rho S \omega_0}$; $\omega_0^2 = \dfrac{EIk_1^4}{\rho S}$; $c = 0.2k_1^2 L^2$; $d = -0.7k_1^4 L^4$ and $f(\tau) = \dfrac{p(t)}{\rho S L \omega_0^2}$

$$\tag{I-43}$$

L is a reference length. Considering the case of a metallic beam with section $S=0.015m^2$, length *l=2meter* and reference length *L=1meter,* we obtain $c = 0.17$ and $d = -0.54$. We thus arrive at a ϕ^6 model with monostable catastrophic potential which has an advantage not only to describe well the behaviour of large amplitude dynamics, but also helps to derive the critical load leading the rupture of the structure.

III-DYNAMICS OF UNBOUNDED ϕ^6 MONOSTABLE MECHANICAL STRUCTURES UNDER ANHARMONIC EXCITATION

III-1 Condition for escape from a potential well

The equation of motion of the mechanical system as presented above under periodic force can be written as

$$\frac{d^2 q}{d\tau^2} + \lambda \frac{dq}{d\tau} + \omega_0^2 q + cq^3 + dq^5 = f_0 \cos(\Omega \tau) \tag{I-44}$$

We remind that the following parameters are used corresponding to $\lambda = 0.009$, $\omega_0^2 = 0.92$, $c = 0.013$ and $d = -0.0008$. In this section we deal with the frontier

in the (Ω, f_0) plane, which separates two types of motion. Indeed, depending on the value of f_0 and Ω, the structure initially moving inside the potential well can escape to an unbounded motion. It is important to analyse the condition on the parameters of the equation where unbounded (catastrophic) motions appear. For this purpose, according to Virgin *et al* [20] , the best criterion to obtain the escape from a potential well is the condition $E_{max} \geq V_c$ (E_{max} being the maximum of the total energy and V_c the potential energy at the nearest unstable equilibrium point) instead of the condition that stipulates that the maximum displacement should reach the nearest unstable equilibrium state. The total energy of the system can be written as follows:

$$E = \frac{1}{2}\dot{q}^2 + \frac{1}{2}\omega_0^2 q^2 + \frac{1}{4}cq^4 + \frac{1}{6}dq^6 \qquad (I\text{-}45)$$

We consider the symmetrical oscillation around the point *(0,0)* .

For this aim we set

$$q(t) = A\cos(\Omega\tau + \varphi) \qquad (I\text{-}46)$$

where *A* is the amplitude of the oscillation and φ is the phase between the output *q(t)* and the excitation. Inserting equation (I-46) into equation (I-44) and equating the coefficients of $\cos(\Omega\tau)$ and $\sin(\Omega\tau)$ separately to zero (assuming that the terms due to higher frequencies can be neglected), we obtain

$$\begin{cases} \left(\omega_0^2 - \Omega^2 + \frac{3}{4}cA^2 + \frac{5}{8}dA^4\right)A\cos\varphi - \lambda\Omega A\sin\varphi = f_0 \\ -\lambda\Omega A\cos\varphi - \left(\omega_0^2 - \Omega^2 + \frac{3}{4}cA^2 + \frac{5}{8}dA^4\right)A\sin\varphi = 0 \end{cases} \qquad (I\text{-}47)$$

After some algebraic manipulations, it comes that the amplitude A satisfies the 10 th-order algebraic equation given by

$$\frac{25}{64}d^2 A^{10} + \frac{15}{16}cdA^8 + \left[\frac{9}{16}c^2 + \frac{5}{4}d\left(\omega_0^2 - \Omega^2\right)\right]A^6 + \frac{3}{2}c\left(\omega_0^2 - \Omega^2\right)A^4 + \left(\omega_0^2 - \Omega^2 - \lambda^2\Omega^2\right)A^2 = f_0^2$$
$$(I\text{-}48)$$

Now inserting equation (I-46) into (I-45) and after some mathematical transformations, the maximum energy of the system is given by

$$E_{max} = \frac{1}{2} A^2 \Omega^2 + \frac{1}{2}\left(\omega_0^2 - \Omega^2\right) X_m + \frac{1}{4} c X_m^2 + \frac{1}{6} d X_m^3$$

where $X_m = \dfrac{\left(-c - \sqrt{c^2 - 4d\left(\omega_0^2 - \Omega^2\right)}\right)}{2d}$ (I-49)

The potential energy at the nearest unstable equilibrium state

$q_c = \pm\left(\dfrac{-c - \sqrt{c^2 - 4d\omega_0^2}}{2d}\right)^{1/2}$ (see figure I-3a) is

$$V_c = \frac{1}{2}\omega_0^2 q_c^2 + \frac{1}{4} c q_c^4 + \frac{1}{6} d q_c^6 \tag{I-50}$$

At this position, the following equality is satisfied:

$E_{max} = V_c$ (I-51)

Considering equation (I-49) along with (I-50) and (I-51), it comes that the amplitude of motion at the frontier separating bounded from unbounded motions is given as follows:

$$A_b = \left(\frac{2V_c - \left(\omega_0^2 - \Omega^2\right) X_m - \frac{1}{2} c X_m^2 - \frac{1}{3} d X_m^3}{\Omega^2}\right)^{1/2} \tag{I-52}$$

Inserting equation (I-52) into equation (I-48), we find that the amplitude of the excitation at the frontier between the bounded and unbounded motions is given by

$$f_0^2 = \left(\left(\omega_0^2 - \Omega^2\right) A_b + \frac{3}{4} c A_b^3 + \frac{5}{8} d A_b^5\right)^2 + \left(\lambda \Omega A_b\right)^2 \tag{I-53}$$

In figure (I-7), we have plotted the variation of the critical forcing as a function of the external frequency. We also use a direct numerical simulation of equation (I-44) to determine the frontier between bounded and unbounded motions. The result is presented in the same figure. For each curve, the range where the bounded motion is obtained is below the curve. The minimum critical forcing amplitude is $f_c=0.27$ at $\Omega = 0.94$ (this means $f_c=65.34$ *N.m/rad* in the dimensional form), which is associate with a primary resonance. Dips in the curve near forcing frequency of one-half, one third, one fourth, one-fifth and one-sixth of Ω may be related to superharmonic resonances and the dip near twice that frequency may be related to subharmonic resonances. For most forcing frequency Ω the

approximate critical forces are smaller than that those obtained by analytical calculation.
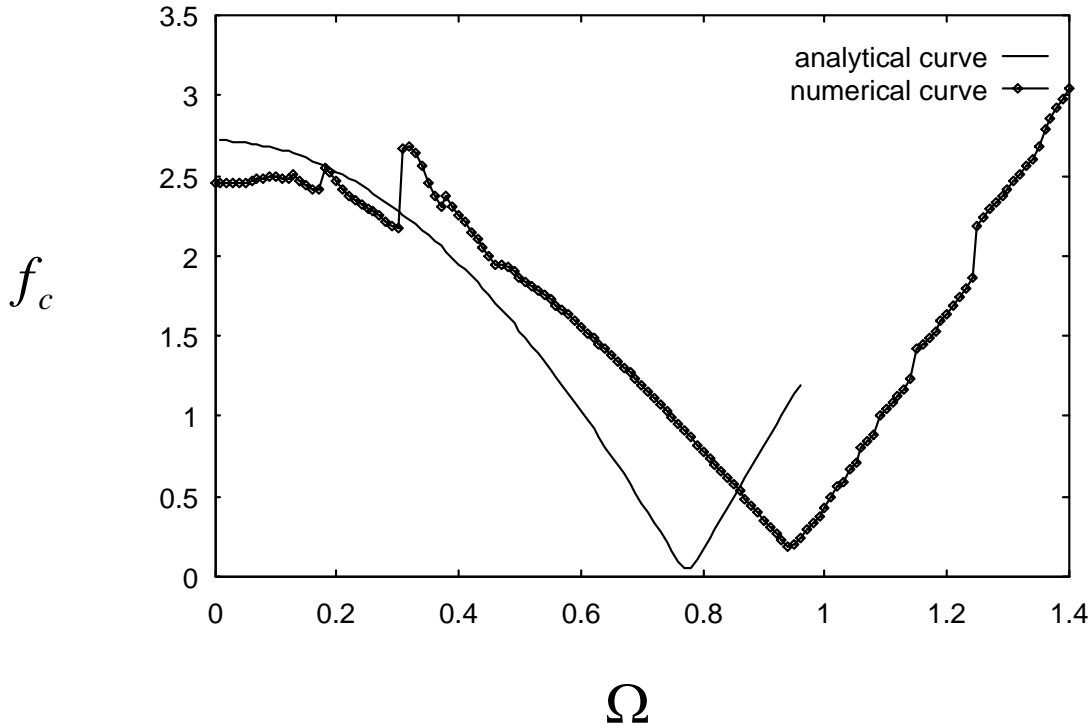
Figure I-7: Escape boundary

III-2 Melnikov criteria for chaos

In this section, we are interested in the study of global bifurcation before and after loss of stability [18,22]. Since these bifurcations can be detected analytically, it is important to obtain the condition for theoretically preventing chaotic dynamics. In view of deriving the condition for the appearance of chaos, we use the Melnikov method. It helps to define the condition for the existence of the so-called transverse intersection points in the sense of Poincaré maps. This may imply the existence of fractal basin boundaries and thus the so-called horseshoes structure of chaos.

Consider the generalised dynamical equation of a given system written in vector form as

$$\dot{U} = g_0(U) + \varepsilon g_p(U,t) \tag{I-54}$$

where $U(q,p),(p=\dot{q})$ is the state vector, $g_0 = (g_1, g_2)$ is the vector field defined as

$$g_1 = \frac{\partial H_0}{\partial \dot{q}} \text{ and } g_2 = -\frac{\partial H_0}{\partial q} \tag{I-55}$$

where H_0 is the Hamiltonian and g_p is a periodic perturbation function. In our model, we have

$$g_0(U) = \left(p, -\omega_0^2 q - cq^3 - dq^5\right) \text{ and } g_p(U,t) = \left(0, -\lambda p + f_0 \cos(\Omega t)\right) \tag{I-56}$$

Let us assume that the unperturbed Hamiltonian system possesses saddle points connected by a separatrix or heteroclinic orbit $u_0(t)$. In the presence of the perturbation $g_p(U,t)$, the orbit is perturbed. When the perturbed and the unperturbed manifolds intersect transversally, the geometry of the basin of attraction may become fractal, indicating the high sensitivity to initial conditions, thus chaos. The Melnikov theorem which gives the condition for the fractal basin boundary can be given as follows [22]. Let the Melnikov's function be defined as

$$M_e(t_0) = \int_{-\infty}^{+\infty} g_0\left(\overline{u}(t)\right) \wedge g_p\left(\overline{u}(t), t + t_0\right) \text{ with } -\infty \prec t \prec +\infty \tag{I-57}$$

If $M_e(t_0)$ has simple zeros so that for a given $t_0 \neq 0$, one has $M_e(t_0)=0$ with $\dfrac{dH(t_0)}{dt_0} \neq 0$ at $t = t_0$ (condition for transversal intersection), then the system (I-54) can present fractal basin boundaries for motions around the stable equilibrium point.

To apply the Melnikov theorem to our model, we first derive the equation for the heteroclinic orbit. The Hamiltonian of the system is defined by

$$H_0(q, \dot{q} = p) = \frac{1}{2}p^2 + \frac{1}{2}bq^2 + \frac{1}{4}cq^4 + \frac{1}{6}dq^6 \tag{I-58}$$

Making use of integrals tables [23] (see also Ref. [17]), we obtain the heteroclinic orbit (connecting the unstable points $-q_c$ and q_c) given by

$$q_0 = \frac{\pm X\xi \sinh(Y\tau)}{\sqrt{2}\left(1 + \left(1 - \xi^2\right)\sinh^2(Y\tau)\right)^{\frac{1}{2}}}$$

$$p_0 = \frac{\pm X\xi Y \cosh(Y\tau)}{\sqrt{2}\left(1 + \left(1 - \xi^2\right)\sinh^2(Y\tau)\right)^{\frac{3}{2}}} \tag{I-59}$$

where

$$X^2 = q_1^2\left(3 + H^2\right), \ Y = q_1^2 H\left(\frac{-d}{2}\left(H^2 + 1\right)\right)^{\frac{1}{2}}, \ \xi = H\sqrt{\frac{2}{3\left(H^2 + 1\right)}}, \ \mathrm{H} = \frac{q_2}{q_1}$$

$$q_1^2 = \frac{-c - \sqrt{c^2 - 4d\omega_0^2}}{2d}, \ q_2^2 = \frac{c - \sqrt{c^2 - 4d\omega_0^2}}{2d}$$

After calculating the Melnikov function, the condition for chaos is

$$f_0 \geq f_c = \frac{Y^2 X \lambda \left(1 - \xi^2\right) \sinh\left(\frac{\Omega \pi}{2Y}\right)}{8\xi\Omega\pi} \left[\frac{3\xi^2 - 1}{1 - \xi^2} + \frac{\left(1 + 3\xi^2\right)}{2\xi} \ln\left(\frac{1 + \xi}{1 - \xi}\right)\right] \tag{I-60}$$

This condition is depicted in Figure (I-8) in the (Ω, f_0) plane along with the escape boundary. The chaotic behaviour occurs in the domain above the curve (thick line).
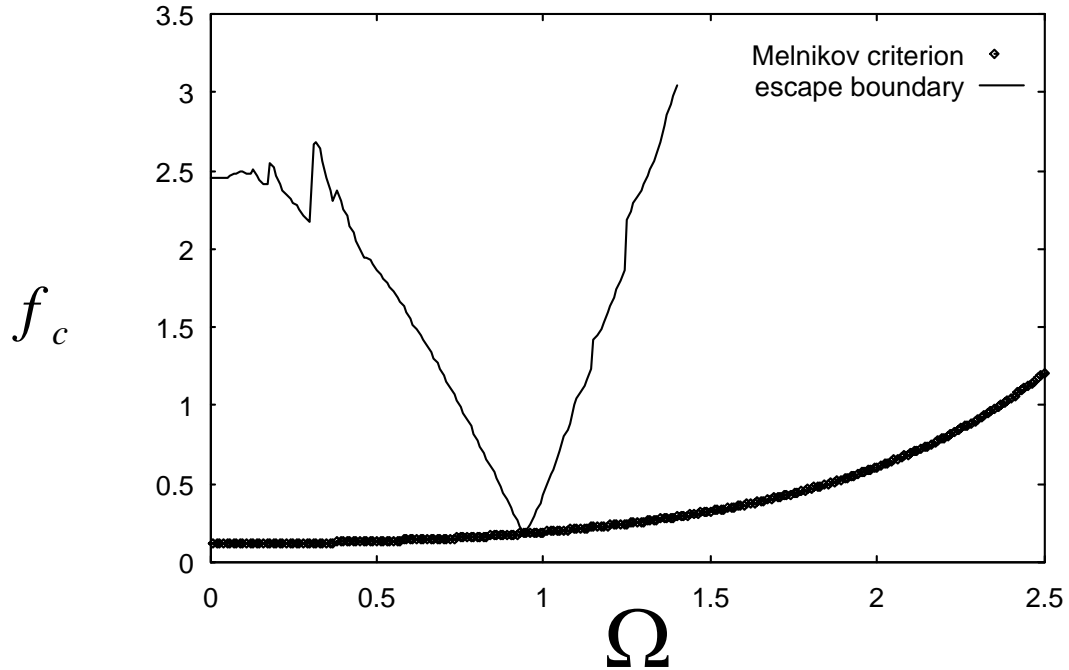

Figure I-8 : Melnikov criterion for the appearance of chaos

It appears in these curves that for certain value of amplitude and frequency of external excitation for which the behaviour are bounded, one can lead to transverse intersection of heteroclinic orbit and at the primary resonant the state the frontier a given by the same values. A particular characteristic of the Melnikov chaos is the fractality of the basin of attraction and the resulting unpredictability due to the dependence on initial conditions. This characteristic has also been analysed here to confirm the validity of our results by performing a scan of the initial condition in the (q_0, p_0) plane for various values of f_0. We find that when the amplitude of the external excitation is less than the critical value, the basins of attraction (marked region) are regular (see figure I-9). For instance in the case of figure I-10a, the basin of attraction presents the classical shape, this implies the non-existence of chaos. As the amplitude of the excitation increases, the regular shape of the basins

of attraction is destroyed and the fractal behaviour becomes more and more visible. (see figures I-9b and I-9c). f_0 increases, the smooth basin boundary first generates small tails (figure I-9b) and finally develops fingers (figure I-9c) , a scenario well known in the case of a ϕ^4 potential with a single well [24].
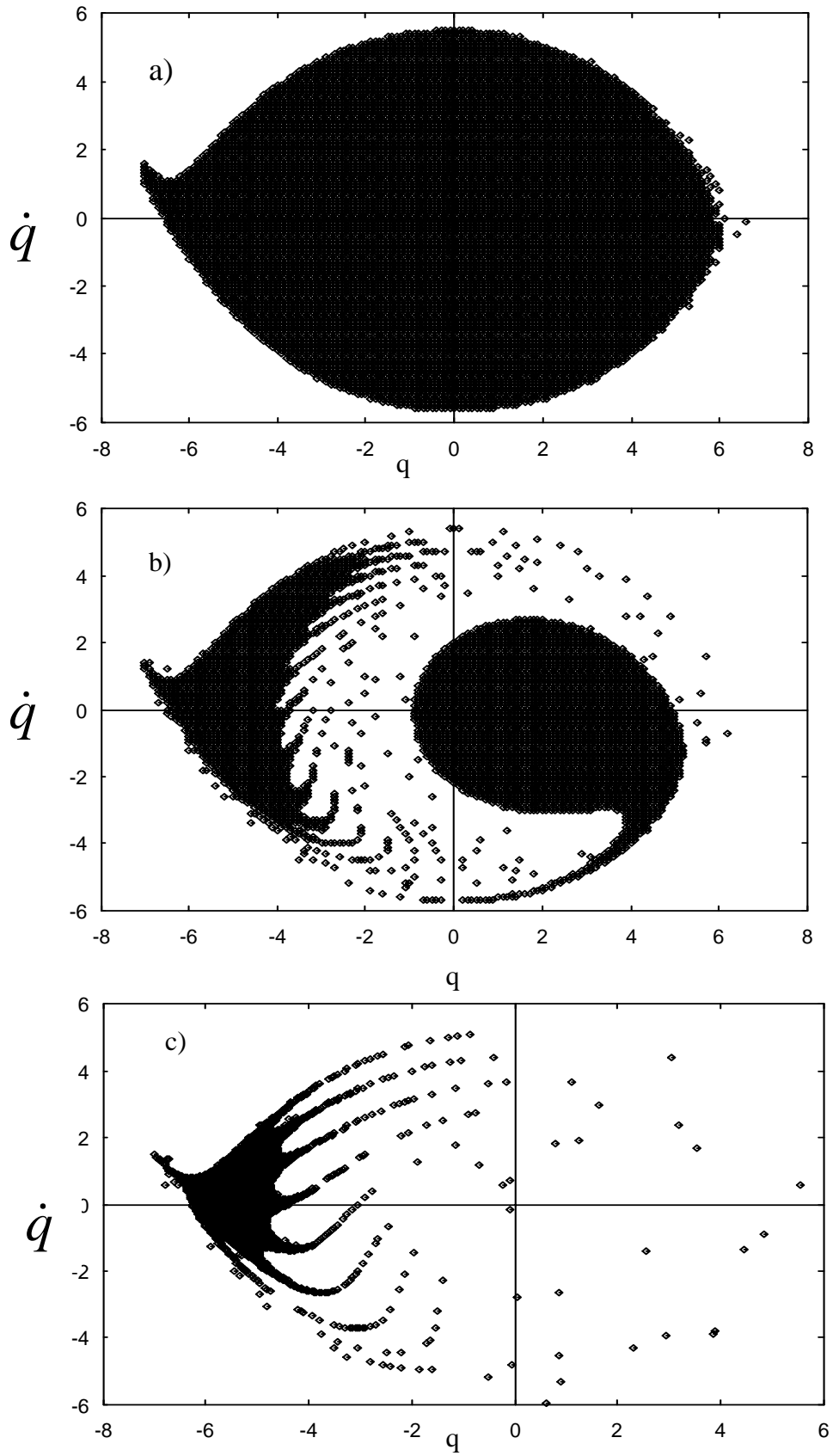
Figure I-9: Basins of attraction for motions around *q=0* with
$\Omega = 0.92$ a) $f_0 = 0.11$; b) $f_0 = 0.25$; c) $f_0 = 0.5$

IV-CONCLUSION

In this chapter, the modelling and dangerous motion of mechanical structures with a catastrophic monostable ϕ^6 potential subjected to a sinusoidal additive excitation have been analysed. It has been shown that the mathematical model of various non-linear structures (inverted pendulum, articulated beam, elastic beam fixed at its base and free at the top) is that of a particle moving in a catastrophic single well ϕ^6 potential. This model seems to be more realistic compared to that described by the classical Duffing oscillator as presented earlier. The conditions for escape from a potential well are obtained. The criteria for the appearance of horseshoes chaos have also been derived using the Melnikov theory. The analytical results have been complemented by the numerical simulation of the original non-linear equation and metamorphoses of the basin of attraction have been observed.

In the next chapter, we will analyse the effects of an active control of the dynamics of structures both in the regular regime (reducing the amplitude of the oscillations and controlling the escape from the potential well) and in the chaotic regime (avoiding Melnikov chaos).

REFERENCES

[1]- J. J. Stokker, "Non-linear vibrations", interscience, New York, 1950.

[2]- C. Hayashi, "Non-linear oscillations in physical systems", McGraw-Hill, New York, 1964.

[3]- A. H. Nayfey, D. T. Mook, "Non-linear oscillations", Wiley,New York, 1979.

[4]- J.M.Thompson, H.B. Stewart, "Non-linear dynamics and chaos", wiley, New York, 1986.

[5]- F. C. Moon, "Chaotic and fractal dynamics", Wiley, New York, 1992.

[6]-P. Woafo, J. C. Chedjou, H. B. Fotsin, Phys. Rev. E 54 (1996) 5929.

[7]-J. C. Chedjou, H. B. Fotsin, P. Woafo, Physica. Scripta 55 (1997) 390.

[8]- J. J. Finnigan, P. J. Mulhear, Boundary-Layer Meteorology 14 (1978) 415.

[9]- T. K. Flesh, R. H. Grant, Boundary-Layer Meteorology 55 (1991) 161.

[10]- B. A. Gardiner, Forestry commission, Edinburg (1989) 1.

[11]- S. Barnett, R. G. Cameron, "Introduction to mathematical control theory", Clarendon Press, Oxford, 1985.

[12]- S. Datta, J. K. Bhattacharjee, Phys. Lett. A 283 (2001) 323.

[13]- M. Debnath, A. R. Chawdhury, Phys. Rev A 44 (1991) 1049.

[14]- P. Holmes, Philos-trans. R. soc. London ser 282(1979)419.

[15]- R. Tchoukuegno, "Dynamique et Contrôle des Vibrations des Poutres Modélisées par le Potentiel ϕ^6 tristable et bistable catastrophique" Ph.D Thesis, University of Yaoundé I, Cameroun, 2003.

[16]- S. P. Timoshenko,"Theorie de la Stabilité Elastique", Paris Dunod, 1966.

[17]- S. Lenci, G. Menditto, A. M. Tarantino, Int. J. of. Non-linear. Mech. 34 (1999) 615

[18]- M. Soutif, "Vibration, propagation, diffusion", Dunod, Paris, 1970.

[19]- H. Favre, "Cours de Mécanique", Paris, Dunod, 1949.

[20]- L. N. Virgin, R. H. Plaut, C. Cheng, Int. J. Non-linear Mech.27 (1992) 357.

[21]- R. Tchoukuegno, P. Woafo, Physica D 167 (2002) 86.

[22]- V. K. Melnikov, Trans, Moskow Math. Soc.12 (1963) 1.

[23]- I. S. Gradshteyn, I. M. Ryzhik, "Table of Integrals, Series and Products", 4th Edition, Academic, New York, 1975.

[24]- A. H. D. Cheng, C. Y. Yang, K. Hackl, M. J. Chajes, Int. J. of Non-linear Mech. 28 (1993) 549.

CHAPTER II:
CONTROL BY SANDWICH AND WITH PIEZOELECTRIC
ABSORBER OF THE DYNAMICS OF UNBOUNDED
MONOSTABLE MECHANICAL STRUCTURES WITH
ϕ^6 POTENTIAL

<div style="border:1px solid black; padding:10px;">

CHAPTER II: CONTROL BY SANDWICH AND WITH PIEZOELECTRIC ABSORBER OF THE DYNAMICS OF UNBOUNDED MONOSTABLE MECHANICAL STRUCTURES WITH ϕ^6 POTENTIAL

</div>

I-INTRODUCTION

In structural engineering, one of the constant challenges is to find new and better means of protecting constructed structures from damaging effects of destructive environmental forces. One avenue opened to researchers and designers is to introduce more conservative design so that structures such as buildings and bridges are better able to cope with large external loads. However, this approach can be untenable both technologically and economically. Another possible approach is to make structures behave more like machines, aircraft, or human beings in the sense that they can be made adaptive or responsive to external forces [1].

In this line, we begin by focussing our attention to the non-linear structures coupled in a sandwich manner with the linear structures. The linear one serves as a control element used to reduce the amplitude of vibration of the non-linear one. In reference [2], Aida *et al.* proposed a plate type dynamics vibration absorber to control the vibration of plates and in reference [3], they also used the beam type dynamic vibration absorber to control the bending vibration of a beam. In these cases, the beams (or plates) are assumed to be in the linear dynamics. So, there is a need to investigate the induced geometrically non-linear effects on static and dynamic characteristics of structures in order to accurately design and effectively control them.

Secondly, in the development of intelligent structures systems, piezoelectric materials are widely used as sensors and actuators for the monitoring and control of structures and mechanical systems [4]. In references [5,6], it has been shown by the authors that piezoelectric materials can be used as passive electromechanical vibration absorbers by shunting them with electrical networks.

The chapter is organised as follows. In section two, we deal with the control models both in the case of sandwich and piezoelectric control and the establishment of the resulting equations of motion is also presented. Section three is devoted to the optimisation of the control design. Firstly we analyse the stability of the system under control and we determine the range of the control parameters that can conveniently reduce the amplitude of vibration. Secondly, we emphasise on the external excitation that can produce the catastrophic failure of the structure or escape from a potential well ([7] and chapter I). In section four, derivation and analysis of the conditions for the appearance of Melnikov chaos as well as the effects of the parameters of the active control strategy on chaotic motions are carried out . Section five summarises the chapter.

II-MODELLING OF THE DYNAMICS OF MECHANICAL STRUCTURES UNDER CONTROL

II-1 Control by sandwich

II-1-1 Case of an articulated beam

To control the bending vibration of this structure, we couple it in a sandwich manner to a linear beam-type dynamic vibration absorber as in references [2,3]. This consists of a dynamic absorbing beam with the same boundaries conditions (figure II-1). In this case, the sandwich component can be a polymer or a fluid.
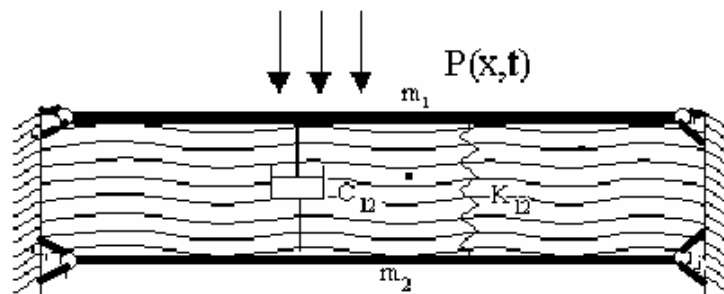

Figure II-1: Beams with sandwich coupling

The equations governing the motion of these two structures are given by

$$\begin{cases} m_1 \frac{\partial^2 w_1}{\partial t^2} + E_1 I_1 \frac{\partial^4 w_1}{\partial x^4} + \delta_1 \frac{\partial w_1}{\partial t} - E_1 A_1 \left[\frac{1}{2l} \int_0^l \left(\frac{\partial w_1}{\partial x} \right)^2 dx - \frac{3}{8l} \int_0^l \left(\frac{\partial w_1}{\partial x} \right)^4 dx \right] \frac{\partial^2 w_1}{\partial x^2} \\ \qquad + k_{12}(w_1 - w_2) + C_{12} \left(\frac{\partial w_1}{\partial t} - \frac{\partial w_2}{\partial t} \right) = P(x,t) \\ m_2 \frac{\partial^2 w_2}{\partial t^2} + E_2 I_2 \frac{\partial^4 w_2}{\partial x^4} + \delta_2 \frac{\partial w_2}{\partial t} + k_{12}(w_2 - w_1) + C_{12} \left(\frac{\partial w_2}{\partial t} - \frac{\partial w_1}{\partial t} \right) = 0 \end{cases} \tag{II-1}$$

where E_i, I_i, m_i and δ_i (i=1,2) are respectively the Young's modulus, the moment of inertia, the mass per unit length and the transversal damping coefficient of the beams. C_{12} and k_{12} are respectively the viscous damping and the stiffness coefficients due to the coupling.

In non-dimensional form, equations (II-1) take the form

$$\begin{cases} \frac{\partial^2 W_1}{\partial \tau^2} + \frac{\partial^4 W_1}{\partial z^4} + \lambda_1 \frac{\partial W_1}{\partial \tau} - k \left[\frac{1}{2l^*} \int_0^{l^*} \left(\frac{\partial W_1}{\partial z} \right)^2 dz - \frac{3k_1}{8l^*} \int_0^{l^*} \left(\frac{\partial W_1}{\partial z} \right)^4 dz \right] \frac{\partial^2 W_1}{\partial z^2} \\ \qquad + \beta(W_1 - W_2) + \alpha \left(\frac{\partial W_1}{\partial \tau} - \frac{\partial W_2}{\partial \tau} \right) = F(z,\tau) \\ \frac{\partial^2 W_2}{\partial \tau^2} + a \frac{\partial^4 W_2}{\partial z^4} + \lambda_2 \frac{\partial W_2}{\partial \tau} + \mu\beta(W_2 - W_1) + \mu\alpha \left(\frac{\partial W_2}{\partial \tau} - \frac{\partial W_1}{\partial \tau} \right) = 0 \end{cases} \tag{II-2}$$

where

$$W_i = \frac{w_i}{r}, z = \frac{x}{L}, l^* = \frac{l}{L}, \tau = \frac{t}{L^2}\sqrt{\frac{E_1 I_1}{m_1}}, F(z,\tau) = \frac{P(x,t)L^4}{E_1 I_1 r}, a = \frac{m_1 E_2 I_2}{m_2 E_1 I_1}, \alpha = \frac{C_{12}L^2}{\sqrt{m_1 E_1 I_1}}$$

$$k = \frac{A_1 r^2}{I_1}, \lambda_1 = \frac{\delta_1 L^2}{\sqrt{m_1 E_1 I_1}}, \lambda_2 = \frac{\mu\delta_2 L^2}{\sqrt{m_1 E_1 I_1}}, r = \left(\frac{I_1}{A_1} \right)^{\frac{1}{2}}, k_1 = \left(\frac{r}{L} \right)^2, \mu = \frac{m_1}{m_2}, \beta = \frac{k_{12}L^4}{E_1 I_1}$$

We assume for both beams simply supported boundaries conditions:

$$W_i(0,\tau) = W_i(l^*,\tau) = 0 \tag{II-3a}$$

$$W_i''(0,\tau) = W_i''(l^*,\tau) = 0 \tag{II-3b}$$

We also assume that the force $F(\tau)$ is a periodic force coinciding with the first mode of the beam and that its time dependence is also sinusoidal (see chapter I, equation (I-23a)). Taking into account the boundaries conditions, we set

$$W_1(z,\tau) = \sum_{j=1}^n q_j(\tau) \sin(\pi j z) \tag{II-4a}$$

$$W_2(z,\tau) = \sum_{j=1}^{n} y_j(\tau)\sin(\pi jz) \tag{II-4b}$$

Inserting equation (II-4) in equation (II-3) and making the same analysis as presented in chapter I, we obtain

$$\begin{cases} \dfrac{d^2q_j}{d\tau^2} + \lambda_1\dfrac{dq_j}{d\tau} + j\pi^4 q_j + \dfrac{k\pi^4}{4}\left[\sum_{r=1}^{n} r^2 q_r^2 - \dfrac{9k_1\pi^2}{16}\sum_{r=1}^{n} r^4 q_r^4\right]q_j \\ \qquad\qquad + \beta(q_j - y_j) + \alpha\left(\dfrac{dq_j}{d\tau} - \dfrac{dy_j}{d\tau}\right) = F_o\cos(\Omega\tau)\delta_{1j} \\ \dfrac{d^2y_j}{d\tau^2} + \lambda_2\dfrac{dy_j}{d\tau} + a\pi^4 y_j + \mu\beta(y_j - q_j) + \mu\alpha\left(\dfrac{dy_j}{d\tau} - \dfrac{dq_j}{d\tau}\right) = 0 \end{cases} \tag{II-5}$$

For the first mode of vibration (*j=1*) we have

$$\begin{cases} \dfrac{d^2q}{d\tau^2} + (\lambda_1 + \alpha)\dfrac{dq}{d\tau} + (\pi^4 + \beta)q + cq^3 + dq^5 - \beta y - \alpha\dfrac{dy}{d\tau} = F_o\cos(\Omega\tau) \\ \dfrac{d^2y}{d\tau^2} + (\lambda_2 + \mu\alpha)\dfrac{dy}{d\tau} + (a\pi^4 + \mu\beta)y - \mu\left(\beta q + \alpha\dfrac{dq}{d\tau}\right) = 0 \end{cases} \tag{II-6}$$

where

$$c = \frac{1}{4}k\pi^4 \quad \text{and} \quad d = -\frac{9}{64}k\pi^6 k_1$$

Here $q=q_1$ and $y=y_1$ (we restrict the analysis on the first modes where the main part of the energy of the system is distributed (see Reference [9, 13]) and chapter I).It is noted that the mass of the controller is greater than the mass of the structure. Taking into account this consideration, the amplitude of vibration of the controller will be small so that the non-linear effect can be neglected, thus the controller will present a linear dynamics.

II-1-2 Case of an inverted pendulum

The inverted pendulum as presented in chapter I (figure I-2), is now tied to another homogeneous pendulum of mass m_2 larger than the mass m_1 $(m_2 \ggg m_1)$ with the mediation of a dissipative and elastic structures (see figure II-2). The damping coefficient of the coupling structure is denoted by C_{12} and the stiffness coefficient by k_{12}. The elastic beam free at the top and fixed at its base can also be subjected to such type of control (see figure II-3). Let us give the equations in the case of an inverted pendulum.
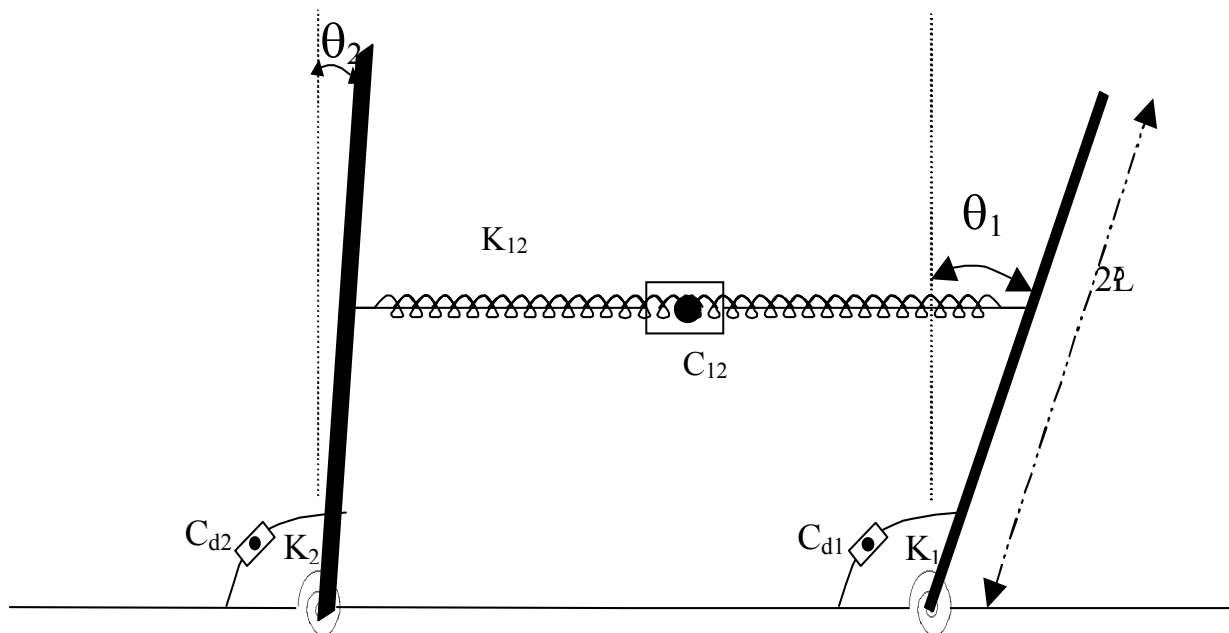
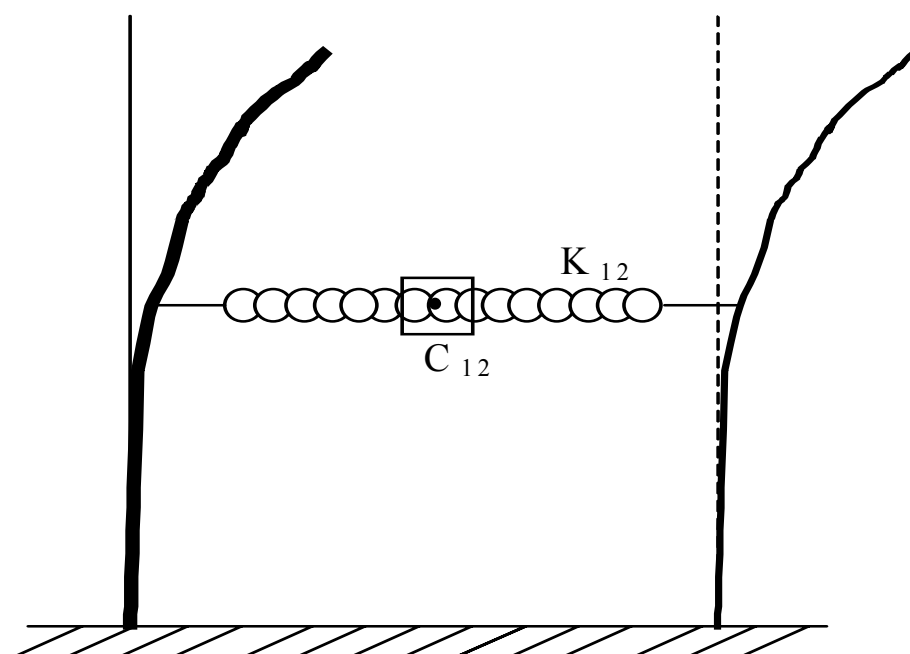**Figure II-2 :** Inverted pendulums with dissipative and elastic coupling

Figure II-3 : Elastic beam under sandwich control

When the system is excited, the energies brought to play are :

-Kinetic energy of the system

$$T = \frac{1}{2}m_1 l^2 \left(\frac{d\theta_1}{dt}\right)^2 + \frac{1}{2}m_2 l^2 \left(\frac{d\theta_2}{dt}\right)^2 \qquad \text{(II-7a)}$$

-Potential energy of the system

$$V = \frac{1}{2}k_1 l^2 \theta_1^2 + \frac{1}{2}k_2 l^2 \theta_2^2 + \frac{1}{2}k_{12} l^2 (\theta_1 - \theta_2)^2 + m_1 gl \cos(\theta_1) + m_2 gl \cos(\theta_2) \qquad \text{(II-7b)}$$

-Dissipation energy of the system

$$F_d = \frac{1}{2}C_{d_1} l^2 \left(\frac{d\theta_1}{dt}\right)^2 + \frac{1}{2}C_{d_2} l^2 \left(\frac{d\theta_2}{dt}\right)^2 + \frac{1}{2}C_{12} l^2 \left(\frac{d\theta_1}{dt} - \frac{d\theta_2}{dt}\right)^2 \qquad \text{(II-7c)}$$

Consider that, the external excitation is $f(t)$ and using the Lagrange formalism, the model is described by the following differential equations system

$$\begin{cases} m_1 \dfrac{d^2\theta_1}{dt^2} + \left(C_{d_1} + C_{12}\right)\dfrac{d\theta_1}{dt} + \left(k_1 + k_{12}\right)\theta_1 - \dfrac{m_1 g}{l}\sin(\theta_1) - k_{12}\theta_2 - C_{12}\dfrac{d\theta_2}{dt} = f(t) \\[3mm] m_2 \dfrac{d^2\theta_2}{dt^2} + \left(C_{d_2} + C_{12}\right)\dfrac{d\theta_2}{dt} + \left(k_2 + k_{12}\right)\theta_2 - \dfrac{m_2 g}{l}\sin(\theta_2) - k_{12}\theta_1 - C_{12}\dfrac{d\theta_1}{dt} = 0 \end{cases} \qquad \text{(II-8)}$$

Equations (II-8) can be normalised and expressed by the following equations

$$\begin{cases} \dfrac{d^2q}{d\tau^2} + \left(\lambda_1 + \alpha\right)\dfrac{dq}{d\tau} + (b+\beta)q + cq^3 + dq^5 - \beta y - \alpha \dfrac{dy}{d\tau} = f(\tau) \\[3mm] \dfrac{d^2y}{d\tau^2} + \left(\lambda_2 + \mu\alpha\right)\dfrac{dy}{d\tau} + (a+\mu\beta)y = \mu\beta q + \mu\alpha \dfrac{dq}{d\tau} \end{cases} \qquad \text{(II-9)}$$

where

$$\tau = \omega_0 t, \; q = \frac{\theta_1}{\theta_0}, \; y = \frac{\theta_2}{\theta_0}, \; \omega_0^2 = \frac{k_1}{m_1}, \; \mu = \frac{m_1}{m_2}, \; \lambda_1 = \frac{C_{d_1}}{m_1\omega_0}, \; \lambda_2 = \frac{C_{d_1}}{m_2\omega_0}, \; \omega_1^2 = \frac{k_2}{m_2} - \frac{g}{l}$$

$$c = \frac{g\theta_0^2}{6l\omega_0^2}, \; d = \frac{-g\theta_0^4}{120l\omega_0^2}, \; \beta = \frac{k_{12}}{m_1\omega_0^2}, \; \alpha = \frac{C_{12}}{m_1\omega_0}, \; f(\tau) = \frac{f(t)}{m_1 l^2\omega_0^2\theta_0}, \; a = \frac{\omega_1^2}{\omega_0^2}, \; b = \omega_0^2 - \frac{g}{l}$$

Throughout this chapter we will use the set of dimensionless parameters which we obtained for the structure as presented in chapter I (this means $\lambda_1 = 0.009$, $b = 0.92$, $c = 0.013$ and $d = -0.0008$), and coupled it with another structure having the following characteristics; $\omega_0 = 2.13$ rad/s, $m_2 = 33.4$ kg, $Cd_1 = 6.83$ Ns/m . Such a structure is compatible to a tree as reported in reference [10]. After mathematical calculations these set of parameters lead us to $\lambda_2 = 0.07$, $a = 0.52$ and $\mu = 0.06$. It is noted that the system with a linear feedback

control is described by the same set of equation for all the control design reported in this chapter. Thus, all the results obtained in the following analysis can also be applied in any of the system under control.

II-2 Control by using piezoelectric absorbers

II-2-1 Generalities on the piezoelectric materials

The piezoelectric effect was first discovered in 1880 by Pierre and Jacque Curie [14] who demonstrated that when a stress field is applied to certain crystalline materials (quartz, lithium, zirconium, titanate, etc), an electrical charge is produced on the material surface. It was subsequently demonstrated that the converse effect is also true; when an electric field is applied to a piezoelectric material, it changes its shape and size. This effect was found to be due to electrical dipoles of the materials spontaneously aligning in the electrical field. Due to the internal stiffness of the material, piezoelectric elements were also found to generate relatively large forces when their natural expansion was constrained. Lead zirconium titanate (PZT) is the most widely used piezoelectric ceramic since its discovery is 1954 [6,14]. Because of their active and passive damping features, piezoelectric materials have been explored for their active-passive hybrid control abilities, which could have the advantages of both the passive and active systems [15-18].

II-2-2 Case of an articulated beam:

a) Physical model

The physical model presented in figure II-4 is an isotropic articulated beam with a piezoelectric actuator. In addition, it can also be assumed that the local vibration in the structure can be monitored using a piezoelectric sensor. The configuration integrates piezoelectric materials with an active voltage source and a passive resistance and inductance shunting circuit. On one hand, structural vibration energy can be transferred to and dissipated in the tuned shunting circuit passively. On the other hand the control voltage will drive the piezo–layer, through the circuit, and actively suppress vibration in the host structure [5]. The passive inductance of the shunt circuit L_p, is selected so that the absorber is tuned to the

nominal or expected excitation frequency. No resistance is intentionally added to the circuit, however the passive inductor may have significant internal resistance which is represented by R_p. An important element of any practical control system
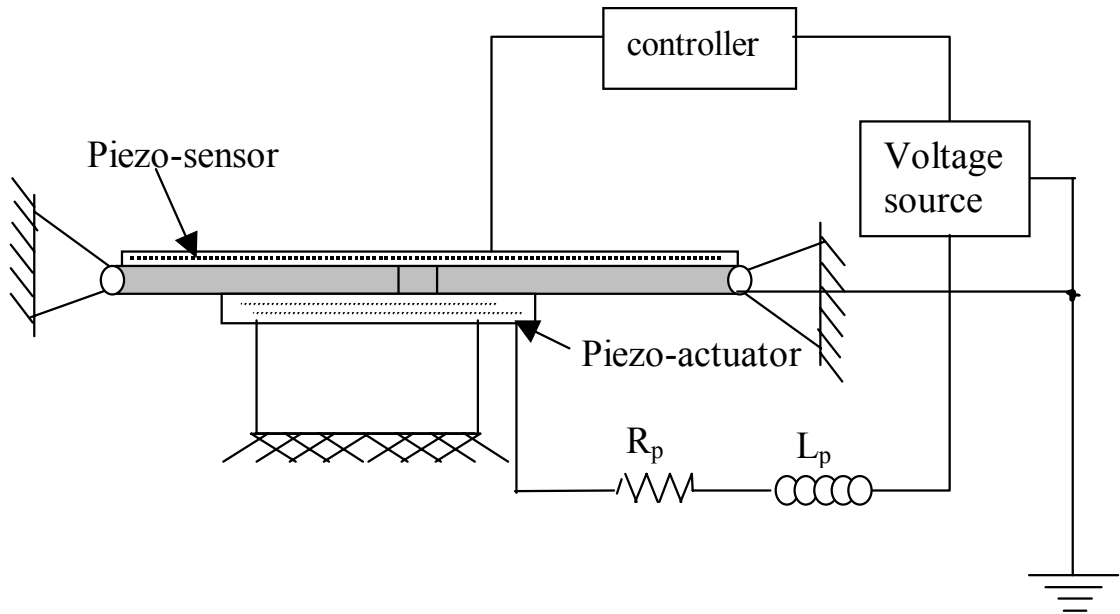

Figure II-4 : General configuration of the system

are the transducers used for implementation of the control . Sensors are needed for measurements which can be used to estimate important disturbance and system variables. Actuators are used to apply control signals to the system in order to change the system response in the required manner. In general sensors provide information to the controller to determine the performance of the control system or to provide signals related to the system response. Thus sensors and actuators provide the link between the controller and the physical system to be controlled and their design and implementation is of prime importance.

b) General mathematical formalism

To derive the system equations, let us assume that the rotational inertia is negligible, the piezoelectric material layers are thin and short compared to the beam, and the applied voltage is uniform. Thus it is assumed that the model of the structure and the piezoelectric absorber can be obtained and it is given by

$$\begin{cases} m\dfrac{\partial^2 w}{\partial t^2} + EI\dfrac{\partial^4 w}{\partial x^4} + \delta\dfrac{\partial w}{\partial t} - ES\left[\dfrac{1}{2l}\int_0^l\left(\dfrac{\partial w}{\partial x}\right)^2 dx - \dfrac{3}{8l}\int_0^l\left(\dfrac{\partial w}{\partial x}\right)^4 dx\right]\dfrac{\partial^2 w}{\partial x^2} + k_c Q = f(t) \\[4mm] L_p\dfrac{d^2 Q}{dt^2} + R_p\dfrac{dQ}{dt} + \dfrac{1}{C_p}Q - k_c w = V_c \end{cases} \tag{II-10}$$

where *E, I, m* and δ are respectively the Young's modulus, the moment of inertia, the mass per unit length and the transversal damping coefficient of the beam. L_p and R_p are the passive inductance and resistance of the shunt circuit, Q is the charge on the piezoelectric material, C_p is the capacitance of the piezoelectric under constant strain and V_c is the control voltage. *L* is the length of the beam and k_c the coupling coefficient represents the conversion from mechanical energy to electrical energy and vice-versa. Using the dimensionless variables.

$W = \dfrac{w}{L}$, $z = \dfrac{x}{L}$, $q = \dfrac{Q}{q_0}$, $l^* = \dfrac{l}{L}$ where q_0 and L are respectively the reference charge and reference length and

$$\tau = \omega_0 t, \quad \omega_0^2 = \frac{EI}{mL^4}, \quad \lambda_1 = \frac{\delta}{m\omega_0}, \quad k = \frac{ES}{m\omega_0^2 L^2}, \quad \beta = \frac{k_c q_0}{mL\omega_0^2},$$

$$F = \frac{f}{mL\omega_0^2}, \quad \lambda_2 = \frac{R_p}{L_p\omega_0}, \quad a = \frac{1}{L_p C_p\omega_0^2}, \quad \mu = \frac{mL^2}{L_p q_0^2}, \quad U = \frac{V_c}{L_p q_0\omega_0^2}$$

then the above two differential equations reduces to the following set of non dimensional differential equation

$$\begin{cases} \dfrac{\partial^2 W}{\partial\tau^2} + \dfrac{\partial^4 W}{\partial z^4} + \lambda_1\dfrac{\partial W}{\partial\tau} - k\left[\dfrac{1}{2l^*}\int_0^{l^*}\left(\dfrac{\partial W}{\partial\tau}\right)^2 dz - \dfrac{3}{8l^*}\int_0^{l^*}\left(\dfrac{\partial W}{\partial\tau}\right)^4 dz\right]\dfrac{\partial^2 W}{\partial\tau^2} + \beta q = F \\[4mm] \dfrac{d^2 q}{d\tau^2} + \lambda_2\dfrac{dq}{d\tau} + aq - \mu\beta W = U \end{cases} \tag{II-11}$$

Taking into account the boundary conditions given by (II-3a) along with (II-4b) and assuming that the force *F* is defined like indicated in chapter I, we obtain for the first mode of vibration

$$\begin{cases} \ddot{y} + (\lambda_1 + \alpha)\dot{y} + \pi^4 y + cq^3 + dq^5 + \beta' q = f_0\cos(\Omega\tau) \\ \ddot{q} + \lambda_2\dot{q} + aq - \mu'\beta' y = U \end{cases} \tag{II-12}$$

where $c = \dfrac{1}{4}k\pi^4$, $d = -\dfrac{9}{64}k\pi^6$, $\mu' = \dfrac{\mu}{2}$ and $\beta' = \dfrac{\pi}{2}\beta$. That form of equation has been obtained earlier (see equation II-6)

II-2-3 Presentation of the control design of inverted pendulum and elastic beam with piezoelectric absorber

Under the horizontal excitation, the displacement of the structure relative to the top may cause the rotation of the rigid arm (see figure II-5). The control force induced by a piezoelectric actuator depends on the restraint of the axial deformation of piezoelectric material produced by the applied voltage. Therefore a lever system is designed to reduce the required axial deformation of the piezoelectric actuator and then reduce the relative displacement of the structure. In the other hand, the two piezoelectric materials can be used as two piezoelectric actuator in a moment controller through the lever system. This is done by applying a voltage to each piezoelectric actuator to generate a pre-compressive force of such magnitude that two actuators work always in compression [12].
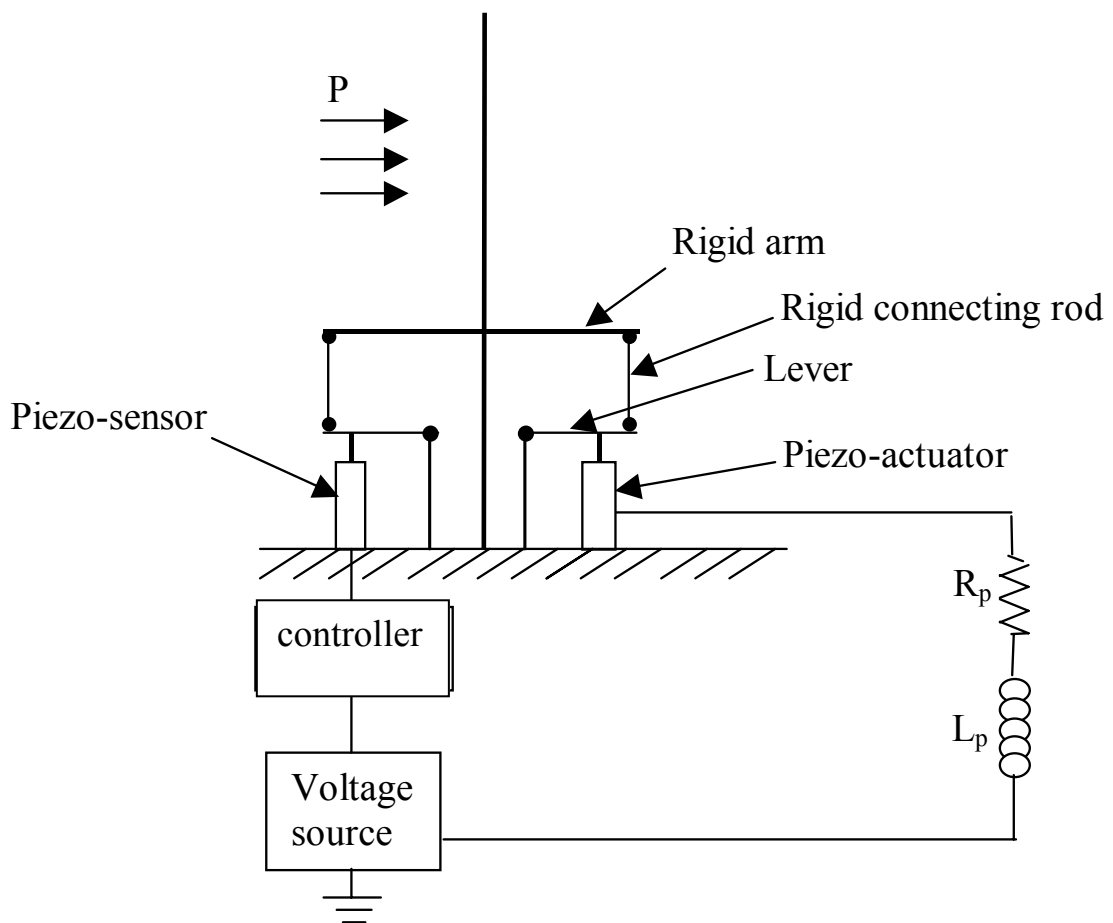

Figure II-5: Elastic or rigid structure under control

A mathematical modelling of the system presented in figure II-5 leads to equation similar to equations (II-9 and II-12).

To end with this section dealing with the modelling of the mechanical structures under sandwich and piezoelectric controls, we note that in both cases, the fundamental equations are the same. Thus the theoretical analysis which follows in this chapter and in chapter III, is more general and the results obtained are applicable both for the piezoelectric control strategy and for the sandwich control strategy.

III- CONTROL OF AMPLITUDE AND UNBOUNDED MOTION

III-1 Stability of active structural control

Following the classical local stability analysis of Lyapunov, we first examine the fixed points of our system. Consider the system of equation II-9, one finds that $u_0 = (0,0,0,0)$ is a fixed points for all parameter values and that there are two more fixed points

$$
u_{\pm} = \left(\pm \left(\frac{-c - \sqrt{4d\left(b + \beta - \frac{\mu\beta}{(a+\mu\beta)}\right)}}{2d} \right), 0, \pm \frac{\mu\beta}{(a+\mu\beta)} \left(\frac{-c - \sqrt{4d\left(b + \beta - \frac{\mu\beta}{(a+\mu\beta)}\right)}}{2d} \right), 0 \right) \text{ the}
$$

local stability can be determined by investigating the linearised system. The autonomous system is obtained for $f_0 = 0$, In this case equation (II-9) becomes in the linear limit

$$
\begin{cases}
\dfrac{dq(\tau)}{d\tau} = v(\tau) \\[2mm]
\dfrac{dv(\tau)}{d\tau} = -(b+\beta)q(\tau) - (\lambda_1 + \alpha)v(\tau) + \beta y(\tau) + \alpha u(\tau) \\[2mm]
\dfrac{dy}{d\tau}(\tau) = u(\tau) \\[2mm]
\dfrac{du}{d\tau}(\tau) = \mu\beta q(\tau) + \mu\alpha v(\tau) - (a+\mu\beta)y(\tau) - (\lambda_2 + \mu\alpha)u(\tau)
\end{cases}
\tag{II-13}
$$

To study the stability of this system, we apply the Lyapunov concept by examining the fundamental solution $e^{s\tau}$. For that we set

$$q(\tau) = q_0 \exp(s\tau), \; v(\tau) = v_0 \exp(s\tau), \; y(\tau) = y_0 \exp(s\tau), \; u(\tau) = u_0 \exp(s\tau) \qquad \text{(II-14)}$$

Inserting (II-14) into equations (II-13) we obtain the characteristic equation of the eigen system given by

$$\begin{vmatrix} -s & 1 & 0 & 0 \\ -(b+\beta) & -s-(\alpha+\lambda_1) & \beta & \alpha \\ 0 & 0 & -s & 1 \\ \mu\beta & \mu\alpha & -(a+\mu\beta) & -s-(\lambda_2+\mu\beta) \end{vmatrix} = 0 \qquad \text{(II-15)}$$

Which gives

$$s^4 + a_0 s^3 + a_1 s^2 + a_2 s + a_3 = 0$$

with

$$a_0 = \lambda_2 + \lambda_1 + \alpha + \mu\beta,$$

$$a_1 = a + b + \beta(1+\mu) + \lambda_1\lambda_2 + \alpha(\lambda_2 + \mu\lambda_1),$$

$$a_2 = \lambda_1(a+\mu\beta) + \lambda_2(b+\beta) + \alpha(a+\mu b),$$

$$a_3 = ba + \beta(a+\mu b).$$

From the classical local stability analysis of Lyapunov, it is known that the fixed points are stable if the real parts of the roots of the characteristics equation are all negative. Otherwise (if at least one root has a positive real part), the fixed points is unstable. Using Routh-Hurwitz criterion [11], for the sign of the real part of roots, we obtain that the real parts of the roots are negative provided that all the coefficients a_0, a_1, a_2 and a_3 are positive and that all the determinants $\Delta_1 = a_0 a_2 - a_2$ and $\Delta_2 = a_0(a_1 a_2 - a_0 a_3) - a_2^2$ are positive also. Knowing that all these coefficients are positive and considering the case where the gain parameters α and β are also positive, the above analysis leads to the following condition for the control for the stability of the fixed points $(0,0,0,0)$ for the system under control

$$(\lambda_1 + \lambda_2 + \alpha + \mu\beta)(a + b + \beta(1+\mu) + \lambda_1\lambda_2 + \alpha(\lambda_2 + \mu\lambda_1))(\lambda_1(a+\mu\beta) + \lambda_2(b+\beta) + \alpha(a+\mu b))$$

$$-(\lambda_1 + \lambda_2 + \alpha + \mu\beta)^2(ba + \beta(a+\mu b)) - (\lambda_1(a+\mu\beta) + \lambda_2(b+\beta) + \alpha(a+\mu b)) \succ 0 \qquad \text{(II-16)}$$

Let us use the dynamics of the controlled system with the parameters defined in section II-1-2. As it appears in the bifurcation diagram of figure II-6, the shaded

region represents the set of control gain parameters leading to instability of the control design.
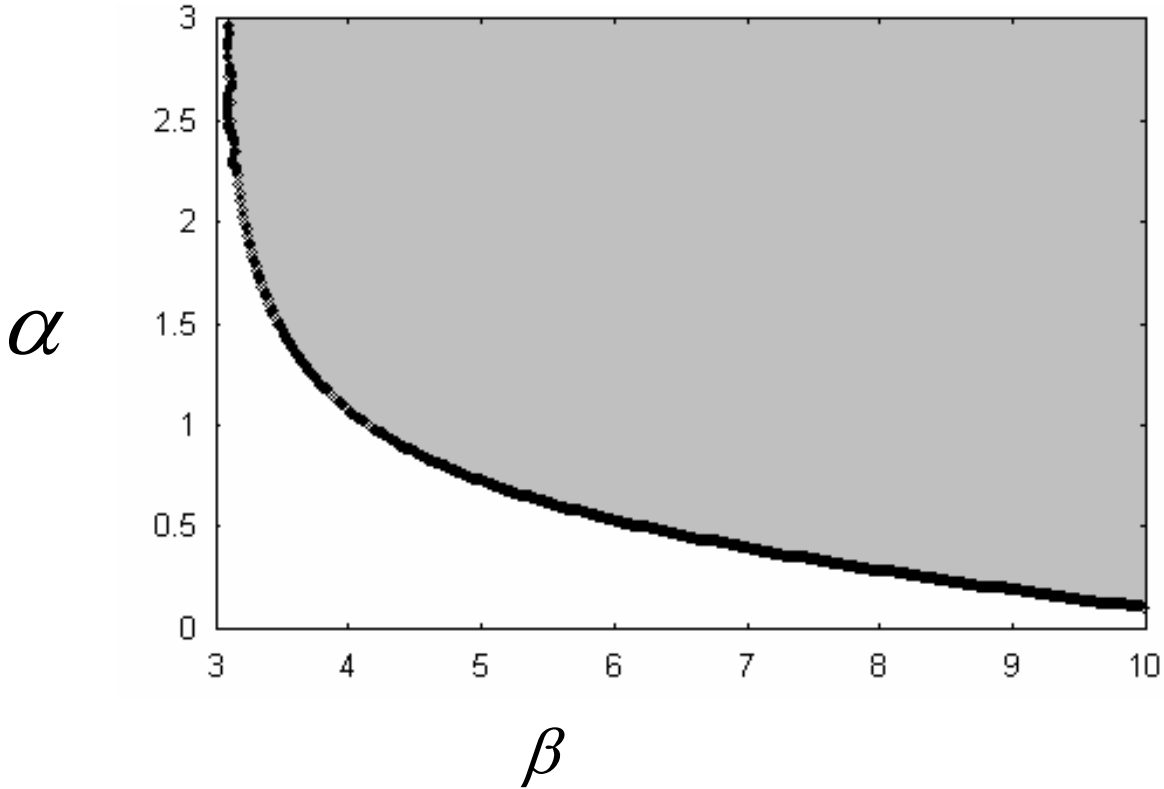

Figure II-6 : Stability boundary in the control gain parameter

III-2 Effects of the control on the amplitude of harmonic oscillations

The harmonic balance method is used to determine the amplitude of the vibration. For that, we set

$$q = A\cos(\Omega\tau + \Phi) \tag{II-17}$$

where *A* is the amplitude of vibration. Let us first consider the system when the effects of the non linear terms are negligible (that is *c=d=0*). In this case, the amplitude of the harmonic oscillations of the controlled system is given by

$$A_c = \frac{F_o}{\left[\left(b-\Omega^2+\beta(1-\varsigma)+\alpha\Omega\eta\right)^2+\left(\Omega(\lambda_1+\alpha)-\eta\beta-\alpha\Omega\varsigma\right)^2\right]^{\frac{1}{2}}} \tag{II-18}$$

Where

$$\zeta = \frac{\mu\left[\beta\left(a+\mu\beta-\Omega^2\right)+\alpha\Omega^2\left(\lambda_2+\mu\alpha\right)\right]}{\left(a+\mu\beta-\Omega^2\right)^2+\Omega^2\left(\lambda_2+\mu\alpha\right)^2}$$

and

$$\eta = \frac{\mu\Omega\left[\alpha\left(a+\mu\beta-\Omega^2\right)-\beta\left(\lambda_2+\mu\alpha\right)\right]}{\left(a+\mu\beta-\Omega^2\right)^2+\Omega^2\left(\lambda_2+\mu\alpha\right)^2}$$

It is necessary to look for the condition fulfilled by the control parameters so that the control should be effective. In fact, the control is effective when

$$A_c \prec A_{nc} \tag{II-19}$$

A_{nc} being the amplitude of the oscillations of the uncontrolled system. It implies that the amplitude of the vibration is reduced, when the control parameters satisfy the following condition

$$\begin{aligned}
\left(\beta(1-\zeta)+\alpha\Omega\eta\right)&\left(2\left(b-\Omega^2\right)+\beta(1-\zeta)+\alpha\Omega\zeta\right) \\
&+\left(\Omega\alpha-\eta\beta-\alpha\Omega\zeta\right)\left(\left(2\lambda_1+\alpha\right)\Omega-\eta\beta-\alpha\Omega\zeta\right) \succ 0
\end{aligned} \tag{II-20}$$

To illustrate this criterion, it is plotted in figure (II-7) in the (α,β) space parameters for $\Omega = 0.52$. The shaded region represents the range where the control is inefficient. Note that α and β are respectively proportional to the elastic coupling k_{12} and damping coupling C_{12}. For instance from the figure for $\beta=2$ the minimum value of α for the effectiveness of the control is 10.33; this means $k_{12}=308.6\ N/m$ and $C_{12}=181.8\ Ns/m$ in the real dimension. Figure II-8 presents the intersection between the stability chart and the domain in space parameters where amplitude is reduced. It appears that to optimise the control strategy it is necessary to use the coupling structure having the parameters in the shaded region.
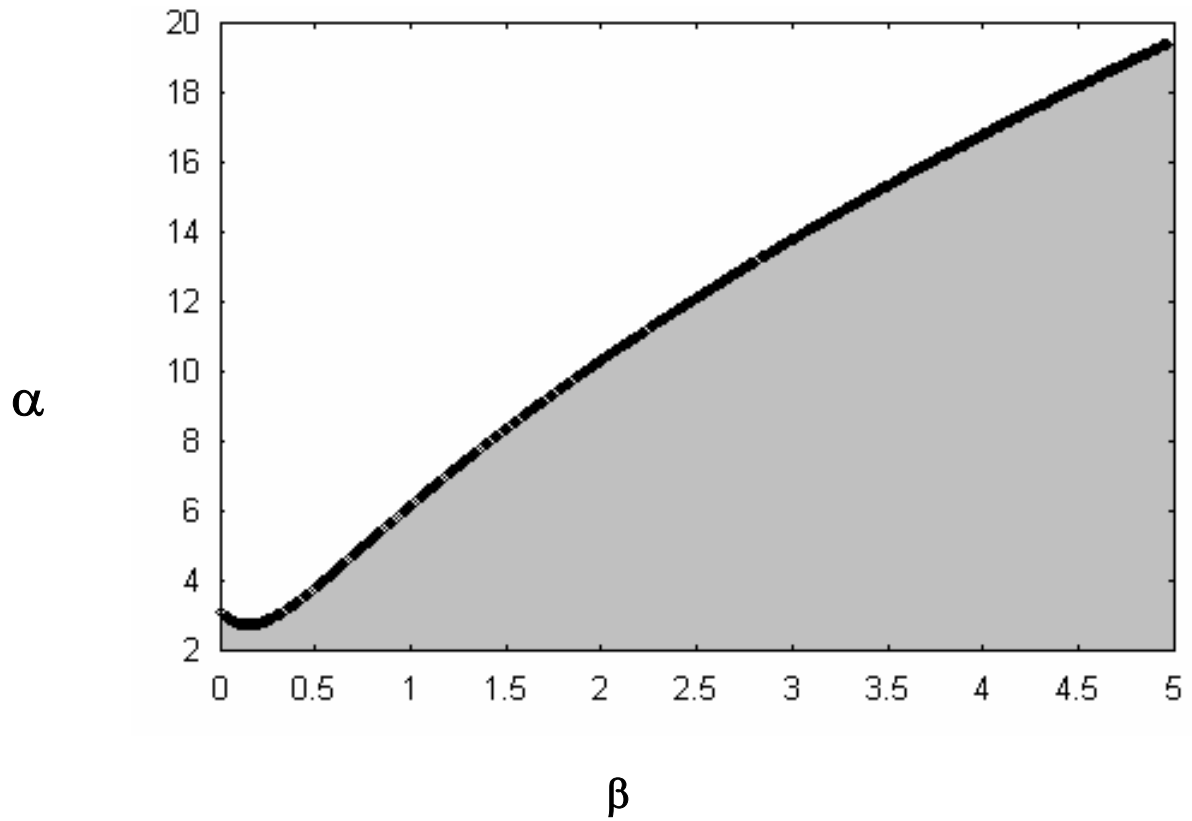
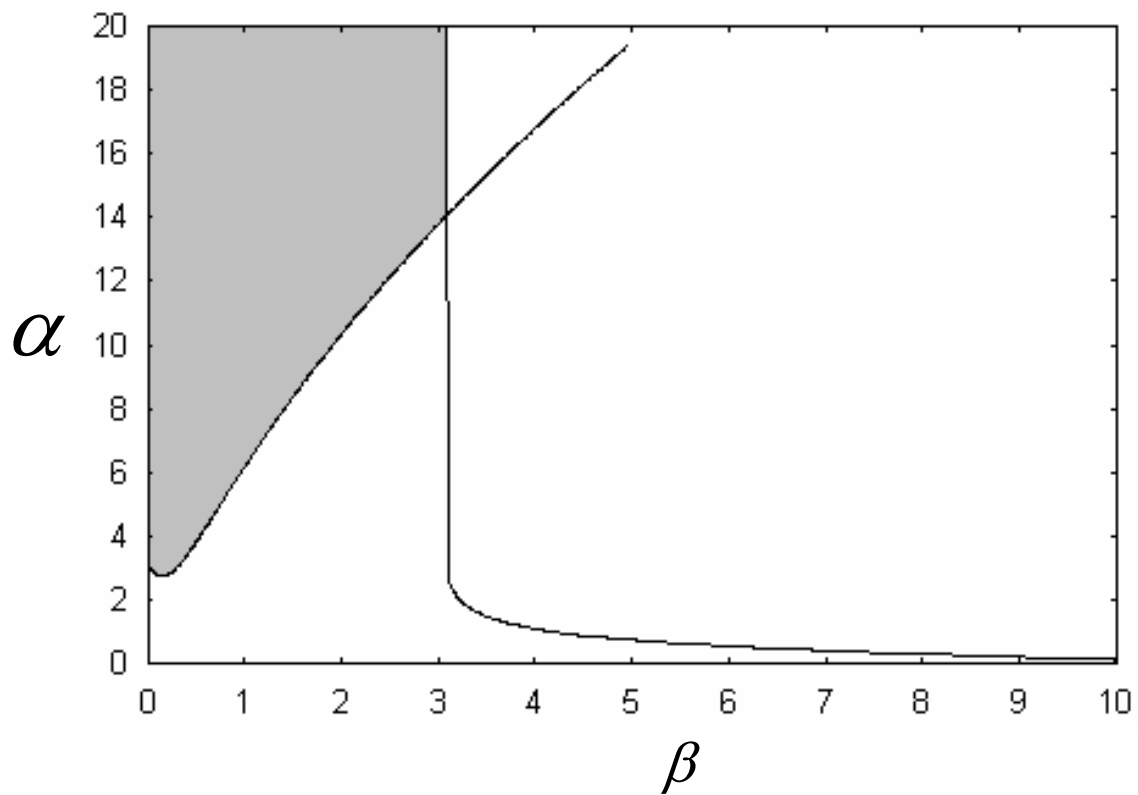**Figure II-7 :**Domain in space parameters (α,β) where the control is efficient.

Figure II-8 : Stability boundary in the parameters (α, β) for which control is

Considering the non-linear case, the amplitude of the oscillations satisfy the following tenth order algebraic equation

$$
\begin{aligned}
F_o^2 = &\frac{25}{64}d^2A^{10} + \frac{15}{16}cdA^8 + \left(\frac{9}{16}c^2 + \frac{5}{4}d\left(b-\Omega^2+\beta(1-\zeta)+\alpha\Omega\eta\right)\right)A^6 \\
&+\frac{3}{2}c\left(\pi^4-\Omega^2+\beta(1-\zeta)+\alpha\Omega\eta\right)A^4 \\
&+\left(\left[b-\Omega^2+\beta(1-\zeta)+\alpha\Omega\eta\right]^2+\left[\Omega(\lambda_1+\alpha)-\eta\beta-\alpha\Omega\zeta\right]^2\right)A^2
\end{aligned}
\tag{II-21}
$$

Assuming that at the frontier separating regions of efficiency and inefficiency of the control, the amplitudes of both the controlled and uncontrolled *(α=β=0)* systems are equal, it comes that the amplitude of the oscillations at this limit is given by

$$
A_l^2 = \left(-3cv-2\sqrt{\Delta}\right)/5dv
\tag{II-22}
$$

where

$$
v = \beta(1-\zeta)+\alpha\Omega\eta
$$

and

$$
\Delta = \frac{9}{4}c^2v^2 - 5dv\left(v(-2\Omega+2b+v)+(\Omega\alpha-\eta\beta-\alpha\Omega\zeta)(2\lambda_1\Omega+\Omega\alpha-\eta\beta-\alpha\Omega\zeta)\right)
$$

This leads us to the following boundary condition for the effectiveness of the control (by inserting equation (II-22) into equation (II-21)):

$$
F_o^2 = \left[\left(b-\Omega^2+\beta(1-\zeta)+\alpha\Omega\eta-\frac{9c^2}{40d}+\frac{\Delta}{10dv^2}\right)^2+\left(\Omega(\lambda_1+\alpha)-\eta\beta-\alpha\Omega\zeta\right)^2\right]\left[\frac{-3cv-2\sqrt{\Delta}}{5dv}\right]
$$

$$
\tag{II-23}
$$

Figure II-9 presents the evolution of the force F_0 as a function of β with $\alpha = 0$ and $\Omega = 0.92$ (we remind the reader that 0.92 is the frequency at the primary resonance). This result is obtained by using the analytical expression given by equation (II-23) (thin line) along with direct numerical simulations of equation II-6 (doted line). This numerical simulation is done using the fourth order Runge Kutta algorithm. The domain of the efficiency of the control is below the curve. As the excitation amplitude increases, we need greater values of β to reduce the vibration of the structure. The contrary is observed in figure II-10 when we look for the effects of α. When α increases, the region of efficiency of the control decreases.
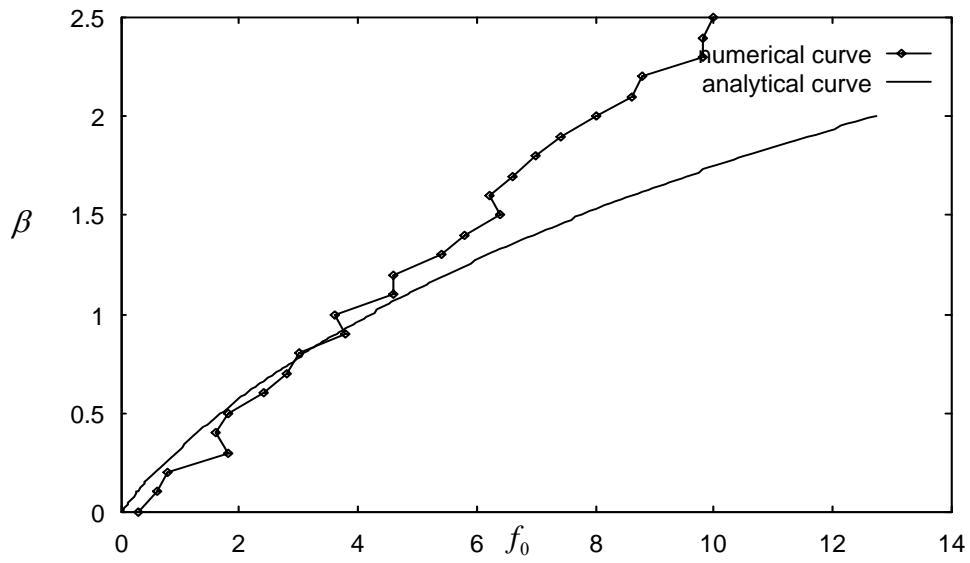
Figure II-9: Boundary of the domains in the space parameters (f_0, β) where the control of amplitude is efficient for α=0
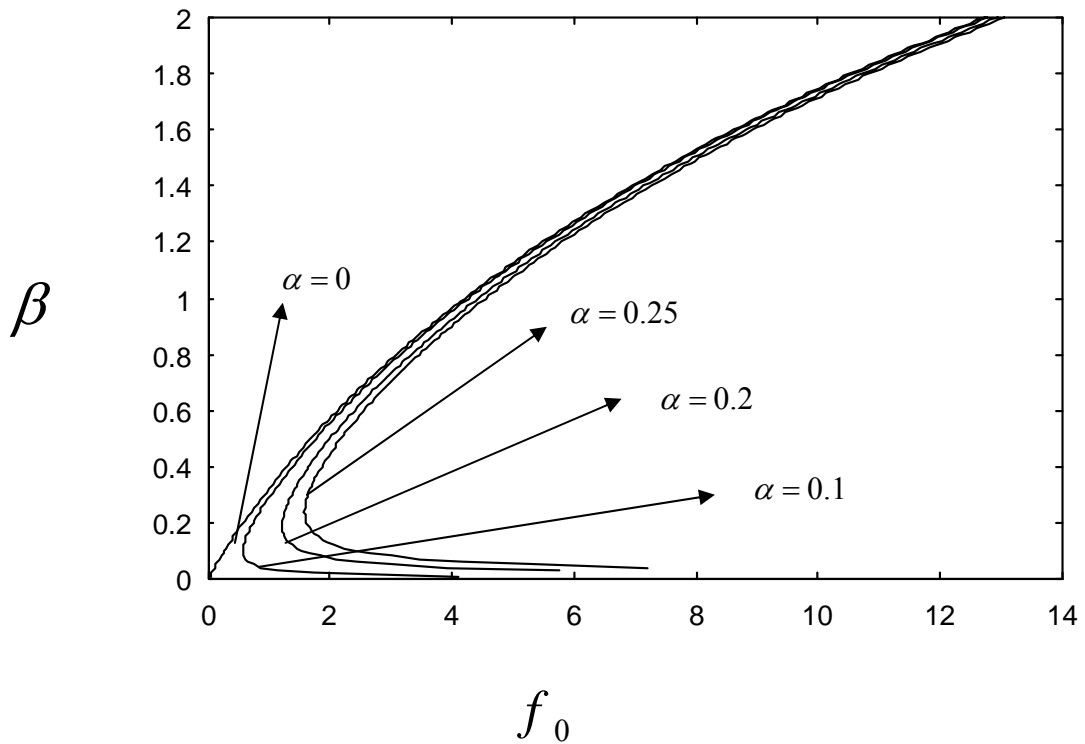

Figure II-10: Boundary of the domains in the space parameters (f_0, β) where the control of amplitude is efficient for $\alpha = 0, \alpha = 0.1, \alpha = 0.2$ and $\alpha = 0.25$.

III-3 Effects of the control on the appearance of unbounded motion

Depending on the value of the external force and those of the other parameters, the system initially moving inside the potential well can cross the barrier of the potential to exhibit unbounded motions leading to failure. It is important to analyse the effects of the control parameters on the condition for the escape from the potential well. We use the method of energy [8,10] as described in chapter I. We thus find that the amplitude of the excitation at the frontier between catastrophic and bounded motions is given by

$$f_c^2 = \left[\left(\left(b - \Omega^2 + \beta(1-\zeta) + \alpha\Omega\eta \right) A_b + \frac{3}{4}cA_b^3 + \frac{5}{8}dA_b^5 \right)^2 + \left(\Omega(\lambda_1 + \alpha) - \eta\beta - \alpha\Omega\zeta \right)^2 A_b^2 \right] \quad \text{(II-24)}$$

with

$$A_b^2 = \left(2V_c - \left(b - \Omega^2 \right) X_m - \frac{1}{2}cX_m^2 - \frac{1}{3}dX_m^3 \right) / \Omega^2$$

Equations (II-24) gives an approximate expression for the critical forcing above which a catastrophe can occur. Its variation as a function of α and β is plotted in figure II-10 (with $\alpha = 0$)and II-11 (with $\beta = 0$) with the results of the direct numerical simulation of equation (II-9). We find that f_c increases with α and β. Practically, this means that the result can be applied as follows: For a stiffness coefficient of the coupling parameter given by $k_{12} = 232.25N/m$ (i.e. $\beta = 1.5$), the critical forcing for the apparition of unbounded motion is $P = 2630.54N$ (i.e $f_c = 10.87$). Taking into account the case of dissipative coupling parameter, for $C_{12} = 26.4Ns/m$ ($\alpha = 1.5$) critical forcing amplitude is given by $p = 1875.5N$ ($f_c = 7.75$). Good agreement is obtained between the analytical and numerical results. This means that the analytical prediction can be used to prevent the failure of the structures.
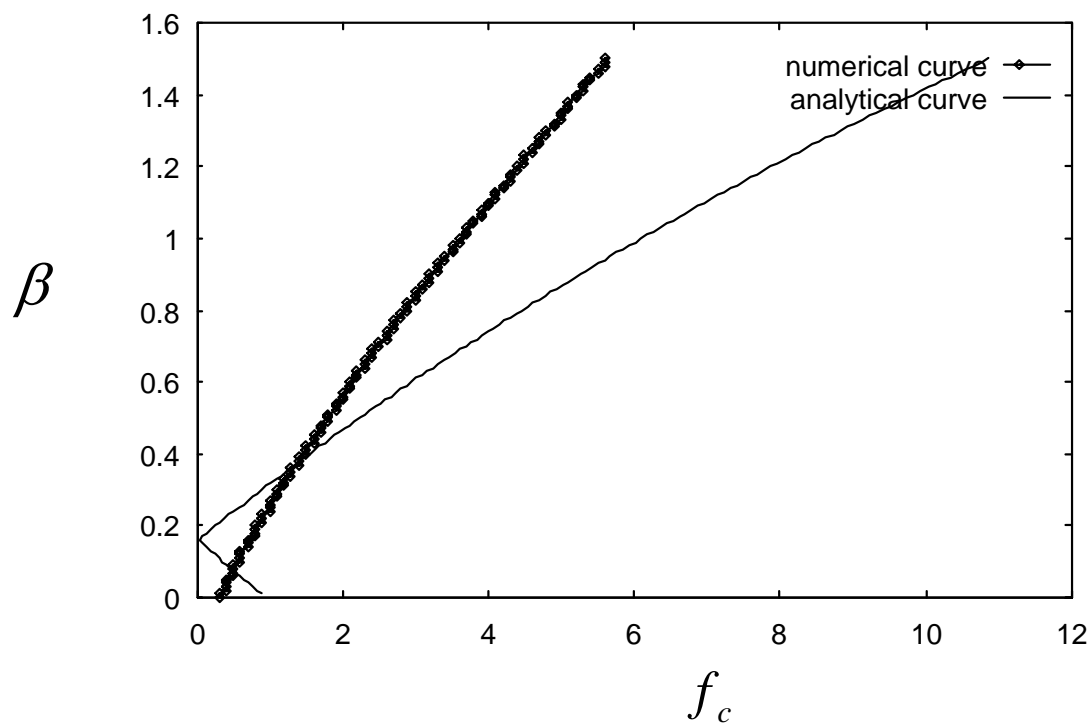
Figure II-11: Critical forcing amplitude for the apparition of catastrophic motion as function of β with $\alpha = 0$
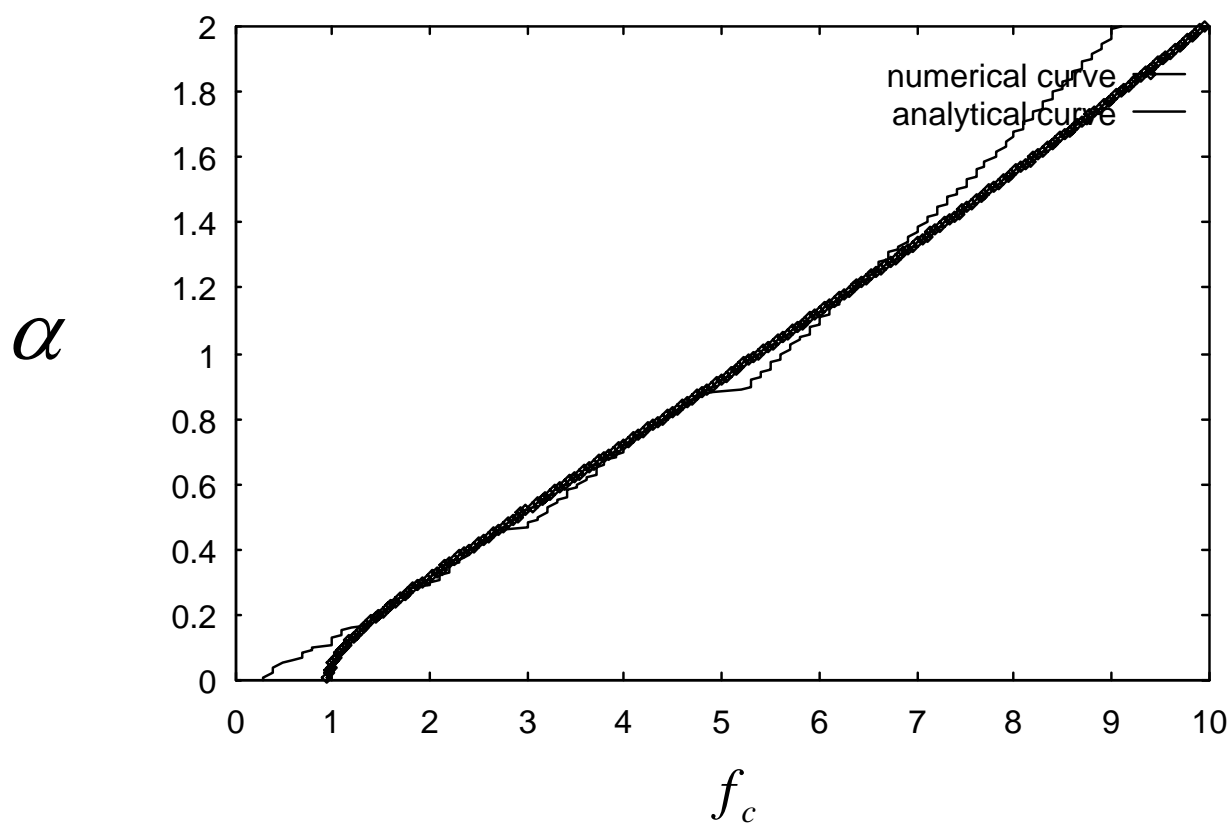

Figure II-12: Critical forcing amplitude for the apparition of catastrophic motion as function of α with $\beta = 0$

IV-Control of Melnikov chaos

IV-1 Analytical study

In chapter I, we derived the condition for the occurrence of horseshoes chaos using the Melnikov theory. One would like to know how the control strategy affects the Melnikov criterion or, in what range of the control parameters the heteroclinic chaos in our model could be inhibited. To deal with such a question, let us express the dynamical structure under control with forcing regarded as a perturbation from an autonomous system in the form

$$\ddot{q} + (\lambda_1 + \alpha)\dot{q} + (b + \beta)q + cq^3 + dq^5 - \beta y - \alpha \dot{y} = f_0 \cos(\Omega \tau) \tag{II-25}$$

where y is the control force and $\dot{y}$ the time derivative. This control force can be obtained by solving the characteristic equation of the control system given by

$$(\lambda_2 + \mu\alpha)\dot{y} + (a + \mu\beta)y = \mu\beta q(\tau) + \mu\alpha \dot{q}(\tau) \tag{II-26}$$

It should be noted that due to the fact that $m_2 \gg m_1$, we have used this assumption $\dfrac{d^2 y}{dt^2} \simeq 0$ in equation (II-9) to obtain equation (II-26). This is done to derive analytically, an approximate criterion for the occurrence of Melnikov chaos. Equation (II-25) can be expressed in the form

$$\dot{U} = g_0(u) + \varepsilon g_p(u, \tau) \tag{II-27}$$

where $u(q, p = \dot{q})$ is the state vector $g_0 = \left(p, -(b + \beta)q - cq^3 - dq^5\right)$ and $g_p = \left(0, f_0 \cos(\Omega \tau) - (\lambda_1 + \alpha)p + \beta y + \alpha \dot{y}\right)$ the heteroclinic orbit is defined be equations (I-61) of chapter I.

Also, by solving equation (II-26), we find

$$
\begin{aligned}
y_0 = &\pm \frac{\mu\beta X\xi}{\sqrt{2}(\lambda_2 + \mu\alpha)} \exp\left(-\left(\frac{a + \mu\beta}{\lambda_2 + \mu\alpha}\right)\tau\right) \int_{-\infty}^{\tau} \frac{\sinh(Y(s - \tau_x))\exp\left(\left(\frac{a + \mu\beta}{\lambda_2 + \mu\alpha}\right)s\right)}{\left(1 + (1 - \xi^2)\sinh^2(Ys)\right)^{1/2}} d\tau \\
&\pm \frac{\mu\alpha XY\xi}{\sqrt{2}(\lambda_2 + \mu\alpha)} \exp\left(-\left(\frac{a + \mu\beta}{\lambda_2 + \mu\alpha}\right)\tau\right) \int_{-\infty}^{\tau} \frac{\cosh(Ys)\exp\left(\left(\frac{a + \mu\beta}{\lambda_2 + \mu\alpha}\right)s\right)}{\left(1 + (1 - \xi^2)\sinh^2(Ys)\right)^{1/2}} d\tau
\end{aligned}
\tag{II-28}
$$

The Melnikov function is defined by

$$M(\tau_0) = \int_{-\infty}^{+\infty} g_0[u_0(\tau)] \times g_p[u_0(\tau), \tau + \tau_0] d\tau$$

$$= \int_{-\infty}^{+\infty} p_0 \left[f_0 \cos(\Omega\tau) - (\lambda_1 + \alpha) p_0 + \beta y_0 + \alpha \dot{y}_0 \right] d\tau \qquad \text{(II-29)}$$

where τ_0 is a phase angle, p_0 and q_0 are the unperturbed separatrices

a) Case of elastic coupling

Taking into account the case where the coupling is only elastic $(\alpha = 0)$ and carrying out the integral in equation (II-29), we obtain:

$$M(\tau_0) = \frac{X\xi\pi f_0}{Y(1-\xi^2)\sinh\frac{\Omega\pi}{2Y}} \cos(\Omega\tau_0) - \frac{\lambda_1 XY}{8} \left[\frac{3\xi^2 - 1}{1-\xi^2} + \frac{1+3\xi^2}{2\xi} \ln\frac{1+\xi}{1-\xi} \right] + k(\beta) \qquad \text{(II-30)}$$

with $k(\beta) = \dfrac{\mu\beta^2 X^2 \xi^2 Y}{2\lambda_2} \displaystyle\int_{-\infty}^{+\infty} \dfrac{\cosh(Y\tau)\exp\left(-\dfrac{(a+\mu\beta)}{\lambda_2}\tau\right)}{\left(1+(1-\xi^2)\sinh^2(Y\tau)\right)^{3/2}} \left(\displaystyle\int_{-\infty}^{\tau} \dfrac{\sinh(Ys)\exp\left(\dfrac{(a+\mu\beta)}{\lambda_2}s\right)}{\left(1+(1-\xi^2)\sinh^2(Ys)\right)^{1/2}} ds \right) d\tau$

Using the Melnikov criterion, chaos is suppressed when

$$f_0 \leq f_{0c} = \frac{Y(1-\xi^2)\sinh\frac{\Omega\pi}{2Y}}{\Omega\xi\pi} \left[\frac{\lambda_1 X^2 Y}{8} \left[\frac{3\xi^2 - 1}{1-\xi^2} + \frac{1+3\xi^2}{2\xi} \ln\frac{1+\xi}{1-\xi} \right] + k(\beta) \right] \qquad \text{(II-31)}$$

Therefore, the critical value of amplitude of the external excitation depends nonlinearly on the control parameter through $k(\beta)$. Thus we need the evaluation of this quantity as β varies. To deal with such a problem, let us set $\upsilon = \exp(Ys), \eta = \exp(Y\tau)$, therefore

$$k(\beta) = \frac{2\mu\beta^2 X^2 \xi^2}{\lambda_2 Y} \int_0^{+\infty} \frac{(\eta^2+1)\eta^{-\frac{(a+\mu\beta)}{\lambda_2 Y}+1}}{\left[4\eta^2 + (1-\xi^2)(\eta^2-1)^2\right]^{3/2}} \left(\int_0^{\eta} \frac{(\upsilon^2-1)\upsilon^{\frac{(a+\mu\beta)}{\lambda_2 Y}-1}}{\left[4\upsilon^2 + (1-\xi^2)(\upsilon^2-1)^2\right]^{1/2}} d\upsilon \right) d\eta$$

$$\qquad \text{(II-32)}$$

Then assuming that $\eta = \dfrac{\psi}{\psi-1}$ and $\upsilon = \dfrac{p}{p-1}$, we obtain

$$k(\beta) = \frac{2\mu\beta^2 \xi^2 X^2}{\lambda_2 Y} \int_0^1 \frac{(\psi-1)^2(2\psi^2-2\psi+1)\left(\dfrac{\psi}{\psi-1}\right)^{-\frac{(a+\mu\beta)}{Y\lambda_2}+1}}{\left(4\psi^2(\psi-1)^2 + (1-\xi^2)(2\psi-1)^2\right)^{3/2}} \left(\int_0^{\psi} \frac{(2p-1)\left(\dfrac{p}{p-1}\right)^{\frac{(a+\mu\beta)}{Y\lambda_2}-1}}{(p-1)^2\left(4p^2 + (1-\xi^2)(2p-1)^2\right)^{1/2}} dp \right) d\psi$$

With the above, we can numerically compute the variation of $k(\beta)$. Figure II-13

shows that $k(\beta)$ increases with β. This implies that f_{0c} increases with β. Consequently, the control becomes more and more efficient when β increases
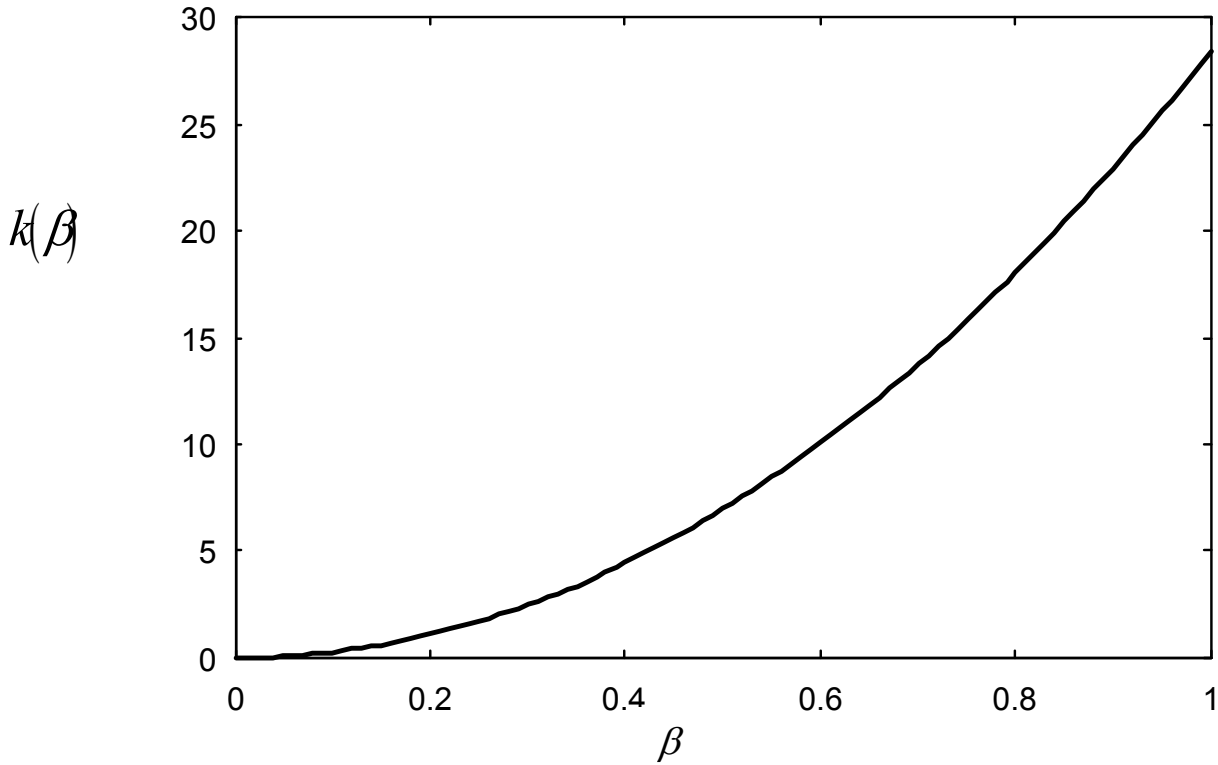

Figure II-13 : Evolution of $k(\beta)$ as a function of β for $\Omega = 0.92$

b) Case of a dissipative coupling

Considering now the case where the coupling is only dissipative, the Melnikov criterion is given by

$$M(\tau_0) = \frac{X\xi\pi f_0}{Y(1-\xi^2)\sinh\frac{\Omega\pi}{2Y}}\cos(\Omega\tau_0) - \frac{\lambda_1 XY}{8}\left[\frac{3\xi^2-1}{1-\xi^2} + \frac{1+3\xi^2}{2\xi}\ln\frac{1+\xi}{1-\xi}\right] + k(\alpha) \qquad \text{(II-33)}$$

with

$$k(\alpha) = \frac{\mu\alpha^2 X^2\xi^2 Y^2 a}{2(\lambda_2+\mu\alpha)^2}\int_{-\infty}^{+\infty}\frac{\cosh(Y\tau)\exp\left(-\frac{a}{(\lambda_2+\mu\alpha)}\tau\right)}{\left(1+(1-\xi^2)\sinh^2(Y\tau)\right)^{3/2}}\left(\int_{-\infty}^{\tau}\frac{\cosh(Ys)\exp\left(\frac{a}{(\lambda_2+\mu\alpha)}s\right)}{\left(1+(1-\xi^2)\sinh^2(Ys)\right)^{1/2}}ds\right)d\tau$$

$$+\frac{\mu\alpha^2 X^2\xi^2 Y^2}{2(\lambda_2+\mu\alpha)}\int_{-\infty}^{+\infty}\frac{\cosh^2(Y\tau)\exp\left(-\frac{a}{(\lambda_2+\mu\alpha)}\tau\right)}{\left(1+(1-\xi^2)\sinh^2(Y\tau)\right)^2}d\tau$$

Carrying out the same expansion like in the previous section, we can conclude that the critical forcing for the appearance of chaos increases with α.

IV-2 Basin of stability

To complement and validate the analytical predictions, we have simulated numerically the system of equations (II-9) to look for the effects of the control parameters on the onset of the fractality in the basins of attraction. Considering firstly the case of the system without control, figure II-14a shows that the boundary is fractal when $f_0 = 0.2$ (i.e f_0=48.4N in real dimensions) and becomes more and more visible as f_0 increases (see chapter I figure I-10). The corresponding value predicted by the Melnikov boundary is $f_0 = 0.18$ ($f_0 = 43.56N$ in real dimension) . Now taking into account the presence of the control, we begin by considering only the effects of β on the critical value f_{0c} (we have set $\beta = 0.8$ (or k_{12}=*117.2N/m*)). Figure II-14b shows that with the same parameters as in figure II-14a, the system and this is accompanied by an enlargement of the basin of attraction. By varying f_0 the fractality reappears only when $f_0 \geq 1.5$ or *$f_0 \geq 363N$*   in real dimension (see figure II-14c). Consider now the case of dissipative coupling ,we realise in figure II-15 that the fractal basin boundary disappear for $\alpha = 1$ and reappear for $f_0 = 4.5$. This means that by making a good choice of the coupling parameters we can conveniently suppress chaos in our system.
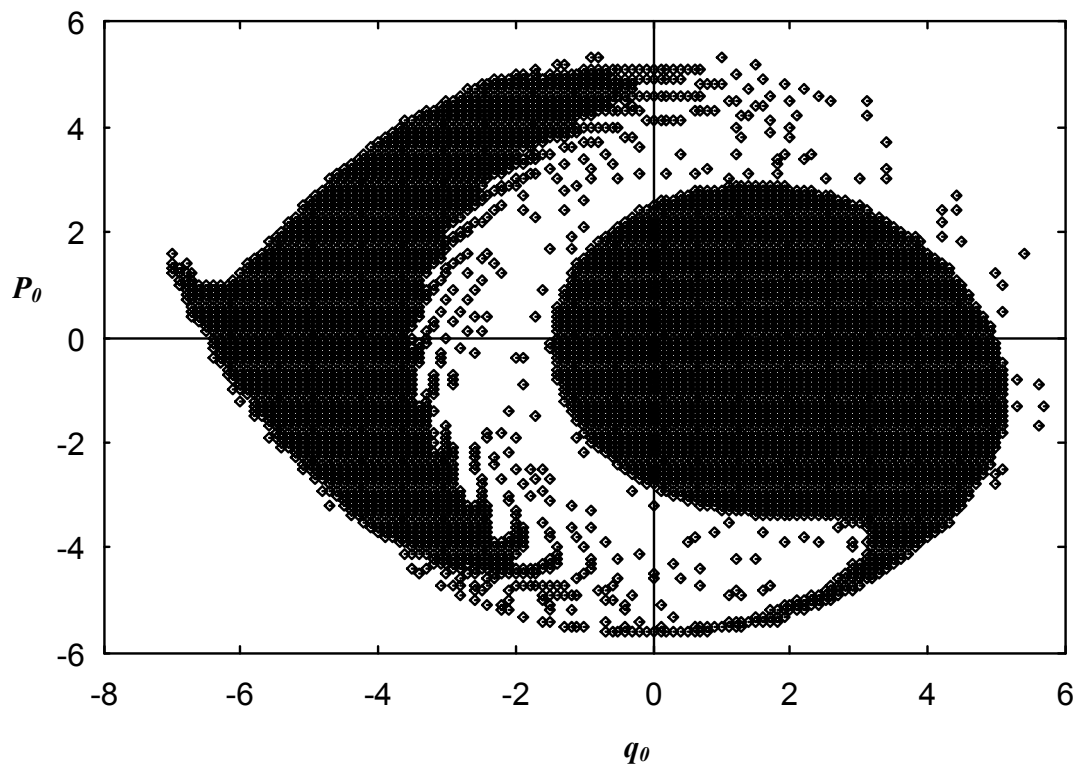
Figure II-14a : A fractal basin boundary diagram for the uncontrolled system for $\Omega = 0.92$ and $f_0 = 0.2$
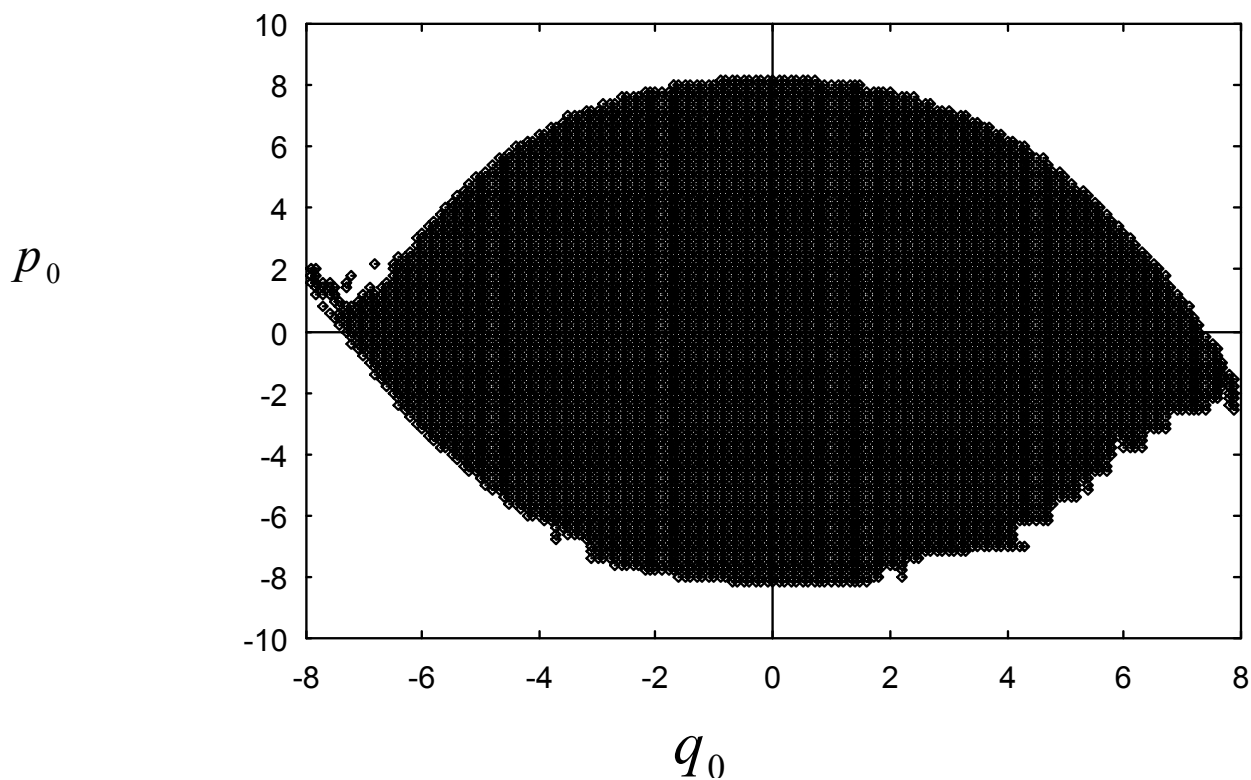

Figure II-14b: Basin of attraction for the case where control is efficient with $\beta = 0.8$, $f_0 = 0.2$ and $\Omega = 0.92$
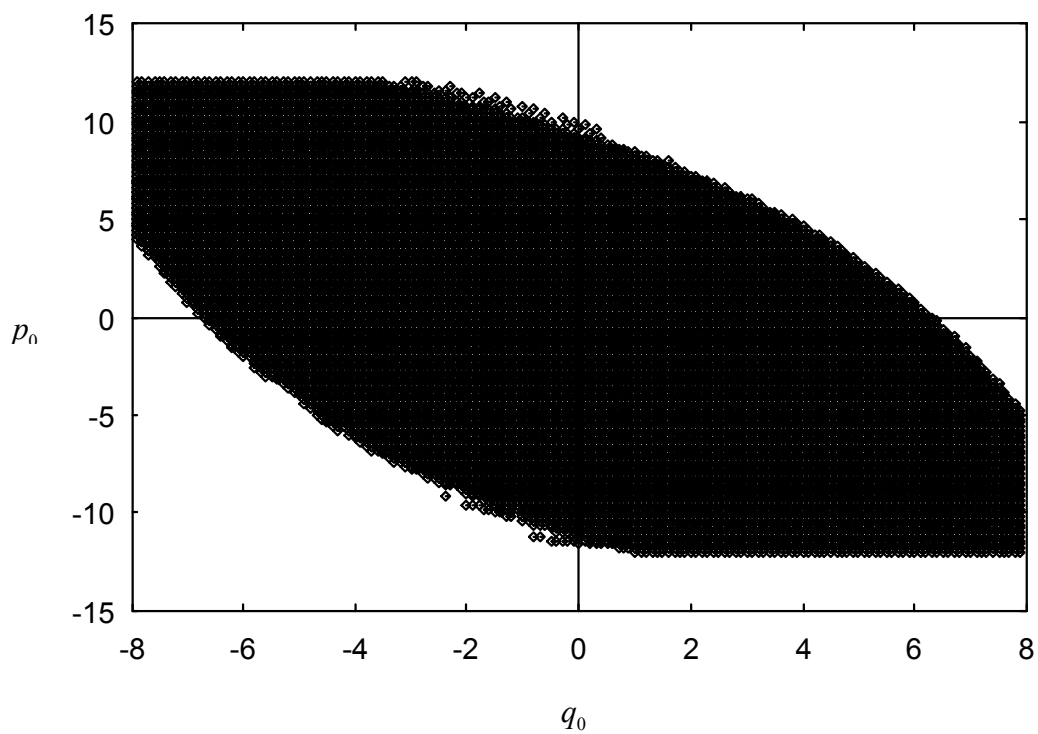
Figure II-15a : Basin of attraction for $\alpha = 1, \Omega = 0.92$ and $f_0 = 0.2$
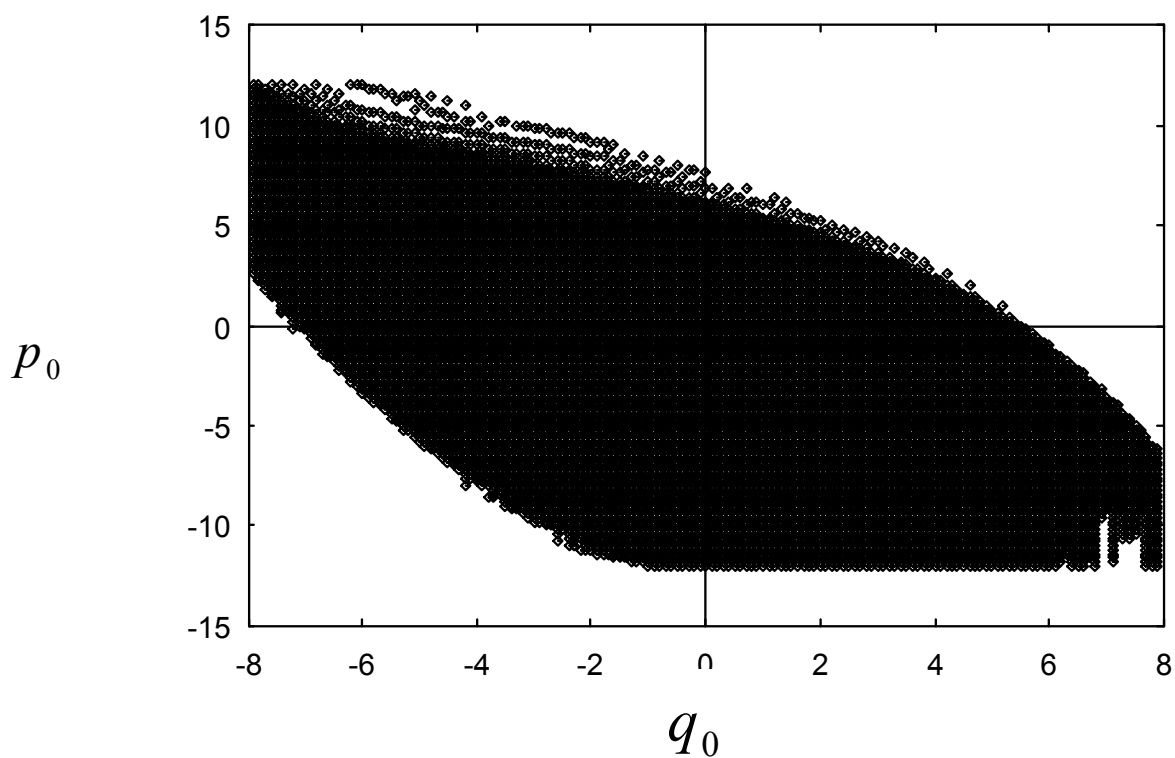

Figure II-15b : uncontrolled basin for $\alpha = 1, \Omega = 0.92$ and $f_c = 4.5$

IV-CONCLUSION

In this chapter, the possibility of using linear structure and piezoelectric absorber to control the dynamics of a non-linear structures has been presented. After the modelling, we have derived the amplitude equation of the mechanical structure with ϕ^6 potential coupled with a linear oscillator. The effects of the control parameters on the dynamical behaviour of the system has also been analysed and the conditions for the effectiveness of the control as well are obtained. Numerical simulation has been performed to confirm and complement the analytical calculations. Another part of this chapter deals with the analysis of the effects of control parameters on the onset of horseshoes chaos. It appears that for a good choice of these parameters one can suppress the Melnikov chaos.

In the next chapter particular attention will be paid on the effects of time delay between the detection of vibration and the action of the control on the effectiveness of the control strategy.

References

[1]- T. T. Soong, "Active structural control: theory and practice", john wiley & Sons, Inc, New York,1950.

[2]-T.Aida, K. Kawazoe, S Toda, J. of Vibration and Acoustics 117(1995)332

[3]- T. Aida, S Toda, S. N. Ogawa, Y. Imada, ASCE J. Engineering Mechanics 118 (1992) 163.

[4]- J X Gao, Y P Shen, Journal of Sound and vibration 264 (2003) 911.

[5]- R A Morgan, R W Wang, Journal of Vibration and Acoustics 124 (2002)77

[6]- M. S. Tsai, K. W. Wang, Journal of Sound and Vibration 221(1) (1999)1

[7]- N. Virgin, L. A. Cartee, Int. J. of Non-linear Mechs. 26 (1991) 449.

[8]- N. Virgin, R.H Plant, C. C. Cheng, Int. J. of Non-linear Mechs.27 (1992) 357.

[9]-A H. Nayfey, D. T. Mook, "Non-linear Oscillation" Wiley, New York, 1996.

[10]-B. A. Gardiner, "Mathematical modelling of forest ecosystems, proceeding of a workhop organized by Forstliche Versuchsenstalt Rheiland-Plalz and zentrun für prektische mathematik, 1991.

[11]- C Hayashi," Non-linear oscillation", Mc Graw-Hill, New York, 1964.

[12]- Y.L. Xu, W. L. Qu, B. Chen, Journal of sound and vibration, 261 (2003) 277.

[13]- P. J. Holmes, Proc. R Soc. London, 292 (1979) 419.

[14]- C. R. Fuller, S. J. Elliott, P. A. Nelson, "Active Control of Vibration" Academic Press, London, 1997.

[15]- E. F. Crawly, J. Luis, AIAA Journal 25 (10) (1987) 1373.

[16]- A. Baz, S. Poh, Journal of Sound and Vibration 126 (2) (1988) 327.

[17]- A. J. Young, "Active Control of Vibration in Stiffened Structures" Ph.D Thesis, Department of mechanical Engineering, University of Adelaide, south Australia 5005, 1995.

[18]- J. F. Rivory, C. H. Hansen, J. Pan, Journal of intelligent Material Systems and structures 5 (1994) 654.

CHAPTER III
ACTIVE CONTROL WITH DELAY OF THE DYNAMICS
OF UNBOUNDED MONOSTABLE MECHANICAL
STRUCTURE WITH ϕ^6 POTENTIAL

> # CHAPTER III:ACTIVE CONTROL WITH DELAY OF THE DYNAMICS OF UNBOUNDED MONOSTABLE MECHANICAL STRUCTURES WITH ϕ^6 POTENTIAL

I-INTRODUCTION

In this chapter we will continue to make the assumptions in the previous chapter: that the system under control is a non linear mechanical structure with ϕ^6 potential and that the secondary structure is fully active. In reference [1,2], the authors showed that one of the most important effects which limit the performance of the control strategy is the time delay between the detection of the structure motion and the restoring action of the control. In fact, they showed that time-delay can even lead to the instability of the control process in linear structures. In reference [3-7], the authors presented many control strategies in non-linear structures but did not take into account the effects of the inevitable time delay. Thus, it is of interest to analyse the same problem for structures with non linear dynamics as presented in this thesis.

The organisation of the chapter is as follows. Section 2 presents the model and the results of the stability analysis. Section 3 deals with the effects of time delay of the control of the harmonic vibration, catastrophic escape from the potential well. Section IV deals with the problem of inhibition of Smale-horseshoes chaos in the model. Concluding remarks will come in the last section.

II-MODEL AND STABILITY ANALYSIS
II-1 The model

The governing equations of the mechanical systems under control as presented in chapter II are repeated in the following

$$\begin{cases} \dfrac{d^2 q}{d\tau^2}(\tau) + (\lambda_1 + \alpha)\dfrac{dq}{d\tau}(\tau) + (b+\beta)q(\tau) + cq^3(\tau) + dq^5(\tau) - \beta y(\tau) - \alpha\dfrac{dy(\tau)}{d\tau} = f_0 \cos(\Omega\tau) \\[3mm] \dfrac{d^2 y}{dt^2}(\tau) + (\lambda_2 + \mu\alpha)\dfrac{dy}{d\tau}(\tau) + (a+\mu\beta)y(\tau) = \mu\beta q(\tau) + \mu\alpha\dfrac{dq}{d\tau}(\tau) \end{cases} \qquad \text{(III-1)}$$

The delay is materialised by the fact that the control system doesn't act at the same time with the excited structure. Mathematically, this effect is taken into account by using the retarded functional differential equation [1]. Thus, for a control system with delay, the differential equation given by (III-1) becomes:

$$\begin{cases} \dfrac{d^2q}{d\tau^2}(\tau)+(\lambda_1+\alpha)\dfrac{dq}{d\tau}(\tau)+(b+\beta)q(\tau)+cq^3(\tau)+dq^5(\tau)-\beta y(\tau)-\alpha\dfrac{dy(\tau)}{d\tau}=f_0\cos(\Omega\tau) \\ \dfrac{d^2y}{dt^2}(\tau)+(\lambda_2+\mu\alpha)\dfrac{dy}{d\tau}(\tau)+(a+\mu\beta)y(\tau)=\mu\beta q(\tau-\tau_x)+\mu\alpha\dfrac{dq}{d\tau}(\tau-\tau_{\dot{x}}) \end{cases} \quad \text{(III-2)}$$

Where τ_x and $\tau_{\dot{x}}$ are the time delays for displacement and velocity feedback force in the system respectively.

II-2 Stability of the control system

Following the method presented in chapter II section III-1, the local stability of the fixed points $(0,0,0,0)$ leads us to the equation of eigen system as follow

$$\begin{vmatrix} -s & 1 & 0 & 0 \\ -(b+\beta) & -s-\lambda_1 & \beta & \alpha \\ 0 & 0 & -s & 1 \\ \mu\beta e^{-s\tau_x} & \mu\alpha e^{-s\tau_{\dot{x}}} & -(a+\mu\beta) & -s-(\lambda_2+\mu\beta) \end{vmatrix}=0 \quad \text{(III-3)}$$

the characteristic equation for the stability of the system under control with delay is thus given by

$$s^4+\left[\lambda_2+\lambda_1+\alpha(1+\mu)\right]s^3+\left[a+b+\beta(1+\mu)+(\lambda_2+\mu\alpha)(\lambda_1+\alpha)-\mu\alpha^2\exp(-s\tau_{\dot{x}})\right]s^2+$$
$$\left[(b+\beta)(\lambda_2+\mu\alpha)+(\lambda_1+\alpha)(a+\mu\beta)-\mu\alpha\beta\left(\exp(-s\tau_x)+\exp(-s\tau_{\dot{x}})\right)\right]s \quad \text{(III-4)}$$
$$+(b+\beta)(a+\mu\beta)-\mu\beta^2\exp(-s\tau_x)=0$$

To obtain the stability boundary in the plane of the control parameter (β,τ_x), we use the D-subdivision method (see reference [3]). According to this method, the stability boundary in the plane (β,τ_x) is determined by the points that yield either to a root *s=0* or a pair of pure imaginary roots of equation (III-4)

Substituting s=0 into equation (III-4), one finds

$$\beta=\dfrac{-ba}{\mu b+a} \quad \text{(III-5)}$$

setting $s = i\gamma$ (where γ is a real constant) into the characteristic equation (III-4), gives the system of equation

$$
\begin{cases}
\gamma^4 - \left(a + b + \beta(1+\mu) + (\lambda_2 + \mu\alpha)(\lambda_1 + \alpha) - \mu\alpha^2 \cos(\gamma\tau_x)\right)\gamma^2 - \mu\alpha\beta\gamma\left(\sin(\gamma\tau_x) + \sin(\gamma\tau_{\dot{x}})\right) + \\
\qquad (b+\beta)(a+\mu\beta) - \mu\beta^2 \cos(\gamma\tau_x) = 0 \\
-\left(\lambda_1 + \lambda_2 + \alpha(1+\mu)\right)\gamma^3 - \mu\alpha^2\gamma^2 \sin(\gamma\tau_x) - \\
\qquad \left((b+\beta)(\lambda_2 + \mu\alpha) - \mu\alpha\beta\left(\cos(\gamma\tau_x) + \cos(\gamma\tau_{\dot{x}})\right) + (\lambda_1 + \alpha)(a+\mu\beta)\right)\gamma + \mu\beta^2 \sin(\gamma\tau_x) = 0
\end{cases}
\qquad \text{(III-6)}
$$

The stability boundary in plane (α, β) can be found from the bifurcation curve defined by the parametric equation (III-6) and the bifurcation line defined in equation (III-5). For our set of parameter equation (III-5) lead to a negative value of β thus, we present the stability boundaries in figure III-1 using equation III-6 for $\tau_x = \tau_{\dot{x}} = \tau_0 = 0, 0.2, 0.4$ and 0.6. The region *(B)* situated below the curve is the region where instability is obtained, domain *(A)* presents the stable position It appears that as the delay increases the region of stability decreases. We are reminded that in order to to plot this graph we have set $\gamma = 1$, this parameters can be the frequency of the external excitation.
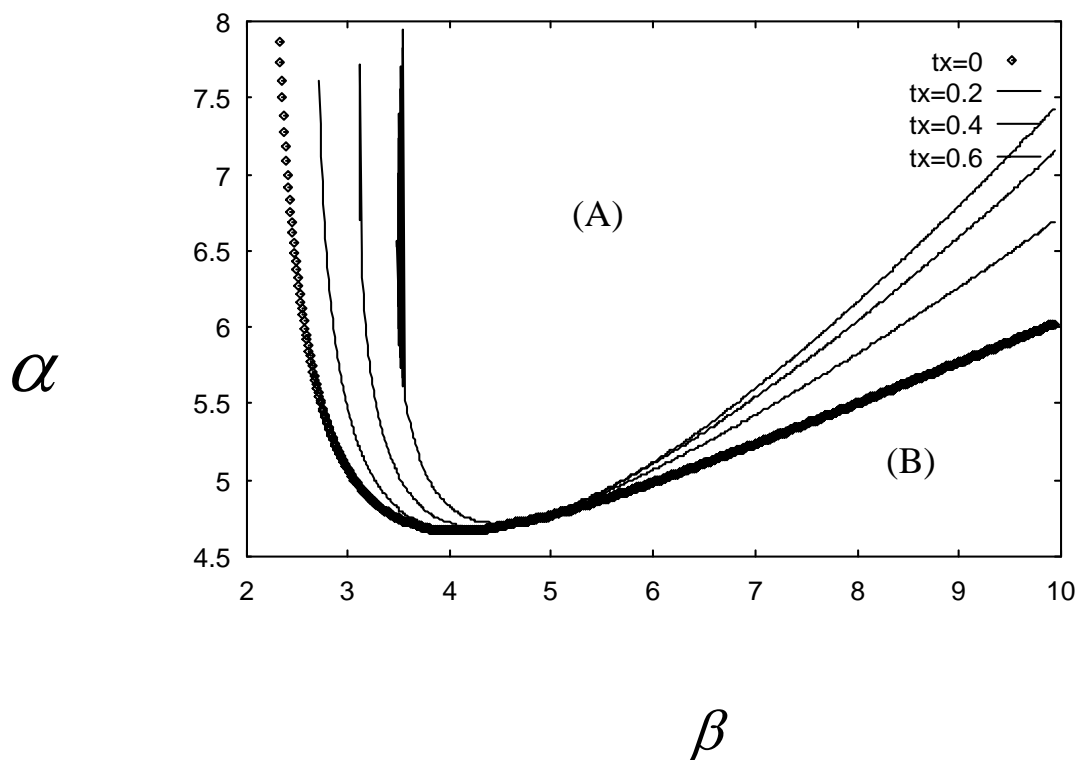
Figure III-1 : Stability boundary in the control space parameters (α, β) for $\tau_0 = 0$, $\tau_0 = 0.2$, $\tau_0 = 0.4$ and $\tau_0 = 0.6$

III-CONTROL OF VIBRATION AND CONTROL OF ESCAPE FROM A POTENTIAL WELL : EFFECTS OF TIME DELAY

III-1 Effects of time-delay on the control of vibration

In the linear limit ($c=d=0$), the amplitude of the harmonic oscillation of the controlled system is

$$A_c = \frac{f_0}{\left[\left(b+\beta-\Omega^2-\beta\eta_1-\alpha\Omega\eta_2\right)^2+\left(\Omega\left(\lambda_1+\alpha\right)+\beta\eta_2-\alpha\Omega\eta_1\right)^2\right]^{\frac{1}{2}}} \tag{III-6}$$

where

$$\eta_1 = \mu\left[\frac{\left(\beta\cos\left(\Omega\tau_x\right)+\alpha\Omega\sin\left(\Omega\tau_{\dot{x}}\right)\right)\left(a+\mu\beta-\Omega^2\right)-\Omega\left(\lambda_2+\mu\alpha\right)\left(\beta\sin\left(\Omega\tau_x\right)-\alpha\Omega\cos\left(\Omega\tau_{\dot{x}}\right)\right)}{\left(a+\mu\beta-\Omega^2\right)^2+\left(\Omega\left(\lambda_2+\mu\alpha\right)\right)^2}\right]$$

$$\eta_2 = \mu\left[\frac{\left(\beta\sin\left(\Omega\tau_x\right)-\alpha\Omega\cos\left(\Omega\tau_{\dot{x}}\right)\right)\left(a+\mu\beta-\Omega^2\right)+\Omega\left(\lambda_2+\mu\alpha\right)\left(\beta\cos\left(\Omega\tau_x\right)+\alpha\Omega\sin\left(\Omega\tau_{\dot{x}}\right)\right)}{\left(a+\mu\beta-\Omega^2\right)^2+\left(\Omega\left(\lambda_2+\mu\alpha\right)\right)^2}\right]$$

Comparing A_c to the amplitude A_{nc} of the vibrations of the uncontrolled system, we see that the control is efficient if $A_c < A_{nc}$. This means that the control parameters satisfy the following condition:

$$\left[\left(\beta\left(1-\eta_1\right)-\alpha\Omega\eta_1\right)\left(\beta\left(1-\eta_1\right)-\alpha\Omega\eta_2+2\left(b-\Omega^2\right)\right)\right]$$
$$+\left[\left(\Omega\alpha+\beta\eta_2-\alpha\Omega\eta_1\right)\left(\Omega\alpha+\beta\eta_2-\alpha\Omega\eta_1+2\Omega\lambda_1\right)\right] \succ 0 \tag{III-7}$$

Figure III-2 displays the stability boundary in plane (α,β) with $\tau_x = \tau_{\dot{x}} = \tau_0$ and $\Omega = 0.52$. The curve with a thick line represents the case where the delay is not considered and the region below this curve represents the case where control is inefficient. Taking into account the effects of delay, we present in the same graph the case where the delay is given by $\tau_0 = 0.2$ and $\tau_0 = 0.4$ and we arrive at the following conclusion. Due to the fact that every graph presents three regions, the inefficient region can increase or decrease depending on the value of time delay. To complement and validate this result, we display in figure III-3 the

evolution of amplitude versus the time for $\tau_x = 0.4$ and $f_0 = 0.5$ with α and β taken in every
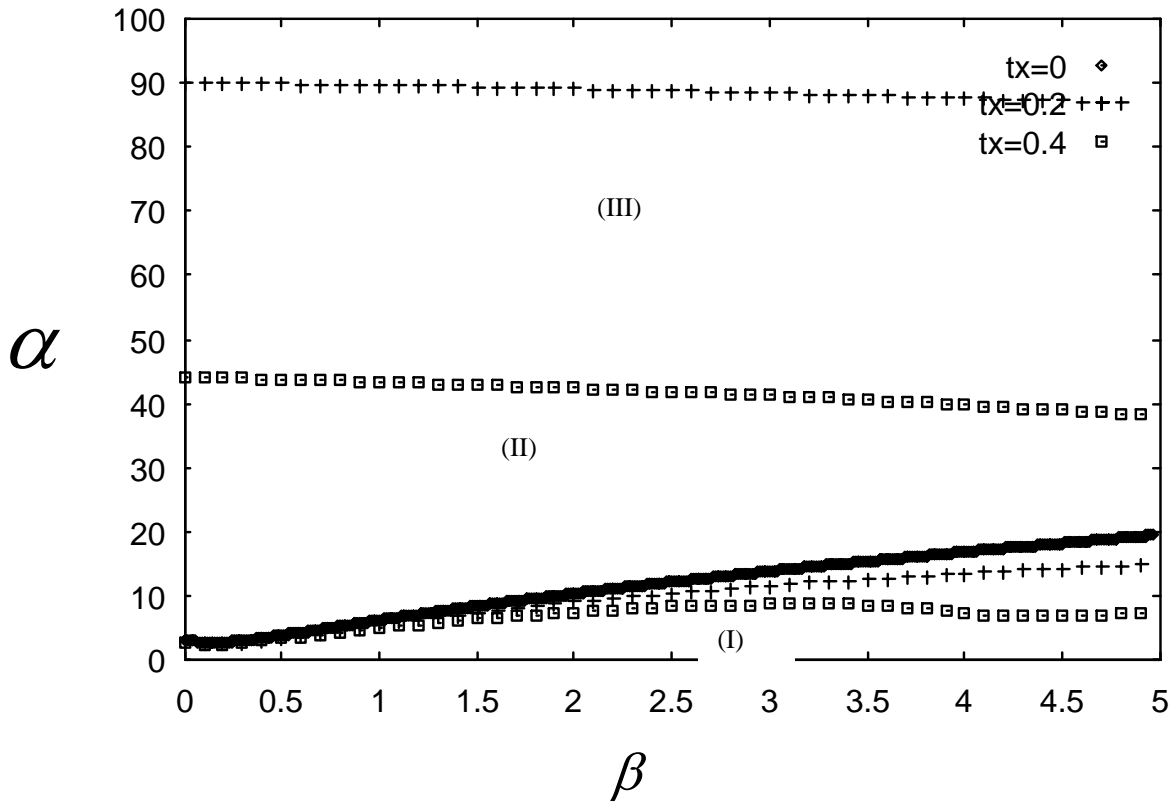

Figure III-2 : Effect of time delay on the two control gain parameters (α, β)
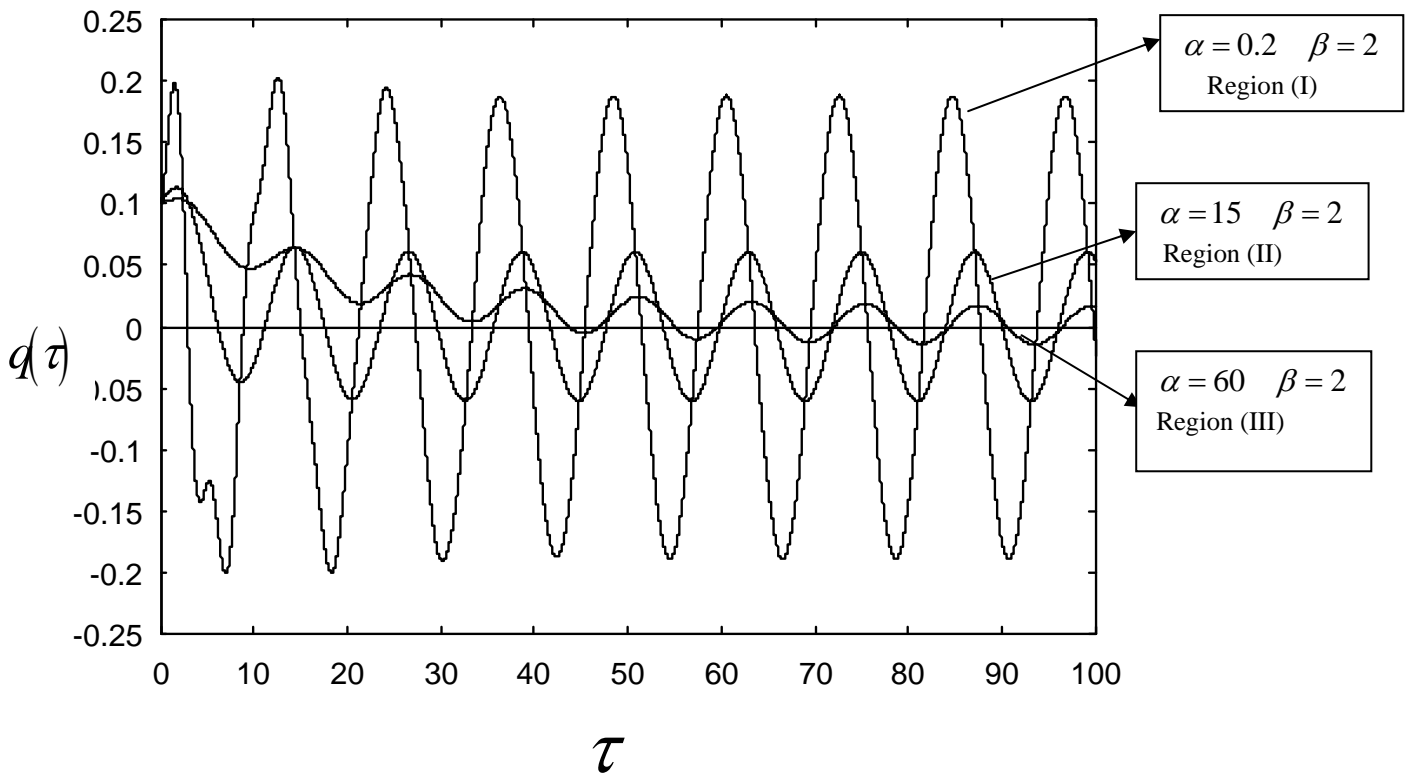

Figure III-3 : Evolution of amplitude versus the time for $\tau_0 = 0.4$ with α and β taken in the three region of figure III-2

region as presented in figure III-2. It appears that to optimise the reduction of amplitude of vibration in the system the value of control gain parameters (α, β) should be taken in region (III).

In the non linear case, the amplitude A of harmonic vibrations obeys the following non linear algebraic equation:

$$\frac{25}{64}d^2A^{10} + \frac{15}{16}cdA^8 + \left[\frac{9}{16}c^2 + \frac{5}{4}d\left(b + \beta - \Omega^2 - \beta\eta_1 - \alpha\Omega\eta_2\right)\right]A^6 + \frac{3}{2}c\left(b + \beta - \Omega^2 - \beta\eta_1 - \alpha\Omega\eta_2\right)A^4$$

$$+\left[\left(b + \beta - \Omega^2 - \beta\eta_1 - \alpha\Omega\eta_2\right)^2 + \left(\Omega(\lambda_1 + \alpha) + \beta\eta_2 - \alpha\Omega\eta_1\right)^2\right]A^2 - f_0^2 = 0 \qquad \text{(III-8)}$$

We remind the reader that η_1 and η_2 are function of τ_x and $\tau_{\dot{x}}$ as given here before. To determine analytically the domain in the parameter space where the control of amplitude is efficient, we proceed as presented in chapter II. In this spirit, we find that at the boundary, the amplitude is given by

$$A_b^2 = \frac{-3c\left(\beta(1-\eta_1) - \alpha\Omega\eta_2\right) - 2\zeta^2}{5d\left(\beta(1-\eta_1) - \alpha\Omega\eta_2\right)} \qquad \text{(III-9)}$$

where

$$\zeta = \frac{9}{4}c^2\left(\beta(1-\eta_1) - \alpha\Omega\eta_2\right)^2 - 5d\left(\beta(1-\eta_1) - \alpha\Omega\eta_2\right)\left[\left(\beta(1-\eta_1) - \alpha\Omega\eta_2\right)^2 + \left(\Omega\alpha + \beta\eta_2 - \alpha\Omega\eta_1\right)^2\right]$$

Inserting equation (III-9) in equation (III-8) (with $A=A_b$), we obtain the boundary separating the domain where the control is efficient (reduction of amplitude of vibration) to the domain where it is inefficient. In figure III-4, we have plotted this boundary in the (τ_x, f_0) plane, assuming that $\tau_x = \tau_{\dot{x}}$ along with the case where delay is not taken into account (solid horizontal line). This is done for α=0, β=0.2 (figure III-4a) and for α=0.5, β=0 (figure III-4b). The choice of α and β take into account the fact that we have demonstrated in chapter II that for a good choice of coupling parameters, the control is efficient. It is found that f_0 is a periodic function of τ_x. Thus, we find that with a good choice of time delay, a better protection of the structure can be obtained. However for some values of time-delay the control is affected in the bad direction.
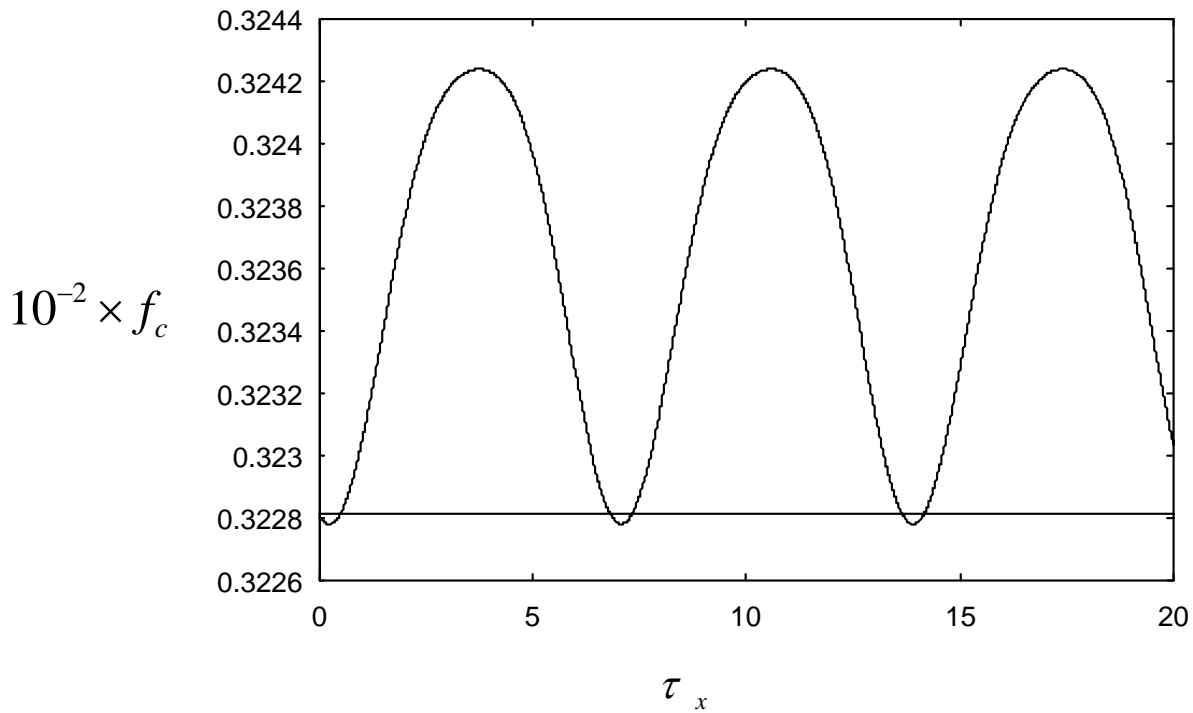
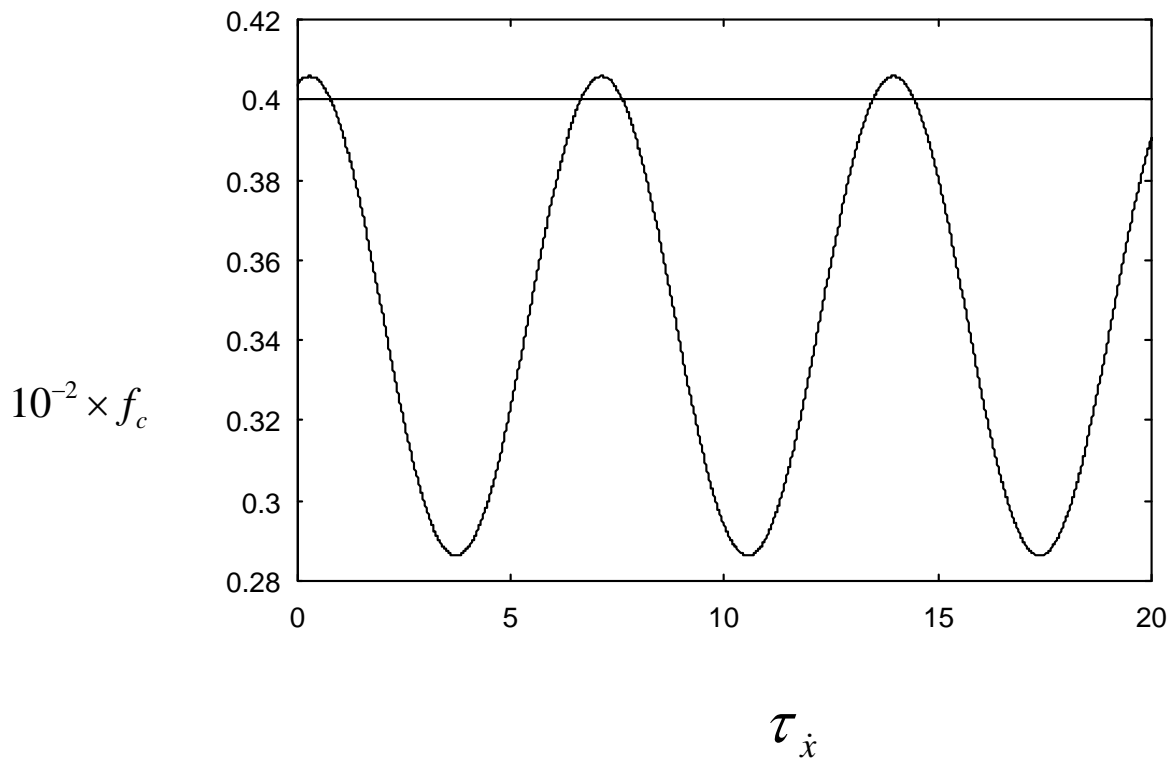**Figure III-4a :** Evolution of amplitude as function of time delay with α=0 and β=0.2.

Figure III-4b : Evolution of amplitude as function of time delay with α=0.5 and β=0

III-2 Effects of time-delay in the control of catastrophic escape

Using the same procedure as presented in chapter II, section III-3 and taking into account the effect of time-delay we obtain the critical force characteristics leading the system to catastrophic motion as follow

$$f_c^2 = \left(\frac{5}{8} dA_b^5 + \frac{3}{4} cA_b^3 + \left(b + \beta - \Omega^2 - \beta\eta_1 - \alpha\Omega\eta_2 \right) A_b \right)^2 + \left(\Omega(\lambda_1 + \alpha) + \beta\eta_2 - \alpha\Omega\eta_1 \right)^2 A_b^2$$

(III-10)

with $A_b^2 = \dfrac{6bq_c^2 + 3cq_c^4 + 2dq_c^6 - 6\left(b - \Omega^2 \right) X_m - 3cX_m^2 - 2dX_m^3}{6\Omega^2}$

where

$$X_m = \frac{\left(-c - \sqrt{c^2 - 4d\left(b - \Omega^2 \right)} \right)}{2d} \quad \text{and} \quad q_c = \pm\left(\frac{-c - \sqrt{c^2 - 4db}}{2d} \right)$$

We display in figure III-5 the variation of the critical force as function of time delay for $\alpha= 0$, $\beta=0.2$ (figure III-5a) and $\alpha= 0.1$, $\beta=0$ (figure III-5b), The horizontal line represents the results in the case where there is no delay. We find that for a certain choice of time delay, f_c is greater than that of the case without delay. We can thus conclude that the time delay can render, for a good choice of time delay, the control of escape more efficient.
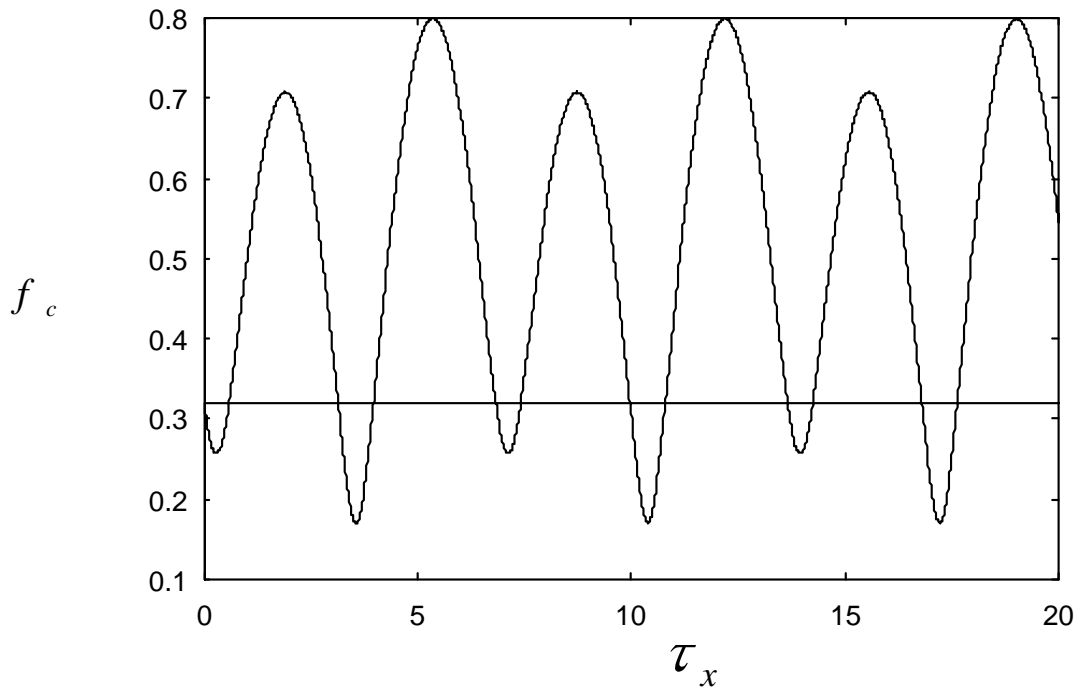
Figure III-5a : Evolution of the critical force as a function of time-delay for $\beta = 0.2$ and $\alpha = 0$
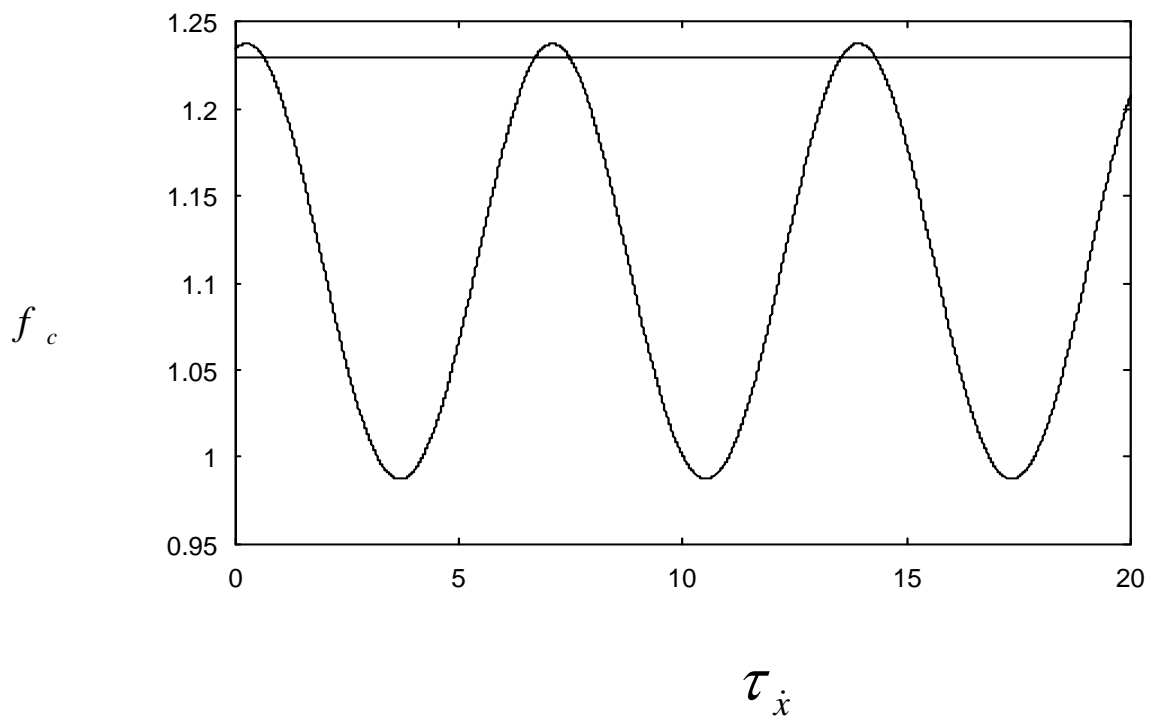

Figure III-5b : Evolution of the critical force as a function of time-delay for $\beta = 0$ and $\alpha = 0.1$

III-3 Effects of time delay of the control of Melnikov chaos

Our aim in this section is to find how the time-delay of the active control strategy affects the Melnikov condition for chaos. As in chapter II, we assume for the analytical treatment that $\frac{d^2 y}{d\tau^2} \simeq 0$. In this case, the components of the heteroclinic orbit are given by equations (I-68) of chapter I and the component y_0 is now given by

$$
y_0 = \pm \frac{\mu\beta X\xi}{\sqrt{2}(\lambda_2 + \mu\alpha)} \exp\left(-\left(\frac{a+\mu\beta}{\lambda_2+\mu\alpha}\right)\tau\right) \int_{-\infty}^{\tau} \frac{\sinh(Y(s-\tau_x))\exp\left(\left(\frac{a+\mu\beta}{\lambda_2+\mu\alpha}\right)s\right)}{\left(1+(1+\xi^2)\sinh^2(Y(s-\tau_x))\right)^{1/2}} d\tau
$$

$$
\pm \frac{\mu\alpha XY\xi}{\sqrt{2}(\lambda_2 + \mu\alpha)} \exp\left(-\left(\frac{a+\mu\beta}{\lambda_2+\mu\alpha}\right)\tau\right) \int_{-\infty}^{\tau} \frac{\cosh(Y(s-\tau_{\dot{x}}))\exp\left(\left(\frac{a+\mu\beta}{\lambda_2+\mu\alpha}\right)s\right)}{\left(1+(1+\xi^2)\sinh^2(Y(s-\tau_x))\right)^{1/2}} d\tau
$$

$$
\text{(III-11)}
$$

Thus the Melnikov function is given by (assuming the dissipate coupling absent)

$$
M(\tau_0) = \frac{X\xi\pi f_0}{Y(1-\xi^2)\sinh\frac{\Omega\pi}{2Y}} \cos(\Omega\tau_0) - \frac{\lambda_1 XY}{8}\left[\frac{3\xi^2-1}{1-\xi^2} + \frac{1+3\xi^2}{2\xi}\ln\frac{1+\xi}{1-\xi}\right] + k(\beta,\tau_x) \quad \text{(III-12)}
$$

with

$$
k(\beta,\tau_x) = \frac{\mu\beta^2 X^2\xi^2 Y}{2\lambda_2} \int_{-\infty}^{+\infty} \frac{\cosh(Y\tau)\exp\left(-\frac{(a+\mu\beta)}{\lambda_2}\tau\right)}{\left(1+(1-\xi^2)\sinh^2(Y\tau)\right)^{3/2}} \left(\int_{-\infty}^{\tau} \frac{\sinh(Y(s-\tau_x))\exp\left(\frac{(a+\mu\beta)}{\lambda_2}s\right)}{\left(1+(1-\xi^2)\sinh^2(Y(s-\tau_x))\right)^{1/2}} ds\right) d\tau
$$

Therefore the condition for the absence of chaos is

$$
f_0 \leq f_{0c} = \frac{Y(1-\xi^2)\sinh\frac{\Omega\pi}{2Y}}{\Omega\xi\pi}\left[\frac{\lambda_1 X^2 Y}{8}\left[\frac{3\xi^2-1}{1-\xi^2} + \frac{1+3\xi^2}{2\xi}\ln\frac{1+\xi}{1-\xi}\right] + k(\beta,\tau_x)\right] \quad \text{(III-13)}
$$

The critical value of amplitude of the external excitation f_{oc} depends nonlinearly on the control parameter and the time-delay through $k(\beta,\tau_x)$. We have found in chapter II that as β increases, the critical forces leading to horseshoes chaos

increases too. Consider that β is known, we can evaluate the evolution of $k(\beta, \tau_x)$ as τ_x varies. Carrying out the development used in the previous section , by setting $\upsilon = \exp(Ys), \eta = \exp(Y\tau)$ and $\chi = \exp(-2Y\tau_x)$, we obtain

$$k(\beta, \tau_x) = \frac{2\mu\beta^2 X^2 \xi^2}{\lambda_2 Y} \int_0^{+\infty} \frac{(\eta^2 + 1)\eta^{-\frac{(a+\mu\beta)}{\lambda_2 Y} + 1}}{\left[4\eta^2 + (1-\xi^2)(\eta^2 - 1)^2\right]^{3/2}} \left(\int_0^{\eta} \frac{(\chi\upsilon^2 - 1)\upsilon^{\frac{(a+\mu\beta)}{\lambda_2 Y} - 1}}{\left[4\chi\upsilon^2 + (1-\xi^2)(\chi\upsilon^2 - 1)^2\right]^{1/2}} d\upsilon \right) d\eta$$

(III-14)

then assuming that $\eta = \dfrac{\psi}{\psi - 1}$ and $\upsilon = \dfrac{p}{p-1}$ we obtain

$$k(\beta, \tau_x) = \frac{2\mu\beta^2 \xi^2 X^2}{\lambda_2 Y} \int_0^1 \frac{(2\psi^2 - 2\psi + 1)\left(\dfrac{\psi}{\psi-1}\right)^{-\frac{(a+\mu\beta)}{Y\lambda_2} + 1}}{(\psi - 1)\left(4\psi^2 + (1-\xi^2)(2\psi - 1)^2\right)^{3/2}} \left(\int_0^{\psi} \frac{(\chi\upsilon^2 - (\upsilon-1)^2)\left(\dfrac{\upsilon}{\upsilon-1}\right)^{\frac{(a+\mu\beta)}{Y\lambda_2} - 1}}{(\upsilon - 1)^3 \left(4\chi\upsilon^2 + (1-\xi^2)(\chi\upsilon^2 - (\upsilon-1)^2)^2\right)^{1/2}} d\upsilon \right) d\psi$$

(III-25)

With the above, we can numerically compute the variation of $k(\beta, \tau_x)$. Figure III-6 which reports the variations of $k(\beta, \tau_x)$ as τ_x varies for $\beta=0.8$, it shows that $k(\beta, \tau_x)$ decreases when τ_x increases. Consequently, the control becomes less and less efficient when the time-delay increases. More generally, to deal with the effect of delay on the critical forcing leading to Melnikov chaos, we derive that the critical forcing decreases with the increasing of time delay. This means that in the presence of time delays chaos appears for smaller values of f_c as compared to the system without delay
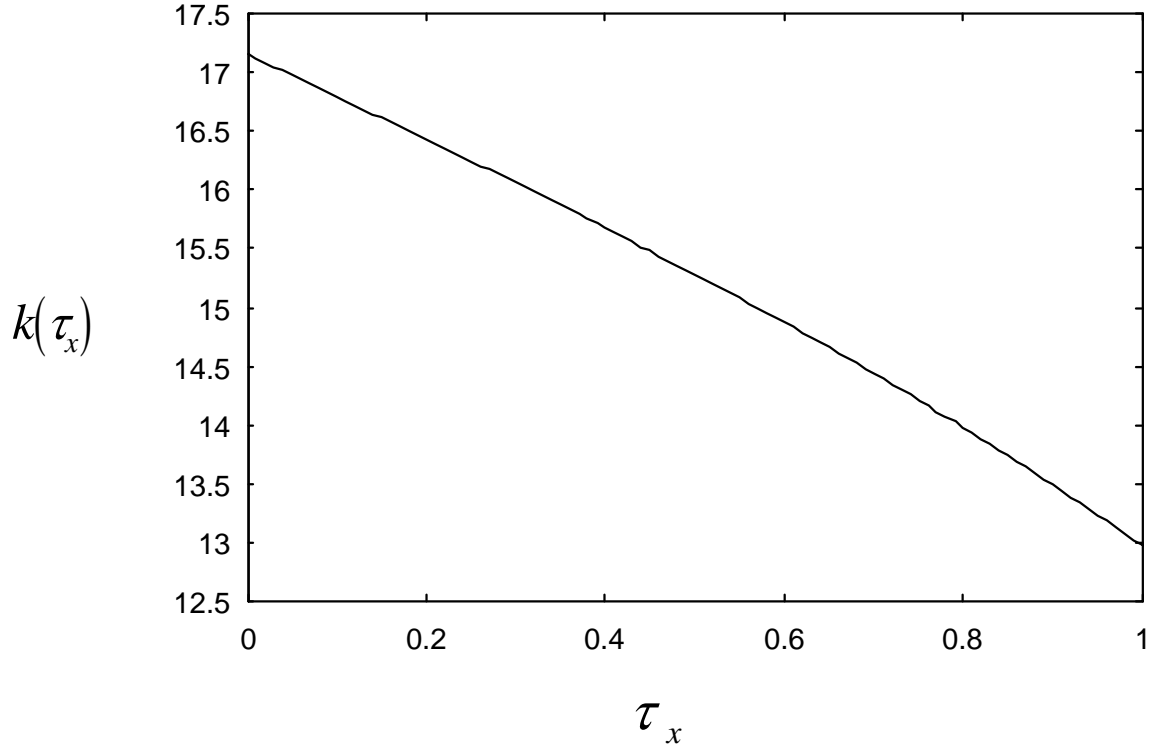
Figure III-6 : Evolution of k(β,τ$_x$) with τ$_x$ for β=0.8

Consider now the case of dissipative coupling ($\beta = 0$); the Melnikov function is given by

$$M(\tau_0) = \frac{X\xi\pi f_0}{Y(1-\xi^2)\sinh\frac{\Omega\pi}{2Y}}\cos(\Omega\tau_0) - \frac{\lambda_1 XY}{8}\left[\frac{3\xi^2-1}{1-\xi^2}+\frac{1+3\xi^2}{2\xi}\ln\frac{1+\xi}{1-\xi}\right]+k(\alpha,\tau_{\dot{x}}) \quad \text{(III-16)}$$

with

$$k(\alpha,\tau_{\dot{x}}) = \frac{\mu\alpha^2 X^2\xi^2 Y^2 a}{2(\lambda_2+\mu\alpha)^2}\int_{-\infty}^{+\infty}\frac{\cosh(Y\tau)\exp\left(-\frac{a}{(\lambda_2+\mu\alpha)}\tau\right)}{\left(1+(1-\xi^2)\sinh^2(Y\tau)\right)^{3/2}}\left(\int_{-\infty}^{\tau}\frac{\cosh(Y(s-\tau_{\dot{x}}))\exp\left(\frac{a}{(\lambda_2+\mu\alpha)}s\right)}{\left(1+(1-\xi^2)\sinh^2(Y(s-\tau_{\dot{x}}))\right)^{1/2}}ds\right)d\tau$$

$$+\frac{\mu\alpha^2 X^2\xi^2 Y^2}{2(\lambda_2+\mu\alpha)}\int_{-\infty}^{+\infty}\frac{\cosh(Y\tau)\cosh(Y(s-\tau_{\dot{x}}))\exp\left(-\frac{a}{(\lambda_2+\mu\alpha)}\tau\right)}{\left(1+(1-\xi^2)\sinh^2(Y\tau)\right)^{1/2}\left(1+(1-\xi^2)\sinh^2(Y(s-\tau_{\dot{x}}))\right)^{3/2}}d\tau$$

Carrying out the same manipulation as presented in the previous section we arrive to the fact that $k(\alpha,\tau_{\dot{x}})$ also decreases when time-delay ($\tau_{\dot{x}}$) increases.

III-4 Effects of time-delay on the basin of stability

The investigation has so far been carried out in a completely analytical context. In this section some numerical simulations are performed to verify the theoretical prediction. Of course a comprehensive numerical study would require the description of the whole dynamics by taking a general equation given by

$$
\begin{cases}
\dfrac{d^2q}{d\tau^2}(\tau)+(\lambda_1+\alpha)\dfrac{dq}{d\tau}(\tau)+(b+\beta)q(\tau)+cq^3(\tau)+dq^5(\tau)-\beta y(\tau)-\alpha\dfrac{dy(\tau)}{d\tau}=f_0\cos(\Omega\tau) \\
\dfrac{d^2y}{dt^2}(\tau)+(\lambda_2+\mu\alpha)\dfrac{dy}{d\tau}(\tau)+(a+\mu\beta)y(\tau)=\mu\beta q(\tau-\tau_x)+\mu\alpha\dfrac{dq}{d\tau}(\tau-\tau_{\dot{x}}) \qquad \text{(III-27)}
\end{cases}
$$

And by constructing their basins of attraction. Turning our interest on the effects of the time delays, we find that the fractality appears more earlier because it is found in chapter II that for the external excitation given by $f_0 = 0.2$, $\alpha=0$ and $\beta=0.8$. Taking the case of $f_0 = 1.5$ and $\beta = 1.5$, figure III-7 confirm that Melnikov chaos is suppressed in the system. It appears now in figure III-7 that for the one value of delay given by $\tau_x = 2.005$ the fractality reappear. This effect when we look for the effect of dissipative coupling parameters (α).
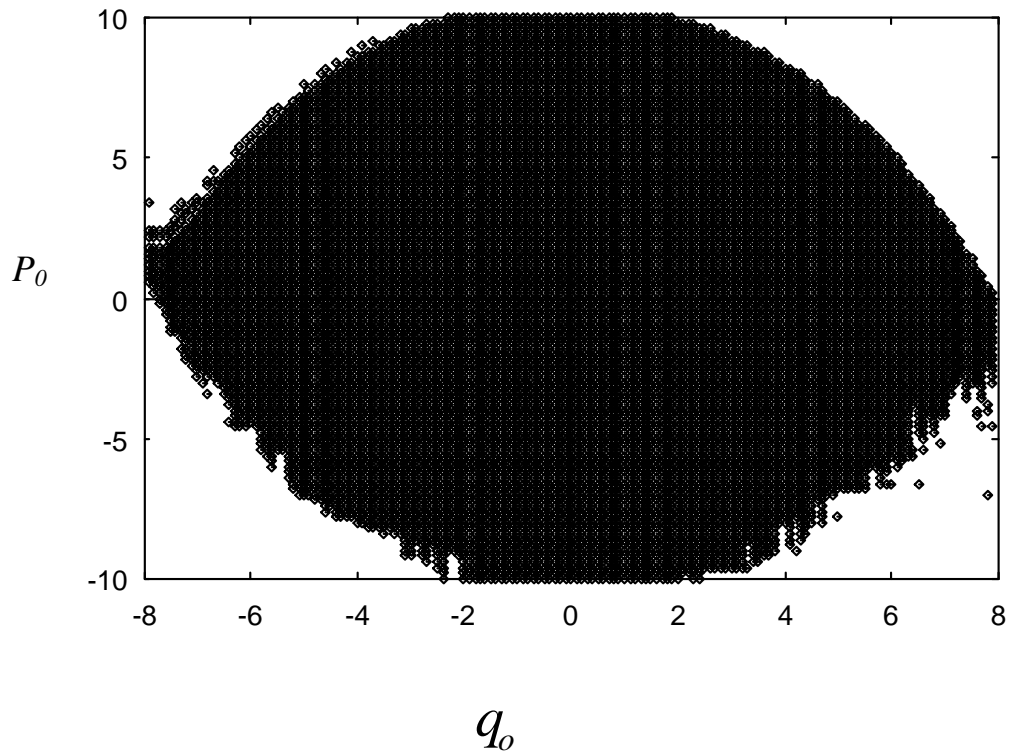

q_o

Figure III-7 : Basin of stability for $\Omega = 0.92$, $\beta = 1.5$, $\alpha = 0$ and $f_0 = 1.5$

Another effect which arises in the system is the extreme sensibility of the system because of delay. For instance, with $\tau_x = 2$, the boundary of the basin remains regular this for $\beta = 1.5$, and *fo=1.5* (figure III-8a). Setting now the value of $\tau_{\dot{x}} = 2.005$ the fractality reappears (figure III-8b) in the system which was regular. This in also confirmed in figure III-8c when the value of delay is $\tau_x = 2.1$, The fractality becomes more and more visible. This means that the best estimation of the optimal parameters for the efficiency of the control should not neglect the effects of time-delays.
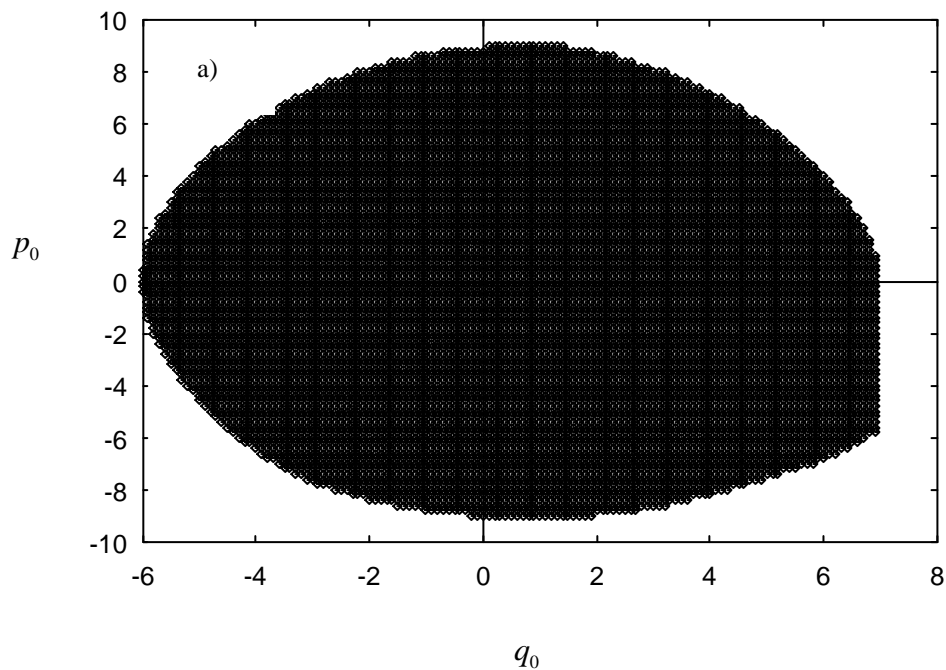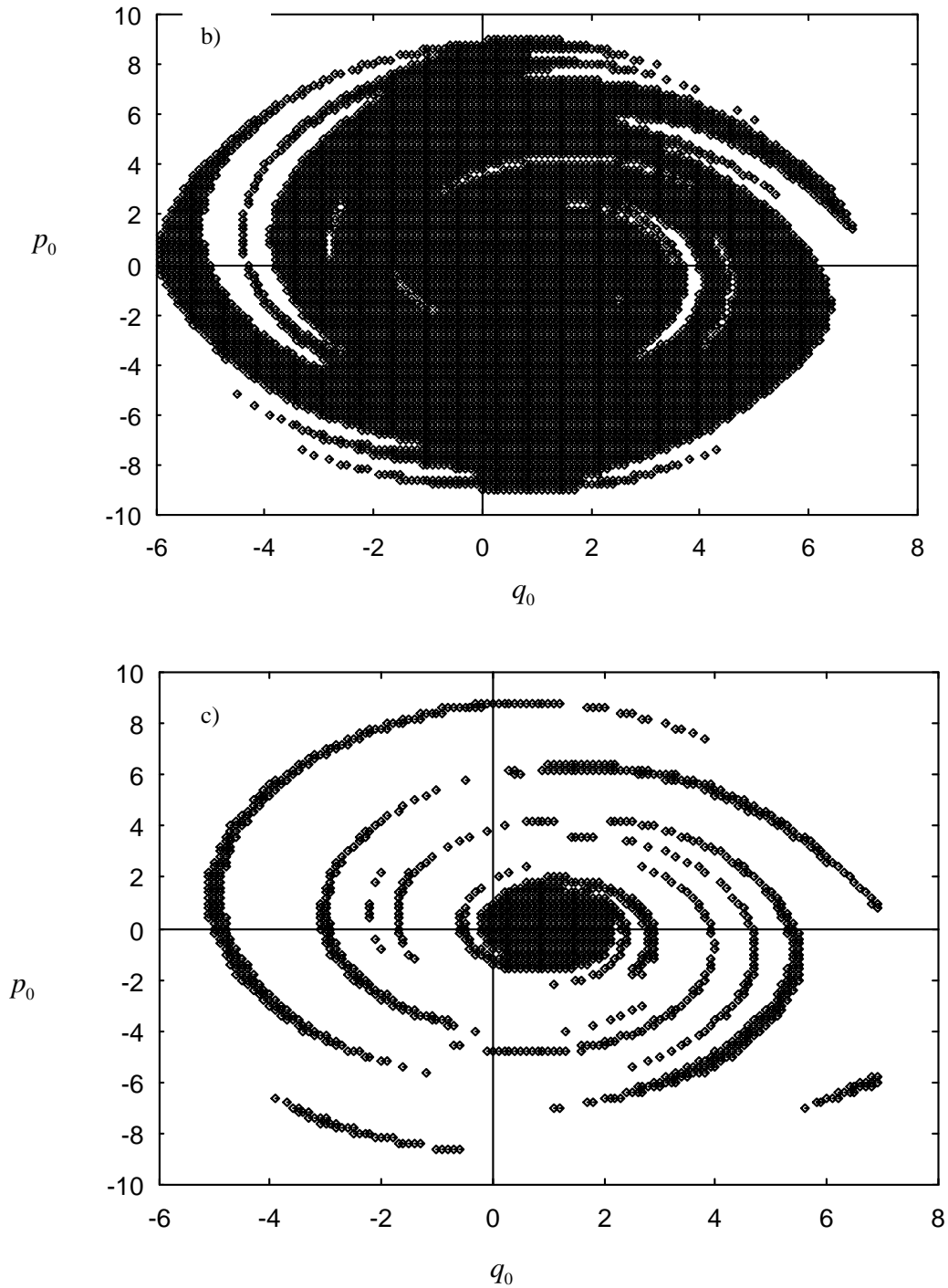
Figure III-8 : Early appearance of the fractal behaviour because of time delay
$a)\tau_x = 2$ b) $\tau_x = 2.005$ c) $\tau_x = 2.01$

IV-CONCLUSION

In this chapter, we have analysed the effects of time delay on the control of vibration, the escape and horseshoes chaos of an harmonically excited system in a catastrophic (unbounded) single well ϕ^6 potential. The stability of the system under control has been studied using the Lyapunov concept and D-subdivision method. The effects of time-delay in the approximate critical force leading to reduction of amplitude and the effects of control parameters and time delays on the critical forces for Melnikov chaos, appear to be important and should be taken into account for the designing of control devices.

REFERENCES

[1]-L. Zhang, C. Y. Yang, M. J. Chajes, A. H. D. Cheng, J Engng. Mech. Div ASCE 119 (1993) 1017.

[2]-T. T. Soong, "Active Structural Control: Theory and Practice", John Wiley & Sons, Inc, New York, 1950.

[3]-K. Hackl, C. Y. Yang, A. H. D. Cheng, Int J. Non-linear Mech. 28 (1993) 441.

[4]-A. H. D. Cheng, C. Y. Yang, K. Hackl, M. J. Chajes' Int. J. Non-linear Mech.28 (1993) 549.

[5]-C. R. Fuller, S. J. Eliot, P. A. Nelson, "Active Control of Vibration" London, Academic Press, 1997.

[6]-R. Tchoukuegno, P. Woafo, Physica D 167 (2002) 86.

[7]-O. C. Pinto, P. B. Goncalves, Chaos, Solitons & Fractals 14 (2002) 227.

GENERAL CONCLUSION AND PERSPECTIVES

GENERAL CONCLUSION AND PERSPECTIVES

1°) Summary of the main results

Before ending with this dissertation, let us give a summary of the main results. This thesis has dealt with the study of the dynamics and active control with delay of the dynamics of unbounded monostable mechanical structures with ϕ^6 potential.

It has been demonstrated in chapter I that, the mathematical model of such a structure like inverted pendulum, articulated beam and elastic beam fixed at the ends and free at the top, is that of a particle moving in a catastrophic single well ϕ^6 potential. This model is more realistic compared to that described by the classical Duffing oscillator as presented earlier. We have studied the dynamics of a ϕ^6 oscillator submitted to an external sinusoidal excitation. The approximate critical force leading to catastrophic motions has been obtained analytically and verified numerically. The criteria for the appearance of horseshoes chaos have also been derived using the Melnikov theory and metamorphoses of the basin of attraction have been observed.

In chapter II, the control of vibration and catastrophe of a non-linear structure by a linear one coupled in a sandwich manner has been studied. We have also presented a model of control in mechanical structures by using an active-passive piezoelectric absorber. The effects of the control parameters and the dynamical behaviour of the system have been also analysed. The condition for the effectiveness of the control as well as that of the escape from the potential well are obtained. Numerical simulations have been performed to confirm and complement the analytical calculations. We derive and analyse the approximate conditions for the appearance of Melnikov chaos as well as the effects of the control gain parameters. For a good choice of coupling parameters, the control strategy can be optimised.

In chapter III, we have analysed the effects of time delays on the control strategy. The stability of the system under control has been studied. The approximate critical force leading to reduction of amplitude and to catastrophic

motions has been obtained analytically. The effects of control parameter along with time delay on the critical forces for Melnikov chaos have been are obtained and the main conclusion is that the best estimation of the optimal parameters for the efficiency of the control should not neglect the effects of time delay.

2°) Perspectives

Despite the results obtained in this thesis, other points of interests will be solved in the future to complement and get a better understanding of this work.

♦Most of the environmental loads, such as wind and earthquakes, to which civil engineering structures are subjected, are random in nature. Hence, the analysis of the behaviour of an actively controlled as well as an uncontrolled structure will be based on the theory of random vibrations.

♦Another point of interest is to couple many inverted pendulums and see how the coupling influence the dynamics of the system. This may have implication in agriculture.

♦During this dissertation, when we were discussing about beams, we consider only the case of the first mode of vibration. It will be of interest to take into account all the normal modes vibration to ameliorate the precision of our results. Moreover a direct numerical simulation of the non-linear partial differential equation of the beam dynamics should be carried out.

♦Our study has focussed on the analytical and numerical study of the control of the dynamics in mechanicals structures. To complement our knowledge in such devices, experimental studies should be carried out for eventual technological exploitation in engineering and in agriculture.

LIST OF PUBLICATIONS

LIST OF PUBLICATIONS

1°)-R. Tchoukuegno, **B. R. Nana Nbendjo** and P. Woafo, "Resonant oscillations and fractal basin boundaries of a particle in a ϕ^6 potential"
Physica A 304 (2002) 362-378.

2°)-R. Tchoukuegno, **B. R. Nana Nbendjo** and P. Woafo, "Linear feedback and parametric controls of vibration and chaotic escape in a ϕ^6 potential"
International Journal of Non-linear Mechanics 38 (2003) 531-541.

3°)- **B. R. Nana Nbendjo**, R. Tchoukuegno and P. Woafo "Active control with delay of vibration and chaos in a double well Duffing oscillator"
Chaos, Solitons & fractals 18 (2003) 345-353.

4°)- **B. R. Nana Nbendjo**, Y. Salissou and P. Woafo, "Active control with delay of catastrophic motion and horseshoes chaos in a single well Duffing oscillator"
Chaos, Solitons & fractals 23 (3)(2005) 809-816.

5°)- **B. R. Nana Nbendjo**, R. Tchoukuegno and P. Woafo, "Control of vibration and catastrophic motion in a non-linear beam by linear beam with sandwich coupling: Modelling and Dynamical study" International Journal of Non-linear Mechanics (Submitted)

6°)- **B. R. Nana Nbendjo** and P. Woafo, "Active control with delay of vibration and catastrophic motion in a mechanical system with ϕ^6 potential", Proceedings of. The third Symposium on contemporary problems in mathematical physics. (COPROMAPH 3), Cotonou, 2003.